The Evaluation of Sorbent Containing Geotextiles for the Remediation of PAH and NAPL Contaminated Sediment

by

Gabriel Trejo, B.S.

Thesis

Presented to the Faculty of the Graduate School of

The University of Texas at Austin

in Partial Fulfillment

of the Requirements

for the Degree of

Master of Science in Engineering

The University of Texas at Austin

August 2009

The Evaluation of Sorbent Containing Geotextiles for the Remediation of PAH and NAPL Contaminated Sediment

Approved by
Supervising Committee:

Danny D. Reible

_____

Howard M. Liljestrand

_____

Dedication

To my parents, Pablo & Antonia Trejo,

and my brothers; Joel, Paul and Gil.

Acknowldgements

I would first like to thank my advisor, Dr. Danny Reible for his seemly limitless knowledge and experience, and for taking a chance on me and bringing me aboard his research group. I'd like to thank Dr. Reible's post-doc, Xiao Xia Lu, who exhibited the patience of a mother when working with me and never giving up on me. A huge thank you is also in order for my fellow members of the Reible research family: Lisa Moretti for getting me started in the lab and always pointing me in the right direction; Ya Choa Qi for keeping me company in the summer; Casey Forrest for sharing the last bus of the CR/RR route; Wil Sarchet for showing me the Reible way; and Matt, Ryan, and Tim for making my last semester at the University of Texas at Austin a memorable one. A special thank you also goes out to the Ph.D.'s in the Reible Lab including: Y.S. Hong for always being there; Dave Lampert for his modeling and sports trivia expertise; Tony Smith for being great resource in the lab and looking forward to 1:00-3:00 PM every Friday afternoon; and Nate Johnson for hosting me during EWRE Recruitment Weekend '07 and for setting the standard of professionalism and athleticism in the group. A mention is also in order for the night owls of ECJ, especially Lee Blaney and Pat McNamara for letting me know I wasn't the last man on campus. This research was partially funded by the Oregon Department of Environmental Quality and Huesker, Inc.

May 14, 2009

Abstract

The Evaluation of Sorbent Containing Geotextiles for the Remediation of PAH and NAPL Contaminated Sediment

Gabriel Trejo, M.S.E.

The University of Texas at Austin, 2009

Supervisor: Danny D. Reible

As more sites containing contaminated sediments are remedied with sediment caps, so grows the interest among site managers and engineers in the benefits afforded by active capping. While traditional sediment caps can effectively manage strongly solid-associated contaminants in many situations, under certain conditions active caps or amendments may be needed to effectively reduce risk to an acceptable level. This research assessed the predicted and observed breakthrough of dissolved organic contaminants in two newly developed geotextiles; one designed to sorb non-aqueous–phase liquids (NAPLs), the other dissolved-phase contaminants. The performance of the geotextiles was then compared to that of another remediation technology that has been deployed in the field for two years. All active materials were then evaluated based on their sorption capacity and their predicted life under field conditions.

The sorbent containing geotextiles designed for active capping applications were tested in columns to simulate field conditions, where upwelling groundwater would be contaminated by impacted sediments, thereby transporting contaminants to the water column. The contaminants of interest in these studies were three polycyclic aromatic hydrocarbons (PAHs) of varying hydrophobicity. Breakthrough curves for the materials

of interest were constructed for the three PAHs and were fit to an advection-dispersion model to predict the mass of contaminants sorbed onto them. This mass was then compared and verified to be similar to values found in literature.

The performance of the geotextiles was compared to that of organoclay deployed in Portland, OR, at the McCormick & Baxter Creosoting Company Superfund Site. In 2004, over 22 acres of sediment at the site were remedied with both passive and active caps to mitigate the effects of decades worth of contamination. In certain portions of the site, a 12 inch thick layer of organoclay was employed, while at other portions of the site, conventional sand or a thin reactive core mat with the equivalent of approximately 1 cm of organoclay were employed. The continued effectiveness of these sediment caps was evaluated using a variety of laboratory techniques, including measuring samples' hexane extractable material, which is a proxy for NAPL contamination, as well as their PAH bulk concentrations. These analyses performed on core samples allowed for the generation of vertical profiles critical to cap evaluation.

Despite possessing a significantly greater specific sorption capacity, the geotextiles could not offer the same protection for the extended period of time that the bulk organoclay could. The greater mass of organoclay deployed in bulk at the McCormick & Baxter site allowed a much greater sorption capacity to be placed. It would take over sixty stacked layers of the one of the geotextiles evaluated in these studies to achieve the same capacity for dissolved-phase contaminants as the 1 ft organoclay cap. However, no significant penetration of NAPL into the bulk organoclay has been noted, and thus even the thin layer within a geotextile might have been sufficient at the site, despite its significantly lower overall capacity. The data generated provides information as to the expected capacity of the various sorbent placement approaches and can help guide decisions at other sites.

Table of Contents

List of Tables

List of Figures

Chapter 1: Introduction

Sediments are the ultimate sink for a variety of environmental contaminants, because of their tendency to partition to the sorbing components of the sediment. Virtually any contaminant introduced into the environment, whether in the vapor, dissolved, or free phase (i.e. non-aqueous phase), can end up in sediments. Once in sediments, contaminants can bioaccumulate in organisms which reside in either the benthic layer or the overlying water-column, partitioning into their fats and lipids, thereby further mobilizing contaminants, and introducing them into the food chain. Once in the food chain, contaminants can biomagnify in higher order organisms until the point where toxic concentrations are reached, resulting in adverse health effects and possibly death. The combination of elevated risk associated with exposure and the difficulty in remediating impacted sediments are indicative of the need for research in this area. Compounding this need is the absence of extensive studies conducted on the fate and transport of contaminated sediment and of the remedial approaches which have traditionally been employed.

A promising technique for the management of contaminated sediments is that of active capping. Traditional capping is merely the isolation of contaminated sediment by placing a layer of clean material over the impacted sediment. After the cap has been in place for an extended period of time, natural sedimentation will deposit a fresh layer of sediments over the cap, providing a clean habitat necessary for the return of benthic organisms. Active capping improves on this remedial technique by using clean material that can actively sequester contaminants or even promote degradation of contaminants within the cap. Due to the difficulty of maintaining active degradation processes, most active caps are really permeable sorptive barriers, retarding contaminant migration

through sorption. Two of the most capable sorbents for organic contaminants are organoclays and activated carbon, and these sorbents are the focus of this thesis.

Organoclay is natural clay that has been modified to become hydrophobic/organophilic. This switch in affinities is made possible by exchanging cations on the surface of the clay with quaternary amines that have carbon chains attached to them. Organoclays are capable of sequestering free-phase liquids (non aqueous phase liquids, NAPL) as well as dissolved phase contaminates.

Activated carbon is carbon that has been treated at high temperature to increase its internal surface area and sorption capacity. Its use in a variety of industrial, remedial, and municipal water treatment applications has garnered it a well earned reputation as an excellent sorbent of dissolved phase contaminants. It has little or no capacity to absorb NAPL phases however.

1.1 Problem Statement

The process of designing a sediment cap involves both short term (e.g. placement) and long term (e.g. capacity, effectiveness) considerations. Bulk placement of active material has been used at several sites that have employed active capping as a solution to contamination of sediments, yet this solution can be an inefficient means of placing high value, high capacity sorbents. Wet activated carbon has a density near that of water, and any trapped air could lead to an inability to settle in the water column. In addition, bulk placement may require placement of several inches of material to insure good coverage of the contaminated sediments, and, in some instances, only a thin layer may be necessary to achieve satisfactory containment of the contaminants. In such instances, reactive core mats in which the sorbent material is placed within a thin layer (typically 1

cm or less) may be an appropriate approach to implementing an active cap. This research compares bulk organoclay deployed at an EPA Superfund Site, the McCormick & Baxter site in Portland OR, to two sorbent filled geotextiles, one designed for separate phase sorption and the other containing activated carbon and designed for dissolved organic contaminant sorption. The capacity and operational characteristics of the two geotextiles are summarized and compared to that of bulk organoclay.

1.2 RESEARCH OBJECTIVES

A series of batch and column studies were performed on a variety of active capping geotextile mats manufactured by Huesker, Inc., to evaluate their sorptive capacity of both free and dissolved phase contaminants. These tests served to mimic the environment of groundwater upwelling through a contaminated sediment cap. Observed and predicted results from these studies were then compared to core samples including similar mats filled with organoclay and in bulk layers of organoclay taken from the McCormick & Baxter Superfund Site in Portland, Oregon. Cores from this site were taken from an assortment of caps which were deployed in 2005 and 2006 to control creosote seepage into the Willamette River. This research analyzed cores taken from the capped sections of the site; to not only evaluate the effectiveness of the sediment cap but also to predict the performance of Huesker, Inc.'s geotextile mats under similar conditions.

Chapter 2: Literature Review

2.1 Contaminated Sediment

The United States Environmental Protection Agency (EPA) defines contaminated sediments as soil, sand, organic matter, or other minerals that accumulate on the bottom of a water body and contain toxic or hazardous materials at levels that may adversely affect human health or the environment (U.S. EPA 2005b). Contaminated sediment can significantly impair the navigational and recreational uses of rivers and harbors and can be a contributing factor in many of the 3,200 plus fish consumption advisories issued annually nationwide which, as of 2004, covered 24% of the river miles and 35% of the lake acreage in the United States (U.S. EPA 2005a). Since the 2004 release of the EPA's National Sediment Quality Survey, the EPA has since taken remedial action in over 140 sites, of which 14 have currently been classified as Superfund Megasites due to the scale of contamination (remedial costs exceed $50 million). Not accounted among the EPA sites are the numerous projects that are being undertaken by other federal, state, or local authorities.

Sediment may become contaminated by a variety of sources, such as air deposition to water then sediments, soil transport as runoff, erosion of aquatic banks or beds, or during the breakdown or build up of minerals (U.S. EPA 2005b). As can be inferred from this list, contaminated sediments can have anthropogenic and natural sources. When dealing with sediments, the highest risk is associated with contaminants in the biologically active layer which extends from the water column-sediment interface down 10-15 cm. The biologically active layer, or benthic layer, is home to variety of organisms which ingest, burrow and otherwise disturb and rework the surficial sediments. When dealing with sediments, the highest risk is associated with contaminants in the benthic layer which extends from the water column-sediment interface, down 10-15 cm.

The benthos zone is home to variety of organisms which are not present at deeper sediment depths and would only be exposed to deeper sediments during storms or other comparable disturbance events. When benthic organisms are exposed to contaminated sediments, contaminants partition into their tissue, or bioaccumulate, which then opens up the pathway for biomagnification in higher order organisms (such as fish and humans).

The goal of all remedial actions is to reduce the risk at a site to an acceptable level, considering both short and long term effects. Short term risk could be evaluated by the impact of a remedy on and around the site during implementation, while long term risk might be gauged by the reduction of exposure of benthic organisms to contamination, thereby diminishing the pathway of contaminants into the food chain thus reducing contaminant mobility (Moretti 2008). Commonly used remediation techniques that reduce risk include dredging, capping, and natural attenuation.

2.2 SEDIMENT REMEDIATION OPTIONS

2.2.1 Dredging

Although the practice of dredging has existed for centuries, it is not to be confused with environmental dredging, which is relatively a new concept. Traditional dredging is conducted for the purpose of maintaining navigational depths in harbors and waterways; whereas environmental dredging is carried out specifically for the purpose of remediating environmental risks (Bridges, et al. 2008). Environmental dredging is intended to reduce risk by removing the problem sediment from the environment. However, residual contamination and contaminant release are inevitable during the dredging process as a result of sediment resuspension and exposure (Sediment Dredging

at Superfund Megasites: Assessing the Effectiveness 2007). This usually causes a decrease in long term risk at the cost of increased short term risks. Not only are short term risks increased by the resuspension of contaminated sediment, but they are also affected by the release of contaminants from deep sediments not normally exposed to the water column, as well as residual contamination produced from dredging operations (Bridges, et al. 2008). Dredging operations themselves are not an inexpensive matter. In addition to physically removing the contaminated sediment from the environment, the sediment must also be dewatered, treated, transported, and disposed of properly.

2.2.2 Natural Attenuation

Natural attenuation or natural recovery uses the environment's own processes to remediate contaminated sediment. The four main processes involved in natural attenuation are physical isolation (accomplished by natural sedimentation), chemical transformation (via biological degradation), reduction of bioavailability and mobility (by sorption onto media), and dispersion of sediments (diluting the contaminated sediments) (Conder, et al. 2009). Of the four processes, physical isolation is one of the most important in separating contaminants from the benthic organisms that populate the surficial sediments. Without isolation, benthos will continue to uptake contaminants through physical contact, thus initiating their contaminant mobility. Biological degradation is often not important due to the refractory nature of many sediment contaminants. Sorption related reduction in bioavailability and mobility is also important but may not be permanent. Dispersion as dilution is generally not considered a satisfactory remedial approach.

Natural attenuation may also be enhanced by accelerating any of the above mentioned critical processes involved. For example, a thin sand layer could be placed on top of an area with contaminated sediment to mimic and speed up the sedimentation process (Conder, et al. 2009).

2.2.1 Capping

Sediment capping is basically the isolation of contaminated sediment with a clean layer of material, to physically and chemically isolate the contaminated sediment from the water column, while simultaneously providing a clean habitat for benthic organisms. A thin layer (<15-30 cm) might be considered enhanced natural recovery in that it effectively adds many years of natural sedimentation as indicated above. A thicker layer or a layer with more sorptive capacity (an active cap) may also be placed to more effectively contain and confine the contaminants. Both primary functions of a sediment cap aim to reduce the transfer of contaminants to the food chain, where they can bioaccumulate and biomagnify in higher order organisms. In-situ caps on impacted sediments are sometimes deployed with an underlying geotextile used to stabilize the cap along with an overlying armoring cap to protect against scouring of the cap (see Figure 1).

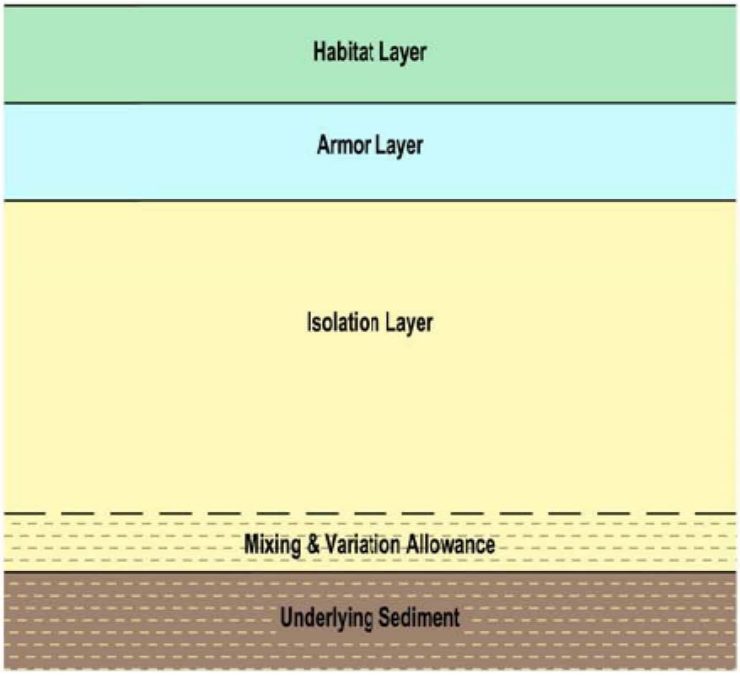

Figure 1: General Sediment Cap Profile (Madalinski 2008)

Capping can be used in conjunction with other remedial techniques and is used frequently to control surficial sediment contamination at environmental dredging sites, where an increase in contaminant concentration levels is common during and for a short time following the dredging. In-situ sediment caps can largely be classified into two kinds of caps: passive and active.

"Passive" Capping

Passive capping usually refers to the placement of inert sand that is typically placed on top of contaminated sediment at a thickness greater than 30 cm. The term passive is associated with these caps because they are inert and provide minimal sorption capacity (McDonough, et al. 2007). The supplemental sand primarily serves as a barrier

to increase the distance between contaminated sediment and the overlying water column, as well as augment the time for natural recovery processes to take place. However, thick caps do little to reduce contaminant's bioavailability considering they have little to no sequestration capabilities due to sand's generally low carbon content. The issue of sand's low sequestration capacity can be addressed by amending the cap with organophilic materials such as coke or activated carbon. All thick caps however, reduce the effective height, or depth of the water column, which can decrease the functionality of the aquatic environment (e.g. shipping waterway or recreational uses). The placement of thick caps can also amplify the issue of consolidation that all capping projects must contend with. When a load is placed on sediment, the underlying sediment will consolidate, decreasing the pore volume of said sediment, thereby expelling contaminated porewater from the sediment to surrounding areas, including the water column.

In-situ containment of contaminated sediment physically separates contaminants from benthic receptors and reduces the flux of contaminants to the water column. Sand provides excellent protection when contaminants are strongly sorbed to the solid phase and when there is an absence of avenues for rapid contaminant migration (Reible, et al. 2006). Under some conditions, however, such as in environments containing high rates of groundwater-surface water exchange, achievement of the desired reductions in flux may require the use of a layer that can sequester or degrade contaminants, rather than simply contain them.

"Active" Capping

Although approximately 100 sediment caps have been deployed in varying environments at contaminated sediment sites in the United States, the vast majority of those have consisted of thick passive sand caps (McDonough, et al. 2007). As of 2007,

fewer than 10 active caps (thin caps or caps amended with sorbents) have been deployed at sites (see Table 1).

Table 1: Current and Future Active Capping Projects (McDonough, et al. 2007)

Cap type	Contaminant or Purpose	Location
Apatite/sand AquaBlock/sand Coke/sand	Sequester heavy metals Hydraulic control Sequester PCBs and PAHs	Anacostia River, Washington, DC
AquaBlock	Evaluate installation techniques	Ottawa River, OH
AquaBlock	Evaluate installation techniques	Fort Richardson, AK
Activated Carbon-RCM[a]	Sequester PAHs	Stryker Bay, Duluth, MN
Organoclay-bulk and in RCM	Contain creosote NAPL	Portland, OR
Sand/topsoil-30 cm Granular bentonite Sand/soil/bentonite slurry Aquablock	Contain PCBs	Grasse River, Massena, NY (Alcoa, 2003)

[a] Planned but not yet installed.

As stated above, the addition of a sorbent layer or sorbent amendments to a cap will prolong contaminant isolation by sequestering contaminants and retarding their transport from the sediment into the bioactive benthic zone (McDonough, et al. 2007). Using sorbents as active capping material isolates contaminants under, or within the cap, to allow for degradation to occur naturally and also increases the cap lifetime by slowing contaminant breakthrough. Apatite, coke, activated carbon, organoclay, and Aqua Block® (a permeability control agent) have all been considered as materials in active caps.

The selection of an active capping material is highly dependent on the site characteristics in which the cap will be deployed. The physical/chemical conditions and

processes at the site along with the feasible approaches that might provide additional control of exposure and/or risk, must all be taken into consideration, not to mention the contaminant of concern plaguing a site (Reible, et al. 2006). Phosphate based materials, such as phytates and apatites, have been shown to effectively stabilize select metals. However, they have simultaneously demonstrated a lack of sorption of organic compounds. Coke on the other hand, which is a byproduct of coal production and readily available at low cost, exhibits an affinity for organic compounds that is comparable to that of sediment with moderate carbon content (Reible, et al. 2006). Activated carbon has exhibited sorption capacities 100-1000 times greater than that of typical sediment. Although it's widely known that fine-grained materials such as clays can be used to provide permeability control, organically modified clays can also sorb dissolved organic contaminants in addition to contain non-aqueous phase liquids (NAPLs) (Galjour Dufreche 2008). Aqua Block®, another clay based material used in active capping applications, acts as a low permeability barrier at the sediment-water column interface, works to reduce the flux of contaminants out of the contaminated layer. Aqua Block® consists of a granular core, which aids in settling, that is covered with a bentonite clay material that swells when exposed to water.

As shown above in Figure 1, caps are typically layered on top of problem sediments in bulk and are often accompanied by sand armoring. Active caps can also be deployed as geotextile mats, which contain active sorbent material, sandwiched between two geotextiles, or interwoven within its matrix. When deployed in this manner, caps are unfurled, much like a roll of carpet, at the bottom of the water column (sediment-water column interface), usually with the aid of machinery and an experienced diver (see Figure 2). This method of active capping deployment ensures nearly uniform coverage of affected areas and also guarantees complete employment of the active material.

Figure 2: Geotextile Mat Placement at Salaberry-de-Valleyfield, Quebec, Canada & the Comtrac Delaware River Project (Honeywell, Tecsult 2006)

2.3 ORGANOCLAYS

As mentioned above, natural clays have established themselves as economical low permeability barriers in the environment. Their high specific surface (surface area to mass ratio), which provides a greater probability for interparticle forces to develop, coupled with their natural negative surface charge produces clay's high affinity towards water molecules (Conduto 1999). Along with its low permeability, these physical properties have made clay almost the automatic choice when seeking an economically favorable and effective barrier in an aquatic environment. Clays have been also used successfully as liners in landfills and secondary containment systems and have even been shown to sequester toxic chemicals and pathogens (Pernyeszi, et al. 2006). However, these barriers have often failed when contacted with organic fluids or petroleum products. Organic fluids compromise clay's natural barriers by reducing their electrical double layer and severely diminishing its plasticity, resulting in an increase in hydraulic conductivity (Lo and Yang 2001).

Organoclay is merely clay that has been treated to exhibit organophilic rather than hydrophilic tendencies. When manufacturing organoclay, inorganic cations (usually sodium and calcium) that reside on the surface of natural clays, are replaced by cationic surfactants (Aqua Technologies of Wyoming Inc. n.d.). In the case of bentonite and zeolite this cation exchange attaches quaternary amines to the surface of the clay. Quaternary amines consist of a positively charged "head" (NR_4^+) with organophilic/hydrophobic carbon chains attached to it. When exchanged onto bentonite or zeolite, NR_4^+ attaches to the negatively charged surface of the clay leaving the organophilic/hydrophobic carbon chains protruding off the clay surface (see Figure 3). It is these carbon chains that alter the surface properties of clay from being organophobic and hydrophilic to organophilic and hydrophobic. The capacity of clay to substitute its inorganic cations for other cations is called its cationic exchange capacity or CEC. Amine generated organoclays can usually be classified as either short chain/adsorptive organoclays or long chain/organophilic organoclays (Groisman, et al. 2004).

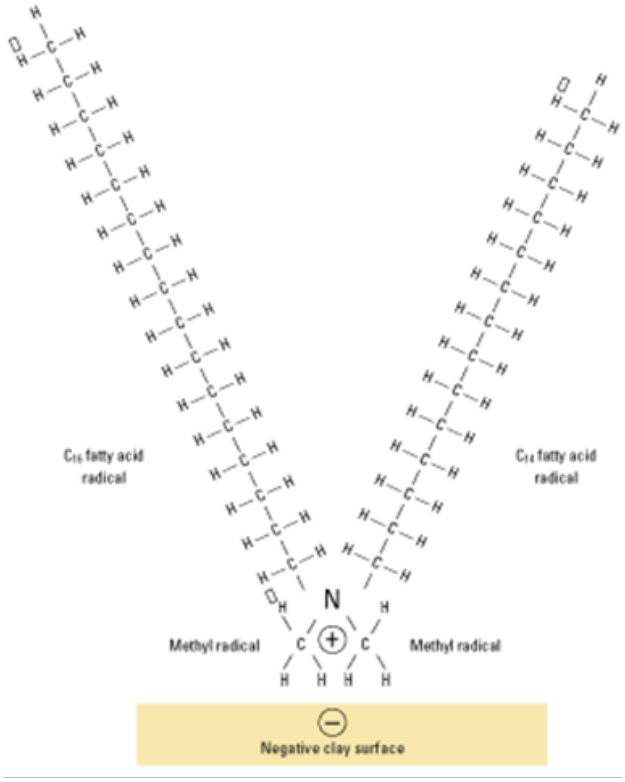

Figure 3: Example of an amine attaching to the surface of a clay, rendering it an organoclay (Moretti 2008)

Short chain organoclays are effective at sorbing low molecular weight non-ionic organic compounds, while long chain organoclays are better sorbents of high molecular weight, strongly hydrophobic compounds (Groisman, et al. 2004). Short chained organoclays exhibit site specific sorption, which is typically modeled with the Langmuir Isotherm (Groisman, et al. 2004).

$$C_{is} = \frac{\Gamma_{max} K_{iL} C_{iw}}{1 + K_{iL} C_{iw}}$$

This type of isotherm is typically used when sorbents possess a finite number of sorption sites. With the Langmuir Isotherm, sorption sites are filled asymptotically as they

approach the maximum sorption capacity ($\Gamma_{\max}$), the point when all specific sorption sites are filled.

Long chain/organophilic organoclays, on the other hand, are commonly characterized by linear isotherms. These organoclays are produced with amines that have carbon chains 10 to 20 carbons long, which behave similar to surfactants (Groisman, et al. 2004). Surfactants (or surface acting agents) act by lowering the surface tension of liquids, enabling greater interaction between fluids. Surfactants are usually amphiphilic, meaning their structure consists of both a hydrophobic and hydrophilic portions (Mulligan, Yong and Gibbs 2001). It is this hydrophobic portion, which consists of long-chained amines that allow organophilic compounds to approach the surface of treated clays and eventually sorb onto them.

As organic sorption occurs, organoclays tend to swell (Lo and Yang 2001) in a manner similar to that of conventional clays when exposed to water. Swelling in organoclays is caused by intercalation, the inclusion of organic compounds into the molecular structure of organoclay. This swelling in turn leads to a decrease in permeability. In a study conducted by Lo and Yang, it was found that permeability of a bentonite organoclay modified with dodecyldimethylammonium bromide (DDDMA, $C_{22}H_{48}BrN$) decreased by two orders of magnitude after exposure to gasoline. This decrease in permeability, brought about by the sorption of organics, can be desired when using organoclay as a liner in landfills to prevent leachate release. However when used as a subaqueous cap, this loss of permeability may have negative impacts. A decrease in permeability could potentially isolate any organoclay beyond the organoclay/organic fluid interface inhibiting further sorption of free-phase organics (NAPL). This change in permeability would also affect the underlying flow regime, altering groundwater flow paths and thereby increasing the probability of contaminant exposure.

Although organoclay is proving useful as an innovative sorbent of both separate and dissolved phase contaminants, the problems raised by decreased permeabilities are serious ones that should be evaluated.

2.4 ACTIVATED CARBON

Much like clay has solidified its niche in permeability management of hydraulic systems, so too has activated carbon become synonymous with filtration and purification of both gases and liquids. Activated carbon had been used in gas purification, gold purification, metal extraction, water purification, medicinal applications, sewage treatment, gas masks, filters for compressed air and many other applications. The chief physical property that characterizes activated carbon and makes it effective as a sorbent is its extensive pore structure, which gives it a considerable amount of surface area for its size. According to IUPAC (International Union of Pure and Applied Chemistry), pores in activated carbon can be classified depending on their pore width as micro- (< 0.2 nm), meso- (> 0.2 nm but < 50 nm), or macropores (>50 nm) (Bandosz 2006) (see Figure 4).

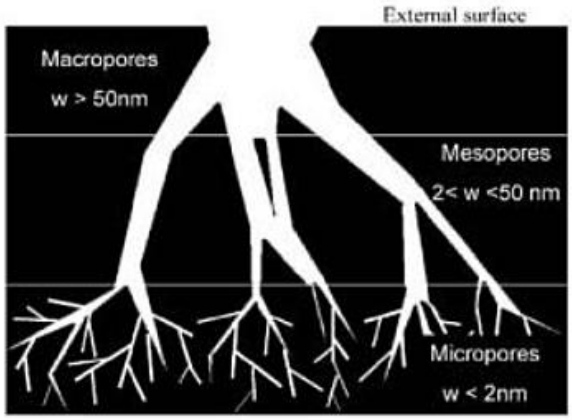

Figure 4: Activated Carbon Pore Structure (Bandosz 2006)

The relatively high specific surface of activated carbon is mainly due to the contribution of micropores in their structure, which coincidently is the location where the majority of adsorption takes place. Micropores can account up to 90-95% of the total surface area of an activated carbon (Bandosz 2006). However, the specific surface area of a carbon is not necessarily proportional to the adsorption capacity of an activated carbon, due to the possibility of molecular sieve effects brought on upon by the pore structure itself. Pore structure therefore is a determining factor in the selection of an activated carbon for a particular application. In general, activated carbons with a high percentage of micropores are desired for the adsorption of vapors and gases, while meso- and macroporous activated carbons are preferred for the adsorption of solutes in the liquid phase (Bandosz 2006). In both processes, molecules or atoms are fixed onto the surface of activated carbon by physical interactions (Van der Waals and London dispersive forces) and/or chemical bonds; hence the importance of an extensive surface area in this sorbent. The selectivity and the amount of a compound that an activated carbon will chemosorb are controlled by the functional groups present on the surface of the carbon. The two principle effects that functional groups can inflict on activated carbons are modifications in a carbon's hydrophobic/hydrophilic nature and the manipulation of their acidic or basic character. Carbons are, in general, hydrophobic in nature. However, in the presence of polar oxygen containing surface groups, their hydrophilicity increases since water molecules can form hydrogen bonds with the oxygen atoms on the carbon surface (Bandosz 2006). These molecules could then in turn form new hydrogen bonds with other surrounding water molecules (see Figure 5). This is important in determining the wetability of a carbon and therefore the degree of impregnation a surface may achieve from a solute in the bulk solution (Bandosz 2006).

A summary of factors influencing the amount of sorption onto activated carbon can be seen in Table 2.

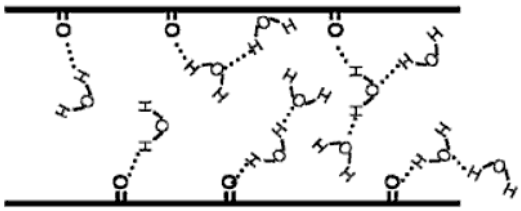

Figure 5: Example of polar oxygen containing surface groups increasing the hydrophilicity of a carbon surface (Bandosz 2006)

Table 2: Factors Influencing the Extent of Adsorption (Bandosz 2006)

	Property	Influence
Adsorbent	Specific surface area	Adsorptive capacity generally increases with S_{BET}
	Pore size distribution	Pore diameters control which sizes of molecules are accessible to them. - micropores (< 2 nm): for microorganics, pesticides - mesopores (2 – 50 nm): for higher molecular weight compounds like dyes, humic substances
	Surface chemistry	Affects the adsorption process through the presence of surface functional groups (aromatics, trihalomethanes) and pH of point of zero charge (acidic or basic compounds)
Adsorbate	Solubility	The lower the affinity between adsorbate and solvent (low solubility, nonpolar), the stronger the adsorption capacity
	Size	The molecular weight and size of the adsorbate affect the adsorptive capacity, related to the pore size distribution of the activated carbon
	Substituent groups	Introduction of substituent groups on phenol results in increased adsorbability in the following order [51]: $-OCH_3 > -CH_3 > -Cl > -NO_2$
Solvent	pH	Very important effect when the adsorbing species is ionized (weak acid and basic species)
	Inorganic salts	Inorganic salts ($CaCl_2$, NaCl) can enhance adsorption of ionized species [52] or humic acids [53]
	Temperature	Due to the exothermic character of adsorption, an increase in temperature generally results in a decrease in adsorption

A variety of adsorption isotherm equations have been used by researchers to model the adsorptive behavior of activated carbon, including those that resemble Henry's Law, the Freundlich, Langmuir, Redlich-Peterson, and Brunauer-Emmett-Teller (BET) equations (see Figure 6 for their typical shapes). These diverse groups of models have all been used to describe sorption onto activated carbon, because each is limited in terms of their applicability to specific systems or to specific concentration ranges (see Table 3). However in studies conducted by Walters and Luthy, where the sorption of 11 PAHs onto activated carbon was evaluated, it was found that the Langmuir Isotherm was the most versatile in describing the sorptive behavior for the PAHs studied.

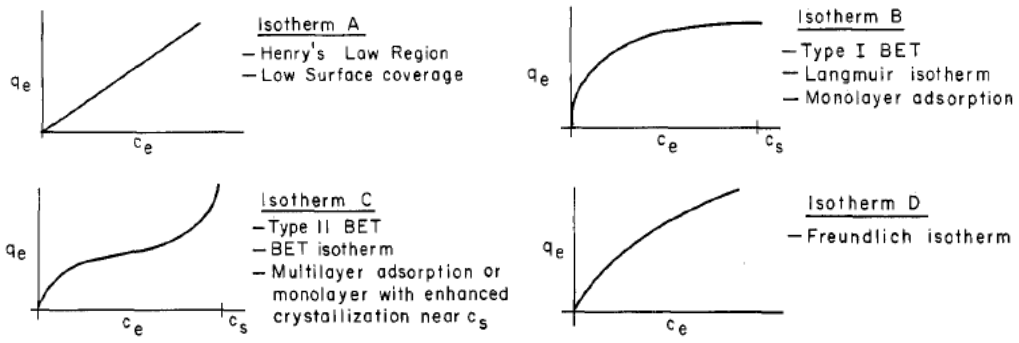

Figure 6: Typical Shapes of Adsorption Isotherm Curves (Walters and Luthy 1984)

Table 3: Adsorption Isotherm Equations (Walters and Luthy 1984)

name	equation[a]	linear form	capacity term	comments
Henry's law	$q_e = K_h C_e$	$q_e = K_h C_e$	K_h, (mg/g)/(mg/L)	limited to low C_e and/or low surface coverage
Langmuir	$q_e = (bq^0 C_e)/(1 + bC_e)$	$C_e/q_e = (1/q^0)C_e + 1/(bq^0)$	q^0 (high C_e), mg/g	describes maximum monolayer capacity
		$1/q_e = [1/(bq^0)](1/C_e) + 1/q^0$	bq^0 (low C_e), (mg/g)/(mg/L)	reduces to Henry's law
BET	$q_e = (Bq^0 C_e)/[(C_s - C_e)[1 + (B - 1)(C_e/C_s)]]$	$C_e/[q_e(C_s - C_e)] = [(B - 1)/(Bq^0)](C_e/C_s) + 1/(Bq^0)$	q^0 (high C_e), mg/g	describes multilayer adsorption
			Bq^0/C_s (low C_e), (mg/g)/(mg/L)	
Freundlich	$q_e = K_f C_e^{1/n}$	$\log (q_e) = (1/n) \log (C_e) + \log (K_f)$	K_f, (mg/g)/(mg/L)$^{1/n}$	empirical
Redlich–Peterson	$1/q_e = 1/(K_{lr} C_e) + 1/(K_{lr} C_e^m)$	nonlinear	K_{lr} (high C_e), (mg/g)/(mg/L)^m	empirical; reduces to Henry's law, Freundlich, or Langmuir under appropriate conditions
			K_{lr} (low C_e), (mg/g)/(mg/L)	

[a]The following are the variables: equilibrium capacity, q_e (mg/g); equilibium concentration, C_e (mg/L); saturation (solubility) concentration, C_s (mg/L).

Activated carbon has been used by mankind since the days of antiquity, and it is impossible to determine its first use. Its precursor in ancient times was either wood char or coal char, and it was employed in the construction of bronze by both Egyptians and Sumerians as early as 3450 BC. Its use in the treatment of water was first recommended in 400 BC by Hippocrates as a method to combat odor and taste problems. Activated carbon, as it is known today, was not discovered until the late 1880's by R. von Ostrejko. Its development and production, though, did not boom until the First World War, where it was used by the Allies to treat water and for the removal of harmful vapors in gas masks.

Activated carbon originates as any carbonaceous based material with an isotropic structure, which means almost any carbonaceous material can be converted into activated carbon. Common source materials for activated carbon include wood, fruit stones, peat, lignan, coals, petroleum coke, and nut shells. A carbon is "activated" by heat treating the original material with medium to high heat to remove solids within its structure, thereby creating pores space within the existing structure and consequently increasing its specific surface.

Activated carbon traditionally has been classified into two categories based on particle size: powdered activated carbon (PAC) and granular activated carbon (GAC).

GAC particles are defined by ASTM as those particles retained by an 80-mesh sieve and those finer as PAC. Because of their physical size discrepancies, their usage is also different. For example, PAC is often directly added to well mix systems due to the high head loss they incur in flow through systems, while GAC is more often packed in columns.

Both PAC and GAC, however, have been shown to experience premature breakthrough in the field when compared to lab studies conducted with DI water. Fouling of field applied activated carbon is often blamed on the presence of dissolved organic matter (DOM) under field conditions. Activated carbon's highly sorptive behavior is its own demise when placed in an environment where DOM is present. The same mechanisms that attract and trap hydrophobic organic contaminants (HOCs) also, attract DOM, which then occupy surface area on the activated carbon that would otherwise be taken up by HOCs. Another issue with using activated carbon in the environment is its propensity to foul in the presence of separate phase contaminants. Although activated carbon exhibits the most sorption of HOCs of any media currently used, its capacity is significantly reduced when contaminants are in the separate phase rather than the dissolved phase. This underperformance is due to clogging of pore space by free-phase liquid, which leaves valuable surface area underutilized.

Chapter 3: Methodology

Column studies were conducted to evaluate the effectiveness of several active capping geotextiles manufactured by Huesker, Inc., under simulated groundwater upwelling conditions. Test methods for measuring water content, nonvolatile hydrocarbon content, and PAH solid concentrations were used to assess the performance of passive and active caps at the McCormick & Baxter Superfund Site.

3.1 McCormick & Baxter Analysis

3.1.1 Water Content and Dry Weight Percentage

In order to evaluate the nonvolatile hydrocarbon content and PAH solid concentration of a sediment sample, its dry density or moisture content must first be determined. To do this, 2 g of sample were placed in a pre-weighted aluminum dish, where M_{i0} is the weight of the dish and M_{i1} is the weight of the dish plus the sample. The sample was then dried in an oven for 24 hours at 105°C to remove any water contained within the sample. After 24 hours the sample was allowed to equilibrate with the ambient temperature in a desiccator and reweighed, M_{i2}. Having recorded these weights, the water content and dry weight percentage of a sample can be calculated as follows:

$$Water\ Content, \omega\ (\%) = \frac{M_{i1} - M_{i2}}{M_{i2} - M_{i0}} * 100\%$$

$$Dry\ Weight\ (\%) = \frac{M_{i2} - M_{i0}}{M_{i1} - M_{i0}} * 100\%$$

3.1.2 Hexane Extractable Material

The hexane extractible test (EPA Method 9071B) can be used to infer the fraction of NAPL or other mobile organic material in sediment. The method used was a modified version of the EPA's method titled n-Hexane Extractable Material for Sludge, Sediment, and Solid Samples (Method 9071B). The hexane extractable material from a sample concists of non-volatile hydrocarbons, vegetable oils, animal fats, waxes, soaps, greases, biological lipids, and related materials. This process is conducted through Soxhlet extraction, in which an extraction solvent is cycled through a solid sample contained within a thimble for an extended period of time. As seen in Figure 7, clean extraction solvent (hexane) is continuously mixed with the sample in the thimble by constantly being evaporated and condensed.

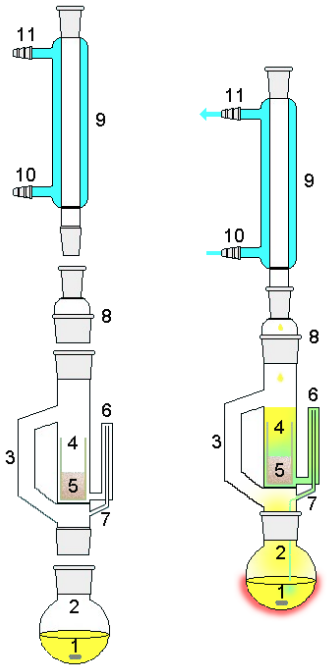

Figure 7: Soxhlet Extractor Apparatus and Setup

1: Stirrer bar **2:** Still pot **3:** Distillation path **4:** Thimble **5:** Solid **6:** Siphon top **7:** Siphon exit **8:** Expansion adapter **9:** Condenser **10:** Cooling water in **11:** Cooling water out
(http://upload.wikimedia.org/wikipedia/commons/3/30/Soxhlet_extractor.png)

The solvent, which is heated and evaporated in a separate chamber underneath the sample, is allowed to rise in the gas phase, only to be condensed in chamber above the thimble. Once condensed, the solvent accumulates in the chamber with the sample, until a siphon is created, thereby transferring the solvent into the chamber where it was being heated. In the process, the solvent extracts organic materials from the matrix of the sample, into the dissolved phase of the solvent, also allowing them to be transferred and ultimately collected in the solvent heating/evaporating chamber. The hexane extractable materials collect in the heating chamber and do not evaporate due to their higher boiling temperatures than hexane.

The Hexane Extractable Material (HEM) of a sample was determined as follows. Samples collected from segmented cores were first homogenized to determine the average HEM in the sampled section of the core. Once homogenized, 8 g of sample were added to a pre-weighed porcelain mortar bowl (sample weight = M_s) and blended with approximately 18 g of anhydrous sodium sulfate (granular, Fisher Scientific) using a porcelain pedestal to dehydrate the sample. This mixture was then placed in a 25 mm diameter, 100 mm long Whatman Cellulose Extraction Thimble, which was in turn placed in a Pyrex® Soxhlet tube. Approximately 90 mL of n-hexanes (Fisher Scientific, Reagent grade) was then poured into a 500 mL round bottom flask containing three to four PTFE boiling chips. The 500 mL flask was attached to the Soxhlet tube containing the extraction thimble, which was also connected to the condenser using a connection tube. The entire extraction apparatus (boiling flask, Soxhlet tube, and condenser) was placed within a hood where it was set on top of a heating plate set at medium-high heat (see Figure 8). Within the hood, the condenser was connected to a cold water source and drain using flexible plastic tubing.

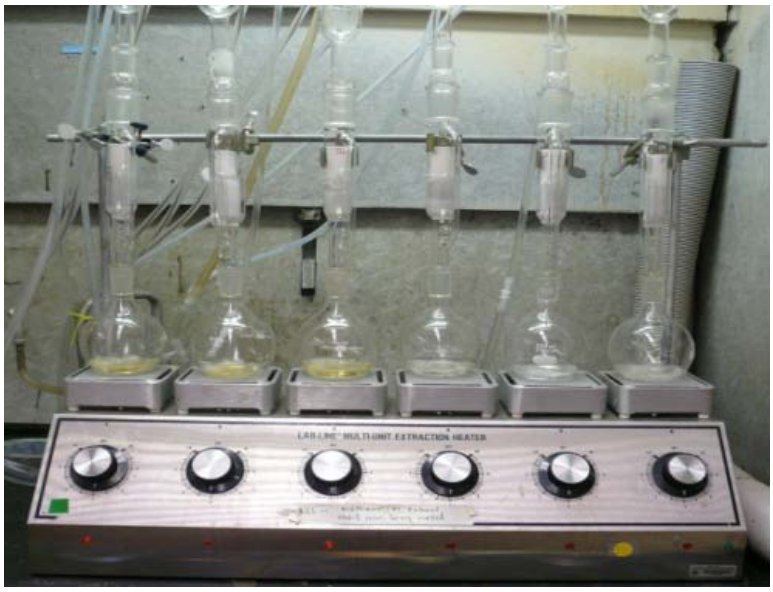

Figure 8: Soxhlet Apparatus

The heat plate temperature was adjusted so that the hexane would cycle through the system at a rate of 12 cycles per hour for 12 hours. As the hexane boiled within the 500 mL flask, its vapor would rise and condense into the Soxhlet tube collecting slowly until enough hexane would amass that a siphon would be created, flushing the hexane and the dissolved extracted materials into the boiling flask. This would continue, eventually reaching the point where the extraction liquid in the Soxhlet tube would turn clear, as opposed to the yellowish color the extract takes on at the onset of the test. After the 12 hours have expired, the heating plate would be turned off and the solvent was allowed to cool. The HEM was then transferred to a pre-weighed 250 mL boiling flask (M_{f0}), rinsing the 500 mL round bottom flask with 3 mL of hexane three times, so as to ensure that all the extract is transferred. The 250 mL boiling flask is then connected to a rotary evaporator and placed in a water bath set at 70° C so as to remove the excess hexane from the extract. Once the hexane was completely evaporated, the boiling flask

was capped with a glass stopper and placed in a desiccator to cool to room temperature. The boiling flask solely containing the HEM was then re-weighted (M_{f1}), allowing for the calculation of the percentage of HEM in a dry sample (the ratio of the HEM weight to the dry sample weight). The percentage of HEM in a dry sample is calculated as follows:

$$Dry\ HEM\ \% = \frac{M_{f1} - M_{f0}}{M_s * \%\ Dry\ Weight}$$

If one's goal is to analyze the PAH solid concentration of sediments, a Soxhlet extraction is necessary in order to harvest the organic material on the solids, and analytical inferences must be removed to facilitate sample analysis. Sample cleanup can be accomplished by using a silica gel column and a series of solvent exchanges. Samples could then be analyzed with High-Performance Liquid Chromatography (HPLC) for a variety of PAHs. Using this technique, a PAH solid concentration profile can be generated from composite samples taken from a sediment core.

3.1.3 Silica Gel Cleanup

Chemical analysis of the HEM required a sample cleanup step. The HEM was concentrated to a volume of 1 mL using a blow-down apparatus (Labconco Rapidvap N_2 Evaporation System) set at 70° C. 6 mL of cyclohexane (Fisher Scientific, Certified A.C.S.) was then added to the blow-down glassware, wetting residual extract on the walls of the glassware, and blowing down the solvents again to 2 mL.

The extract was then cleansed of interferences using the EPA Silica Gel Cleanup procedure (Method 3630C). 7 g of silica gel that was activated by heating to 105°C for 16 hours, and was then packed into a 25 mL burette with a stopcock which served as a column. To minimize the amount of fugitive activated silica gel during the cleanup

process, a small amount of glass wool was placed at the bottom of the column. The glass wool was cleaned prior to its placement in the column by soaking it in dichloromethane (DCM) (EM Science, HPLC Grade) and removing excess DCM. When pouring the activated silica gel into the burette, the stopcock was closed to prevent the loss of any media. The column stand was then tapped to tightly pack the media, which aids in expediting the cleanup process. Once tightly packed, the stopcock was opened and DCM was slowly poured into the burette, saturating the silica.

Once the entire column was saturated with DCM, a 2 cm cap of activated anhydrous sodium sulfate was placed on top of the activated silica gel. The anhydrous sodium sulfate was activated by heating it for 4 hours in a 550°C muffle furnace. The column was then eluted with 40 mL of pentane (Fisher Scientific, Certified) which was wasted. Right as the last of the 40 mL of pentane was about to expose the top of the sodium sulfate to air, 2 mL of HEM in cyclohexane was introduced into the column. Complete transfer was assured by rinsing out the blow down glass with 2 mL of cyclohexane and eluting the rinse through the silica gel column as well.

As the last of the cyclohexane was about to expose the media to the air, 25 mL of pentane was eluted though the column and discarded, followed by a 25 mL solvent mixture of DCM and pentane at a 2:3 v/v ratio. Once the solvent mixture was introduced to the column, a pre-weighed 40 mL vial was used to capture elutriate. 2 mL of elutriate was then transferred to a pre-weighed 5 mL centrifuge vial, weighing both vials afterward. The 2 mL in the centrifuge vial was blown down to 0.1 mL.

The second solvent exchange was then performed by adding 3 mL of acetonitrile (ACN) (Fisher Scientific, HPLC Grade) to the centrifuge vial, blowing down to 2 mL and then weighing the sample one final time.

3.1.4 HPLC Analysis of 14 PAHs

Once a sample had been treated with the cleanup procedure to remove interferences, samples were analyzed using HPLC according to the EPA's Polynuclear Aromatic Hydrocarbon procedure (Method 8310) for a variety of PAHs of varying hydrophobicity. An ACN blank and a procedure control were also analyzed for quality control purposes. Samples were analyzed for the following PAHs using HPLC:

Naphthalene	Benz[a]anthracene
Fluorene	Benzo[b]fluoranthene
Acenaphthene	Benzo[k]fluoranthene
Phenanthrene	Benzo[a]pyrene
Fluoranthene	Dibenz[a,h]anthracene
Pyrene	Benzo[ghi]perylene
Chrysene	Indeno[1,2,3,-cd]pyrene

The PAHs listed above increase in hydrophobicity, with naphthalene and indeno[1,2,3,-cd]pyrene being the least and most hydrophobic PAHs, respectively investigated. Due to analytical limitations, the chromatograms of benzo[ghi]perylene and indeno[1,2,3,-cd]pyrene were unable to be properly separated and were analyzed jointly in an effort to maximize data yield from samples. The HPLC used in these studies was a Waters 2795 Series HPLC that was equipped with a Waters 996 Photodiode Array Detector and a Waters 2475 Multi-Wavelength Fluorescence Detector. The Photodiode Array Detector was used to identify compounds qualitatively using their ultraviolet adsorption at 254 nm as a general indicator, which was then associated to their retention time in the HPLC column to indicate the chemical species. The Fluorescence Detector was used to quantify compounds once their time specific retention times were identified. The column utilized in the HPLC was a Luna C18(2), 250 x 4.6 mm column warmed to 40°C. HPLC Grade Acetonitrile (Fisher Scientific) and Millipore Water were used as the

carrier solvents for samples which were mixed at a 70% to 30% ratio. 25 µL of sample were introduced into the column which operated at a 1.0 mL/min and were allowed to run for 45 min/sample. During the 45 min in which a sample was analyzed, three timed events were programmed into the Fluorescence Detector to maximize compound's responses. The duration, excitation and emission wavelengths (Futona 1981), Energy Units Full Scale (EUFS), and Gain used during each timed event of the analysis can be seen in Table 4.

Table 4: 14 PAH HPLC Timed Events

Event Criteria	Event 1	Event 2	Event 3
Time (min)	0-11	11-21	21-45
Excitation Wavelenth (nm)	280	305	305
Emission Wavelenght (nm)	340	430	430
Energy Units Full Scale (EUFS)	1000	1000	10000
Gain	1	1	1
PAHs Eluted In Each Event	Naphthalene, Acenaphthalene, Fluorene, Phenanthrene	Fluoranthene, Pyrene, Chrysene, Benz[a]	Benzo[b], Benzo[k], Benzo[a], Dibenz[a,h], Benzo[ghi], Indeno[1,2,3]

Peaks on chromatogram's produced by samples were integrated using Waters Millennium 32 Software (Version 3.05.01). From these results, the bulk concentration of a PAH on a sample was calculated as follows:

$$PAH\ Bulk\ Concentration\ (\frac{mg}{kg}) = \frac{Area * RSF * Sample\ Vol.\ in\ ACN * \frac{Total\ Elute\ Mass}{Mass\ of\ Elute\ in\ 5\ mL\ Vial}}{\frac{Sediment\ Sample\ Mass}{1+\omega} * 1000}$$

3.2 HUESKER GEOTEXTILE ANALYSIS

3.2.1 Column Test Setup

Dynamic testing with dissolved phase contaminants was conducted to evaluate the effectiveness of two active capping geotextiles manufactured by Huesker, Inc., one was a proprietary mat capable of sorbing both dissolved and NAPL components and the other was a mat containing activated carbon (Filtermat). Continuous flow column studies were designed to reproduce conditions that were analogous to sediment capping, in which the cap was exposed to sediment contaminated with high molecular weight hydrophobic compounds in an area experiencing high rates of groundwater-surface water exchange via groundwater upwelling. Significant groundwater upwelling will quickly compromise a conventional sand cap and thus active caps are often considered for this situation. Several PAHs of varying hydrophobicity were used in these experiments as the high molecular weight contaminants.

Several columns were set up to mock field conditions in which the performance of both the complete geotextile and active material within the geotextile could be evaluated. The vast majority of the columns' volumes were filled by glass beads, where the material of interest was placed near the top of the column, coinciding with the location of the column's effluent port. The columns were saturated with water before being introduced to water with dissolved contaminants. Samples from the column effluent as well as the reservoirs used as influent were periodically taken and analyzed with HPLC. Measuring concentration of the column's effluent as a function of time allows one to determine the contaminant capacity of the geotextiles and their active materials, as well as develop mathematical models that can predict the effectiveness and the functional life of the geotextiles.

In all, five columns were set up: two testing Huesker's NAPL mat that's designed to absorb separate phase, oily contaminants, as well as dissolved contaminants; two testing the active material (activated carbon) in Huesker's Filtermat 200; and one column testing an intact sample of the Filtermat 200 geotextile. The Huesker Filtermat 200 geotextile is impregnated with 200 g/m^2 of powdered activated carbon derived from coconut shells.

The columns containing the two replicates were 15 cm long, 2.5 cm diameter glass columns (Kontes) with diffusing caps to ensure uniform solution introduction into the column. An additional thin layer of glass wool was also added at the influent port of the column to further ensure the prevention of short circuiting within the column. The majority of these column's volumes were occupied with 3 mm diameter glass beads which served as approximately 14 cm of inert filler in the columns. Thin layers of glass wool were placed on top of the glass beads, followed by the active cap material, which was then proceeded by another thin layer of class wool. The rest of the column volume was then filled with approximately 2-3 layers of 3 mm glass beads (see Figure 9).

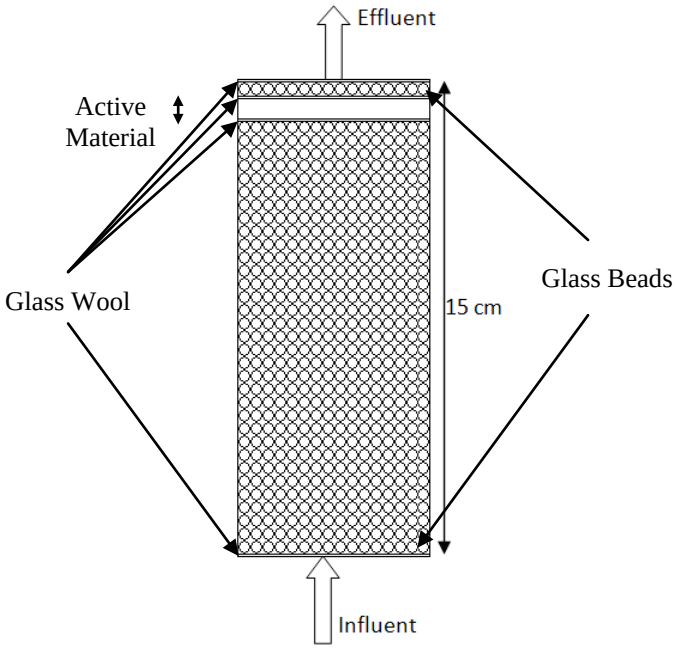

Figure 9: Column setup for 15 cm long columns

The fifth column, which contained the intact Filtermat 200 sample, was prepared using a 7.62 cm diameter, 3.5 cm flange style column. The excess volume in this column which was not taken up by the geotextile was occupied by 3 mm glass beads and a 7.62 cm diameter porous stone. A cross-section of this column can be seen in Figure 10.

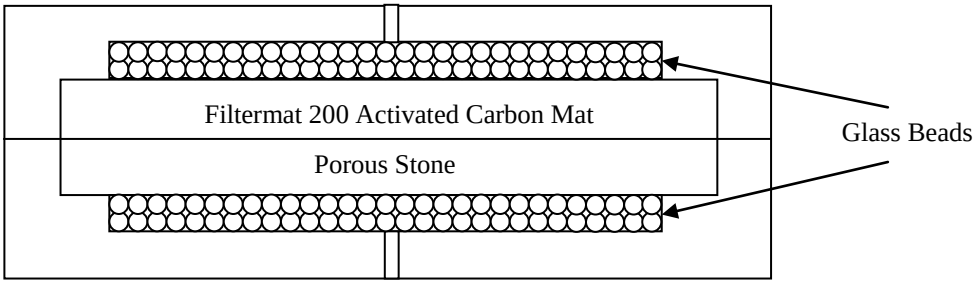

Figure 10: Column setup for 7.62 cm dia., 3.5 cm long column

To minimize losses due to unwanted sorption onto tubing walls, Teflon tubing was used as the influent supply and effluent return lines. Columns were connected to one of either of two 2 L influent reservoirs that were continuously mixed. Each reservoir contained naphthalene, phenanthrene, and pyrene at their respective saturation concentrations, which were produced by maintaining pure contaminant solids in the influent reservoir. Other measures that were taken to prevent losses in the system included covering the reservoirs with aluminum foil (to reduce photodegradation) and adding sodium azide, NaN_3 (Fisher Scientific, Laboratory Grade), at a 0.1 M concentration in order to combat bio-degradation and biological uptake.

One influent reservoir held approximately 2 L of deionized (DI) water, while the second influent reservoir contained water from a fresh water lake (LW), to evaluate the effects of natural organic carbon (NOM) on the active materials. All columns were setup to cycle water from their reservoir, through the column, and back to the reservoir. PAH crystals were periodically added to both reservoirs to maintain a constant concentration (every 10 days for the DI water reservoir and 7 days for the lake water reservoir).

An eight channel peristaltic pump (Cole Parmer, Istamec Model CP 78002-10, Head CP 78002-50), in conjunction with three-stop, black/black 0.76 mm inner diameter tubing (Cole Parmer), provided flow to all five columns at rate of 0.38 mL/min. This translated into a superficial (Darcy) velocity of 102 cm/day in the 15 cm long columns, and 11 cm/day in the 3.5 cm long column. Table 5 contains a summary of the columns experimental names and their corresponding properties, and Figure 11 and Figure 12 exhibit the experimental setup.

Table 5: Column Studies Experimental Setup and Properties Summary

Column	Length (cm)	Diameter (cm)	Water Matrix	Active Material in Column	Flow Rate (mL/min)	Darcy Velocity (cm/day)
NM1	15.0	2.54	DI	NAPL Mat	0.38	102
NM2	15.0	2.54	LW	NAPL Mat	0.38	102
ACB1	15.0	2.54	DI	1 cm of Bulk AC (2.7 g)	0.38	102
ACB2	15.0	2.54	LW	1 cm of Bulk AC (2.5 g)	0.38	102
ACMS	3.5	7.62	LW	Filtermat 200 (0.91 g of AC)	0.38	11

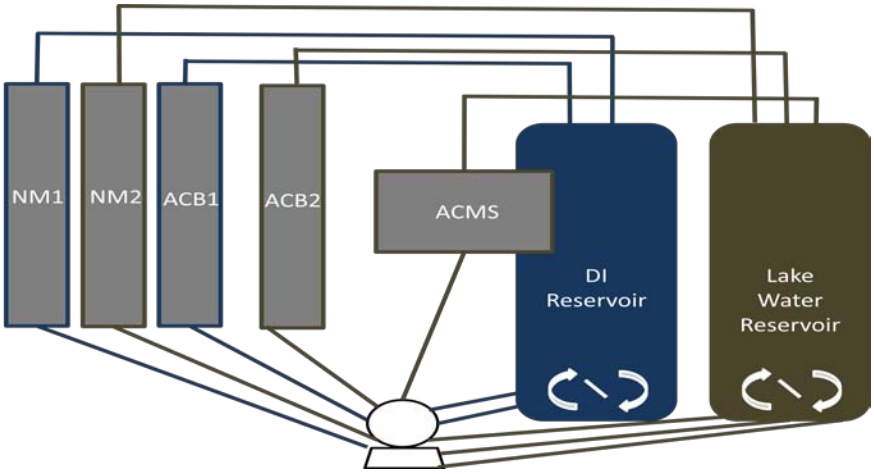

Figure 11: Column Studies Theoretical Experimental Setup

Figure 12: Column Studies Actual Experimental Setup

3.2.2 Column Sampling

As can be seen in Figure 12, the effluent lines (and in columns ACB1 and ACMS the influent lines) from the columns were spliced and had a valve inserted to facilitate sampling. Sampling of the column's influent and effluent initially took place approximately every 3 days, and for the majority of the experiment involved diluting samples for analysis. Dilution was accomplished gravimetrically by weighing either 100 µL (for AC columns) or 180 µL (for NM columns and influent samples) of ACN in pre-weighed 2 mL vials with 200 µL HPLC vial inserts plus caps with septum's before sampling. Sampling was conducted with a 100 µL glass syringe (Hamilton Co., Gastight #1710), by drawing the desired volume (100 µL for AC columns and 20 µL for NM column samples) directly from the effluent lines, and injecting samples directly into the insert contained within the vial. The influent samples were taken from the reservoirs and were first subjected to filtering with a 0.45 µL PTFT syringe filter (VMR) due to the presence of PAH solids contained within the reservoirs. 20 µL of filtrate was then injected into the pre-weighed vials with ACN. The glass syringe was wiped down and rinsed out three times with ACN after every sample was taken to prevent cross contamination during sampling. Samples were then re-weighed and analyzed immediately with HPLC, along with an ACN blank which was used to dilute the samples and a set of PAH standards that contained naphthalene, phenanthrene, and pyrene at 500, 20, and 20 ppb. Samples were analyzed with the same HPLC used for the McCormick & Baxter PAH analysis. However, run times and wavelengths were optimized for these analyses. Samples were analyzed for 8 min and were introduced into the column with an 85% to 15% acetonitrile-water solution. The event characteristics for these tests can be seen in Table 6.

Table 6: HPLC Timed Events for Huesker Columns

Event Criteria	Event 1	Event 2	Event 3
Time (min)	0.0-5.3	5.30-6.50	6.50-8.0
Excitation Wavelenth (nm)	250	244	295
Emission Wavelenght (nm)	340	360	390
Energy Units Full Scale (EUFS)	10000	10000	10000
Gain	1	1	1
PAHs Eluted In Each Event	Naphthalene	Phenanthrene	Pyrene

3.2.3 Tracer Tests

Prior to the commencement of the column studies, a tracer test was conducted on the 15 cm long, 2.54 diameter columns, to determine the hydraulic characteristics of the columns. A 0.1 M NaBr solution was used as the inert tracer in these studies, in which a Cole Parmer bromide probe compatible with a pH/ISE meter was used to measure concentration as a function of time. Prior to conducting the tracer test, the probe was calibrated with solutions of known bromide concentrations. The NaBr solution was introduced to the columns, which were pre-saturated with DI water, at 0.38 mL/min. Bromide concentration measurements in the effluent were taken every 15 min initially, but the sampling interval was reduced to 2.5 min as breakthrough was occurring. Ionic strength adjustment of the effluent was necessary for accurate measurement with the probe and was accomplished by introducing 2 mL of a 5 M $NaNO_3$ for every 100 mL of sample. The tracer effluent concentrations were interpreted to determine several characteristics of the columns such as void volume, interstitial velocity, porosity, and dispersivity.

3.2.4 Batch Sorption Tests

Static batch tests evaluating the potential sorption capacity of free phase contaminants were conducted for both of Huesker's sorbent geotextile mats. Their NAPL Mats are composed of a layer of proprietary sorbent material with filtering layers on both sites; whereas Huesker's Filtermat 200 contains activated carbon at a loading of 200g/m^2 as the mat's active material. The permeable sorbent material in the NAPL Mat consisted of high loft foam that's expected to retain its permeable nature during sorption of free phase liquids, allowing for complete utilization of the mat's capacity.

In these tests, bulk non aqueous phase liquid (NAPL) was slowly added to samples of the geotextiles of known weight, in a pre-weighed glass jar until free NAPL could no longer be absorbed by the media. Once the sorptive mat was saturated, the excess NAPL was decanted from the jar and the saturated sample was reweighed in the jar. The sorbent geotextile mats of interest were exposed to Soltrol – 130 (Chevron Phillips Chemical Company), a light mineral oil dyed with Sudan IV (Sigma Aldrich, Certified). Soltrol was chosen as a representative NAPL due to its comparable sorbing characteristics shared with creosote and manufactured gas plant (MGP) NAPLs.

Chapter 4: McCormick & Baxter Site Description

The McCormick & Baxter Superfund site is located in Portland, OR, just north of downtown Portland, on the northeastern banks of the Willamette River near river mile 7. The site, which spans 41 acres on land and an additional 23 of sediments, lies within the much larger Portland Harbor Superfund Site. The McCormick & Baxter Creosoting Co. operated from 1941 to 1991 as a wood treatment facility, were it would weatherize railroad cross ties and utility and telephone poles using coal-based creosote, pentachlorophenol (PCP), and inorganic preservative solutions containing arsenic, copper chromium, and zinc. From 1945 to 1969, cooling water, wastewater, and other process wastes were disposed of directly in the Willamette River. Other waste streams from storm water, boiler water, and oily wastes were maintained in several above ground disposal tanks onsite until 1971. These disposal tanks ranged in size from 70,000 to 173,000 gallons and were located on the southwestern portion of the site, adjacent to the Willamette River. Also located near this tank farm area was a 750,000 gallon creosote tank. This tank sustained two documented leaks in its life, with one such event releasing over 50,000 gallons of creosote into the environment. In general, there are three major source areas at the site: the Former Waste Disposal Area (FWDA), the central process area, and the Tank Farm Area (TFA).

Investigation of these areas in 1990 by the Oregon Department of Environmental Quality (ORDEQ) revealed substantial levels of PAHs, heavy metals, and PCP in the soil, sediment, and water at the site. Contamination at the site reached depths of 80 ft below grade in soil, which migrated and in turn led to the contamination of sediments as far as 35 ft below the sediment-water interface. This study also concluded that the TFA was a primary source of NAPL contamination in the Willamette River.

This study by the ORDEQ, along with a subsequent expedition in 1992, led to the site being listed by the EPA on its National Priorities List on June of 1994. ORDEQ was designated by the EPA as the lead agency for selection and implementation of the remedy at the site, while the EPA agreed to handle funding and construction at the site. Immediate measures that were taken at the site from 1992 to 1994 by ORDEQ included the demolition of the creosoting plant and the removal of any solids and sludge from the site. These actions were merely precursors to the more involved remedies for the groundwater, soil, and sediments at the site. A site plan for the facility can be seen in Figure 13.

Remedial actions for the creosote contaminated aquifer at the McCormick & Baxter Site began in 1994, where groundwater from the site was pumped and treated with an automated system. However this system only lasted for six years and was terminated in 2000 due to poor product recovery and high operating costs. Manual pumping of the groundwater was determined as a better option and commenced shortly thereafter. Pumping activities at the site have cumulatively yielded approximately 6,300 gallons of creosote since 1989. In order to protect against the further spread of creosote which could not be recovered at the site, a sheet-pile/soil-bentonite slurry barrier wall was constructed to isolate 18 acres at the site.

The soil remedy at the McCormick & Baxter Site consisted of removal and capping of compromised soil. The goal of remedial activities was to eliminate the potential for human contact with contaminants in the soil above predetermined removal action levels. As a result, 4 ft of soil was excavated and disposed of offsite due to the presence of arsenic, PCP, and PAHs. Excavation began in 1999 and since then, over 36,000 tons of soil and debris have been removed and disposed of in landfills. At the same time over 33,000 tons of clean sand have been imported to the site from an offsite

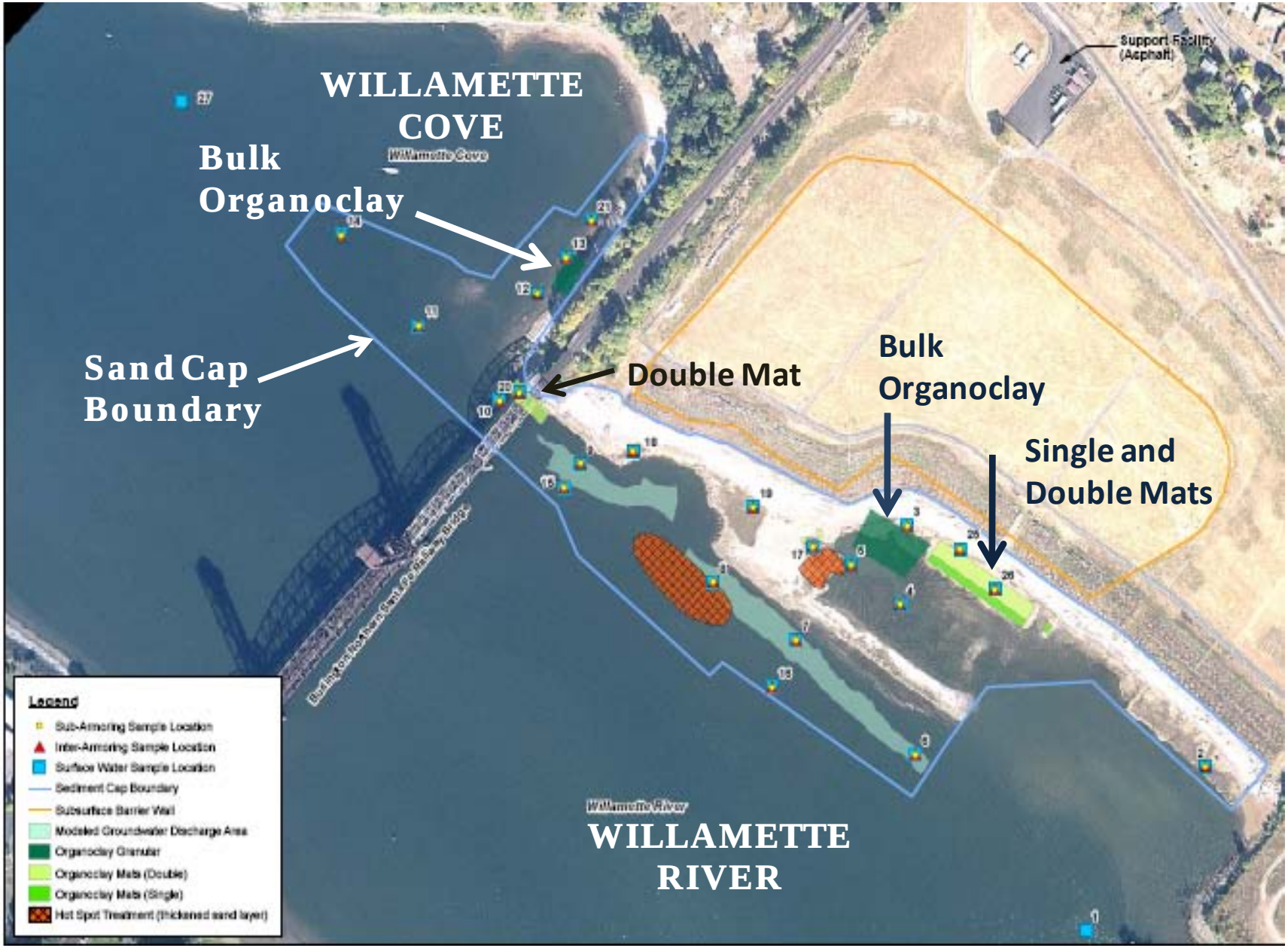

Figure 13: McCormick & Baxter Superfund Site

quarry and used as backfill. Capping of the soil was primarily used for the 14.7 acre area bounded by the subsurface sheet-pile barrier wall, where elevated concentration levels above action levels persisted.

Capping was also used to remediate contaminated sediments at the site. Current sediment remedial actions at the site were implemented in 2004/2005, when both passive and active caps were deployed at the site. Sediments were capped that exhibited contaminant concentrations above human health and ecological risk-based protective levels and/or exhibited significant toxicity to benthic organisms. The caps themselves were covered with a variety of armoring materials in order to protect against an assortment of destructive forces that would compromise the cap's integrity. During implementation of the cap, approximately 1,600 pilings, dock remnants, in-water debris, and an abandoned barge in Willamette Cove were removed. The banks of the Willamette River and Cove at the site were also re-graded and 23 acres of sediment were capped using a multilayer cap consisting of sand, organoclay, and armoring. While the vast majority of the capped area was covered with a 3 ft thick passive sand cap and protective riprap (5 ft thick cap in areas of elevated concentration), organoclay, both in bulk and in geotextile mats, was deployed in areas of known NAPL migration. Theses NAPL seeps predominately were located in Willamette Cove and in the TFA in the Willamette River. Over 600 tons of bulk ET-1 Aqua Technology Organoclay was deployed at these locations at a thickness of 1 ft, in order to prevent NAPL release into the water column. In 2005, a total of 24,350 ft^2 of organoclay mats were deployed at the site at three locations. These mats were deployed on the shore line of the Willamette River, under the Burlington Northern Railroad Bridge, and at two areas in the TFA near a seep. Armoring of all the sediment caps was simultaneously deployed to protect the integrity of the caps. The armoring material selected for the caps was dependent on expected hydraulic and

physical environment (i.e. current, wave, erosive, and impeller energies) to which they would be exposed. For example, articulated concrete blocks were installed on the shores and shallow areas of the site, where erosive forces would be their greatest.

Since the completion of deployment activities in 2005, the sediment caps at the site have been evaluated for their continued effectiveness and available sorptive capacity annually. In the first round of evaluation studies conducted in 2006, the baseline sorptive capacities were determined for fresh ET-1 Organoclay installed at the site and the remaining capacity of the organoclay caps. A subsequent sampling event took place in August 2007, in which a number of cores were taken from several locations, along with a 2 ft^2 segment of the organoclay mat, and analyzed for their continued effectiveness. Samples collected at both times showed little or no movement of NAPL into the organoclay cap and that the organoclay retained its full NAPL sorptive capacity. The individual sorption of contaminants by the organoclay was not evaluated in this round of analysis.

Core samples containing sand, sediment, and organoclay were collected in August 2008 and subjected to tests evaluating their HEM to indicate the presence of NAPL, and select hexane extracts were subjected to PAH component analysis to examine migration of specific contaminants. Separate analyses were also conducted of the interstitial water in the sediments and capping materials but are not presented here.

Chapter 5: Results

5.1 HUESKER MAT ASSESSMENT

A series of column studies were conducted on active capping geotextile mats manufactured by Huesker, Inc., to assess the mat's performance under groundwater upwelling conditions. The objective of these tests was three fold:

- determine the breakthrough times for several PAHs of varying hydrophobicity,
- compare the performance of the different mats to estimates found in literature, and
- predict the performance of the capping materials under varying conditions.

The studies were conducted with water from a fresh water lake source, and carbon free DI water to assess the impacts of matrix affects on the media. These studies were also setup to stimulate upwelling at two velocities. The velocities selected for the tests were chosen to accelerate the breakthrough time of the various media and are not representative of upwelling velocities which would be observed in the field.

In addition to the dynamic tests conducted with the dissolved phase contaminants, the free phase sorption potential of Huesker's sorbent geotextile mats were evaluated in static batch equilibrium studies.

5.1.1 NAPL Sorption Capacity Batch Tests

Static batch equilibrium studies were designed to evaluate the NAPL sorption capacity in Huesker's geotextile mats. In these tests, Soltrol – 130 was slowly added until free NAPL could no longer be absorbed by the media. Table 7 contains results for the batch sorption tests conducted on three Huesker geotextile mats, along with results from similar tests conducted on PM 199 CETCO Organoclay. Two of the Huesker Mats

tested were composed of the same proprietary, sorptive material, with the only difference being the entrained air in the active material in one of the mats which made it more voluminous. Since this voluminous, or high loft, NAPL Mat was composed of the same sorbent material as the other sorptive NAPL mat provided by Huesker, it could be assumed that the sorptive mats would behave similarly.

Table 7: Sorption Capacity of Varying Sorbent Materials using Soltrol-130 as a Representative NAPL

Sorbent Material	Mat Loading of Sorbent Material (g/cm^2)	NAPL Capacity by Weight (g/g)	NAPL Capacity by Area (g/cm^2)
Organoclay CETCO PM 199 (≈ 1 cm thickness)	0.4	1.82 (0.14)	0.73
Activated carbon	0.2 (CETCO)	0.37 (0.02)	0.074
	0.02 (Single layer)		0.007
Original NAPL Mat (0.2 cm thickness)	0.044 (0.0004)	2.60 (0.25)	0.11
High Loft NAPL Mat (1 cm thickness)	0.072 (0.006)	10.5 (0.78)	0.76

Estimates based upon unconsolidated materials (NAPL mat subject to consolidation under load)
CETCO mat loadings based upon 0.8 lb/ft^2 organoclay or 0.4 lb/ft^2 activated carbon
Parenthesesed values represent the Std. Dev. in replicate measurements

As can be seen in the above table, the NAPL mats exhibited have a very high capacity for sorption of NAPL per unit mass of the mat material. The capacity of the voluminous, high loft NAPL mat was equivalent approximately to that of a typical organoclay mat loaded at 0.8 lb/ft^2 (0.4 g/cm^2). Another notable result of the test was the low NAPL sorptive capacity exhibited by the activated carbon, which was expected. NAPL is known to normally foul activated carbon and interfere with its ability to absorb dissolved contaminants. However, the high unit mass sorptive capacity of the NAPL

mats is somewhat offset by the low density of the material. When the sorptive capacity of the high loft NAPL mat is presented in a unit area basis, it's revealed that the mat has a similar capacity (0.76 g/cm^2) as CETCO PM 199 Organoclay (0.73 g/cm^2).

5.1.2 Tracer Studies

Before sorption tests commenced, tracer studies were conducted to determine the physical and hydraulic characteristics of the columns such as void volume, porosity, and hydraulic residence time and dispersivity (see Table 8). Figure 14 shows the results of the tracer tests for the 15 cm long columns in which a conservative bromide tracer was used along with advection-dispersion model outputs, which simulated the data and estimated the columns' dispersivity. The model was fit to the tracer test data by using the least squares method.

Table 8: Column Properties

Column	Void Volume (mL)	Porosity (-)	Hydraulic Residence Time (min)	Model Fit (R^2)
NM1	37.35	0.48	103.75	0.982
NM2	42.75	0.55	118.75	0.999
ACB1	41.40	0.54	115.00	0.996
ACB2	36.45	0.47	101.25	0.986
ACMS*	77.85	0.49	216.25	-

*Tracer test was not conducted for ACMS column prior to tests

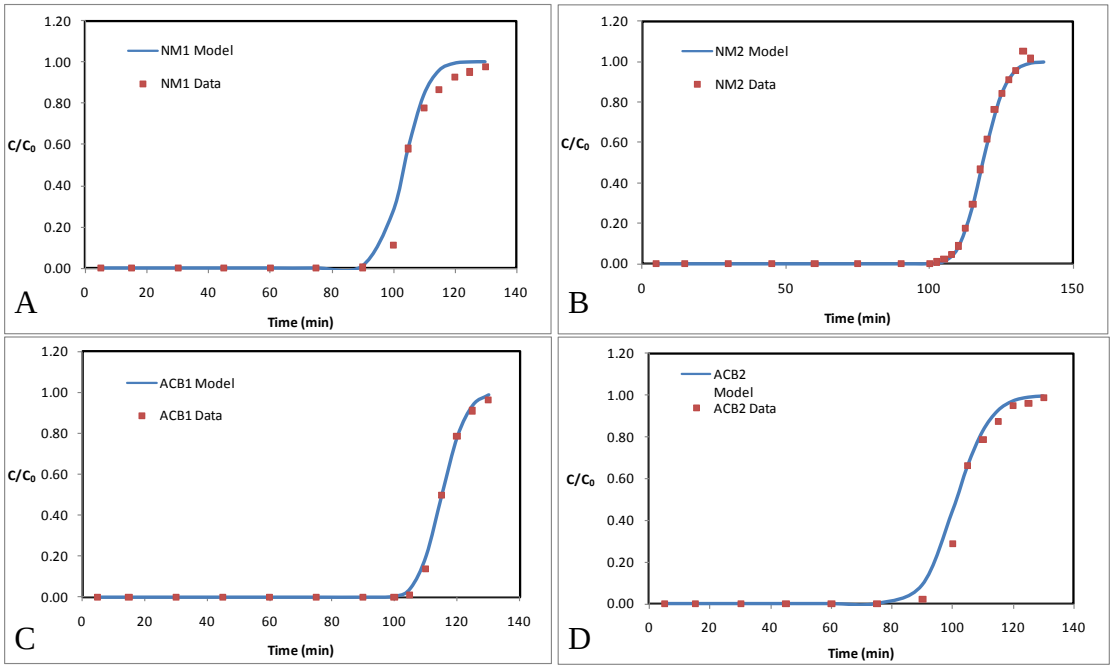

Figure 14: Tracer Tests and Models
(A) NM1; (B) NM2; (C) ACB1; (D) ACB2

An advection-dispersion model with appropriate boundry and initial conditions was used to fit the tracer data as well as model the life of the active materials. The model was programmed into Microsoft Excel by David Lambert, and is of the following form (see Appendix A term definitions):

$$\frac{C}{C_0} = 0.5\left\{e^{\left[\left(\frac{Pe}{2}-u\right)\zeta\right]}erfc\left[\frac{1}{2\tau^{0.5}}(\zeta - 2u\tau)\right] + e^{\left[\left(\frac{Pe}{2}+u\right)\zeta\right]}erfc\left[\frac{1}{2\tau^{0.5}}(\zeta + 2u\tau)\right]\right\}$$

(Van Genuchten 1981)

In order to generate a breakthrough curve for the capping materials, effluent concentrations taken throughout the life of the experiment (identified as concentration C), were normalized by the average influent concentrations (identified as concentration C_0).

5.1.3 NAPL Mat Column Studies

Although the primary focus of the column studies was on Huesker's Filtermat 200 geotextile, two columns were also set up to observe PAH sorption in their NAPL mats. Figure 15 shows normalized effluent concentrations for naphthalene, phenanthrene and pyrene. C_0, for these column studies, was defined by the maximum in the effluent concentrations as shown in Figure 15. C_0 was defined in this manner in order to generate a better fit to the advection-dispersion model, especially for naphthalene. Similar charts pertaining to naphthalene as those shown in Figure 15, with the exception that data was normalized by the steady state concentrations achieved by the columns, can be seen in Appendix B. The initial portions of the breakthrough curves were fit to models to determine sorption capacity of the active material. Despite the use of pure solid contaminants in the influent reservoir, slow dissolution rates, sorption and other losses caused the effluent concentration to remain below saturation and was widely scattered after initial breakthrough of the contaminant. Decreases and variations in the influent concentration (despite the use of pure solid contaminant to attempt to maintain a constant concentration) were also mirrored in the effluent. The experiments were continued in an effort to resolve the cause of both the variations and the relatively low effluent concentrations (see Appendix C & Appendix D) but this was not accomplished.

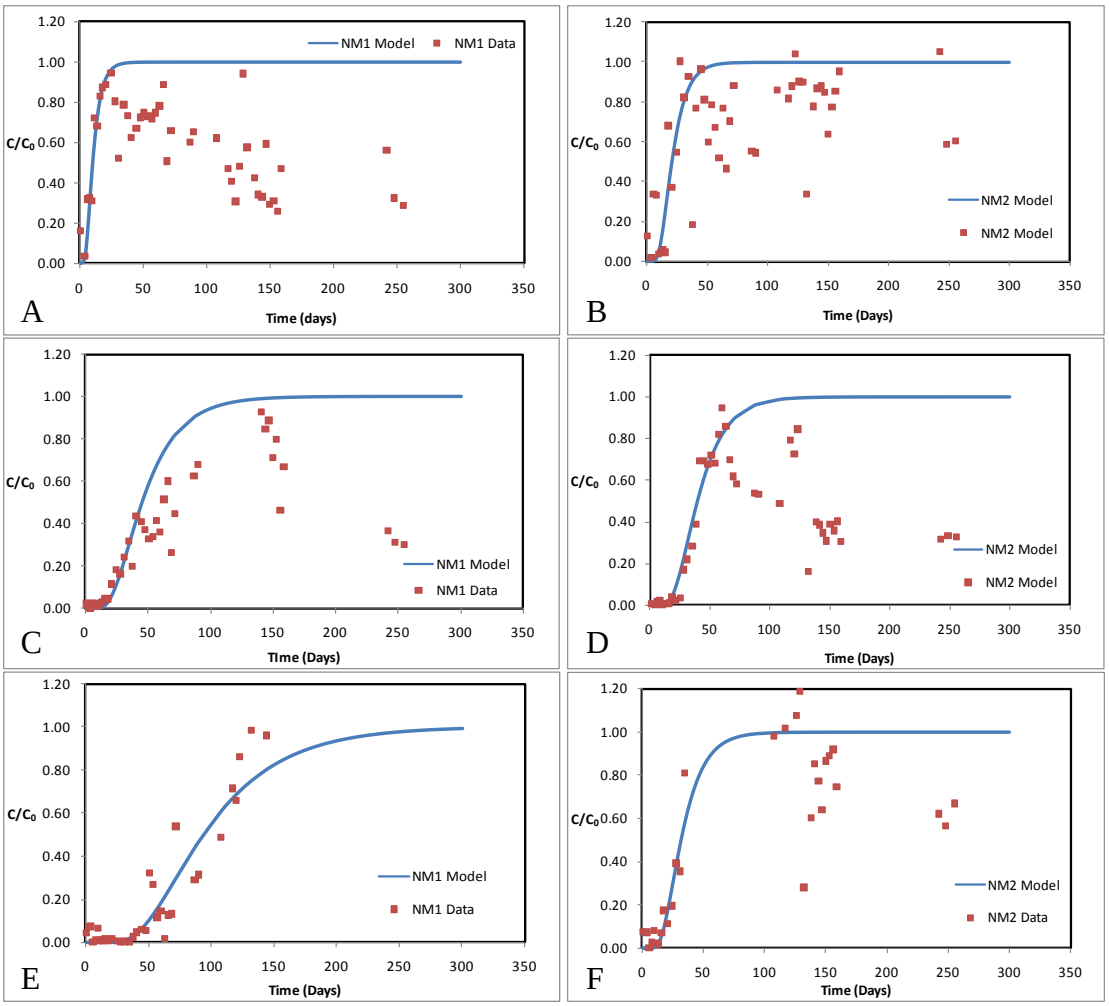

Figure 15: Column Data and Models for Huesker's NAPL Sorbent Mat
(A) NM1 Naphthalene in DI Water; (B) NM2 Naphthalene in Lake Water;
(C) NM1 Phenanthrene in DI Water; (D) NM2 Phenanthrene in Lake Water;
(E) NM1 Pyrene in DI Water; (F) NM2 Pyrene in Lake Water

Also shown in these figures are the model predictions generated by using the one-dimensional advection-diffusion model above. These models were fit to the data using the hydraulic characteristics of the columns determined from the inert tracer test and the least squares method to optimize the one remaining fitting parameter, which was the partitioning coefficient of the active material, K_d. The partitioning coefficient for

dissolved contaminants is the ratio of the concentration of a contaminant on a solid or sorbent material, over the concentration of a contaminant in a liquid or aqueous phase.

$$K_d = \frac{C_S}{C_{aq}}$$

Table 9 contains a summary of the partitioning coefficients of the NAPL mat for the three PAHs, as well as the residuals squared as a measure of the accuracy of the models to predict the data (r^2).

Table 9: Huesker NAPL Mat Partitioning Coefficients

Column	Naphthalene		Phenanthrene		Pyrene	
	K_d (L/kg)	R^2	K_d (L/kg)	R^2	K_d (L/kg)	R^2
NM1	28,205	0.90	125,000	0.84	259,488	0.87
NM2	56,367	0.56	107,779	0.96	85,709	0.96

C/C_0 values were multiplied by a factor to obtain a C/C_0 = 1.00 at the maximum concentration

5.1.4 Activated Carbon Column Studies

Two columns containing activated carbon from Huesker's Filtermat 200 and one column containing an intact sample of Filtermat 200 were run simultaneously with the sorbent mats described above. Even though these tests were conducted for over 250 days, this time frame was still not long enough to capture breakthrough for two of the three PAHs studied, phenanthrene and pyrene. Therefore, the remaining discussion in this section only focuses on the sorption of naphthalene onto activated carbon.

As with the NAPL mat columns, the effluent concentrations, even after the achievement of apparent steady state, were not equal to the expected influent concentration. Since the breakthrough percentage of naphthalene remained low after seemly achieving steady state conditions, this could only mean that the measured influent

concentration was not the actual influent concentration being fed to the columns. This was assumed most likely due to sorption onto tubing leading to the columns. Although it would be expected that any losses due to sorption would reduce over time due to the achievement of saturation in the tubing, the Tygon tubing in the peristaltic pumps needed to be changed on a regular basis due to physical wear in the pump, possibly accelerated by a lack of chemical resistance to the PAHs. Thus, new sorption capacity was continuously placed in line.

This hypothesis was tested in the late stages of the experiment, once effective equilibriums had been achieved for naphthalene in all three of the columns containing activated carbon. Influent samples were taken in two locations: at the reservoir as had been done for the majority of the experiment and at a sampling port located downstream of the Tygon peristaltic pump tubing but upstream of the column. It was shown that unfiltered "influent" samples taken at the influent ports exhibited naphthalene influent concentrations 45% and 42% of that measured in the DI and LW reservoirs respectively. This was also the case for phenanthrene, where influent samples taken at the ports were 61% and 69% of the influent samples taken at the reservoir (see Appendix E). Pyrene actually showed higher concentrations in the influent port than in the reservoir, presumably due to solid phase pyrene or sorption onto dissolved/suspended solids in the unfiltered sample. This data suggests significant losses did occur between the reservoir and the column, and that some solids were carried over into the column influent. The presence of these solids could account for the variability noted previously in the effluent concentrations. Due to the uncertainty in the influent concentration, the effluent data from each of the three columns were fit to C/C_{ss} as was done with the NAPL mat columns. C_{ss} was defined as the average effluent concentration after achievement of

apparent steady state and was taken as the average effluent concentration for samples taken between days 153-255 of the studies.

Figure 16A contains C/C_{SS} as a function of time for both bulk activated carbon columns (ACB1 & ACB2), along with a fit to the one-dimensional advection-diffusion model. Figure 16B contains C/C_{SS} results from the ACMS column and its corresponding model. These models were fit to the data using the known hydraulic parameters determined from the inert tracer test (at least for ACB1 & ACB2), as well as the activated carbon's partitioning coefficient (K_d) which was optimized using the least squares method. Since a tracer test was not conducted on the ACMS column, the dispersivity in the column was determined by visually fitting the shape of the naphthalene breakthrough curve.

Figure 17 displays the experimental C/C_{SS} breakthrough curves and models for all three activated carbon columns, while Table 10 contains their naphthalene partitioning coefficients and the square of the residuals as a measure of the predictive accuracy of the models (r^2).

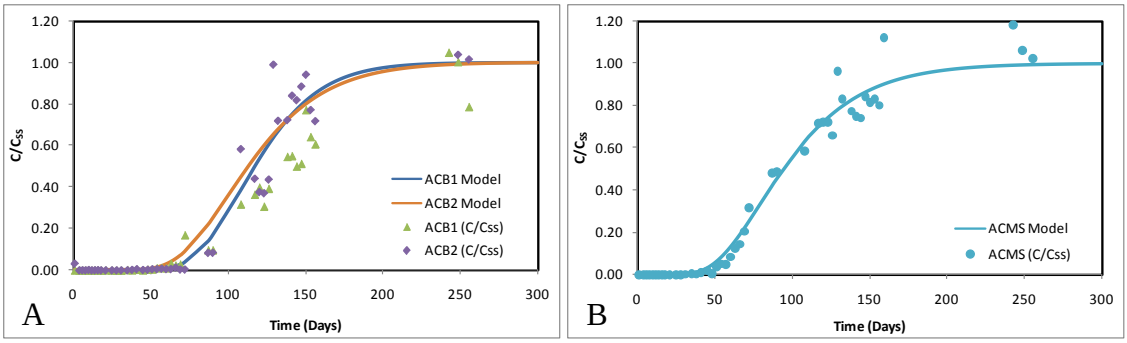

Figure 16: Activated Carbon Naphthalene Breakthrough Data and Models
(A) ACB1 & ACB2 Columns; (B) ACMS Column

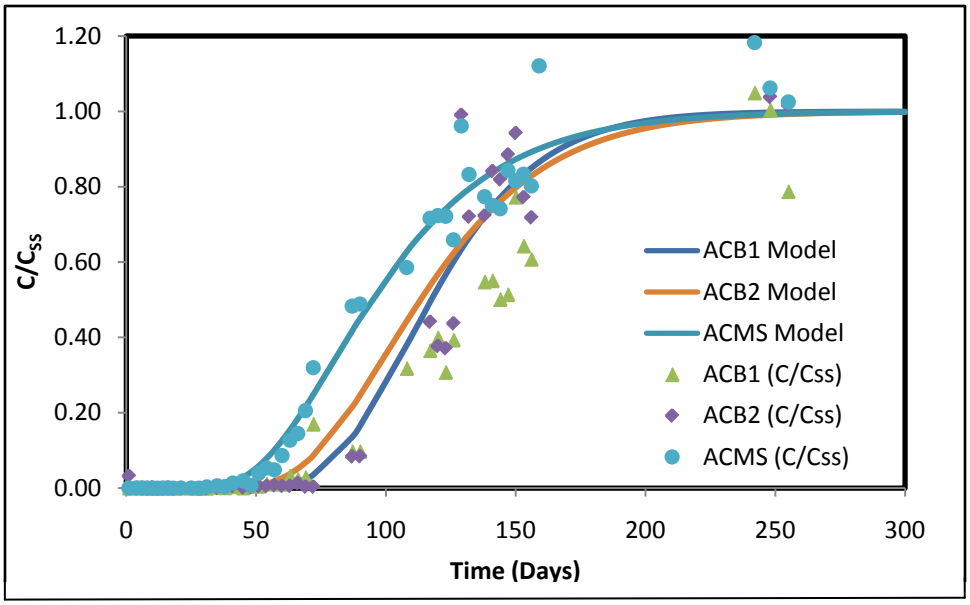

Figure 17: Naphthalene Breakthrough Curves and Models for Columns containing Bulk Activated Carbon (ACB 1&2) and the intact Huesker Filtermat 200 (ACMS)

Table 10: Huesker Activated Carbon Partitioning Coefficients and Model Accuracies

Column	Naphthalene	
	K_d (L/kg)	R^2
ACB1	23,578	0.73
ACB2	24,508	0.92
ACMS	58,357	0.97

Huesker's Filtermat 200 and its active material, activated carbon, showed an expectedly large affinity for sorption of PAH's. More than 35,000 and 64,000 pore volumes of PAH spiked lake water (LW) were passed through the 0.2 cm thick impregnated activated carbon mat and 1.0 cm thick bulk activated carbon cap without witnessing breakthrough for either phenanthrene or pyrene. Depending on the column

configuration, breakthrough of naphthalene ($C/C_{SS} \geq 0.50$) was observed in the effluent of the activated carbon columns after 90 -120 days, which corresponds to 12,000 – 30,000 pore volumes of water.

There seemed to be minimal impact caused by the dissolved organic matter, DOM, in the spike lake water (which contained 8.4 mg C/L) on the activated carbon, as indicated by the results from the two columns containing bulk activated carbon. The breakthrough curves for both of these columns were very similar and nearly collapsed into a single curve. If higher concentrations of DOM were present in the water, the effect would likely be more pronounced.

For a symmetric breakthrough curve, the time until the contaminant achieves 50% of its steady state effluent concentration is directly related to the effective capacity of the sorbent. The sorptive capacity of the activated carbon in the columns, W_s, can be calculated in the following manner:

$$W_s = \frac{C_{in} t_{0.5} Q}{m_{AC}}$$

where C_{in} is the estimated influent naphthalene concentration (mg/L) accounting for sorption losses due to Tygon tubing; $t_{0.5}$ is the time (days) at which the effluent concentration equals 50% of steady state concentration, Q is the volumetric flow into the column (L/day), and m_{AC} is the mass of activated carbon in the column. Since the calculated sorptive capacity is normalized by the mass of activated carbon within each column, all three columns should have theoretically produced the same quantity. However this was not the case, as seen in Table 11.

Table 11: Naphthalene Breakthrough Times and Sorpiton Capacties

Column	C_{in} (mg/L)	$t_{0.5}$ (days)	Q (L/day)	m_{AC} (g)	W_s (mg/g)
ACB1	7.2	120	0.52	2.68	166.39
ACB2	6.8	120	0.52	2.54	166.39
ACMS	6.8	90	0.52	0.91	346.97

The higher naphthalene sorption capacity found in ACMS is likely the result of its increased hydraulic residence time. While the ACB1 and ACB2 columns have hydraulic residence times of 115 min and 101 min, the residence time in the ACMS column was 216 min. This disparity in retention times between the ACMS and the other two columns is due to their varying geometry. ACMS and its 7.62 cm diameter provides approximately 9 times the cross-sectional area than the 2.54 cm diameter ACB1 and ACB2 columns, which translates into slower superficial velocities by that same factor (102 cm/day vs. 11 cm/day). The shorter residence time in the ACB columns apparently led to failure to achieve full equilibrium sorption. Under similar circumstances using F400 Calgon Activated Carbon, models developed by Walters and Luthy (1983) suggested between 546-640 mg/g of naphthalene could be sorbed at concentrations approximately 7.0 mg/L depending on sorption model used. Assuming that the activated carbon in Huesker's Filtermat 200 has similar capacity, one could conclude that the ACB columns achieved approximately 26-30% of their equilibrium sorption capacity and that the ACMS column achieved 54-64% of its equilibrium capacity. Although this could be tested by either batch sorption tests or by column studies at lower flow rates, neither had been performed by the end of this study. For purposes of subsequent simulations, residence times of greater than 500 minutes in the activated carbon (corresponding to a Darcy velocity of 4 cm/day or less with the Huesker activated carbon mat) would be expected to achieve near equilibrium based upon the Walters and Luthy isotherm data.

5.2 McCormick & Baxter Assessment

In August of 2008, sampling was performed at the McCormick & Baxter Superfund Site to determine the continued effectiveness of bulk sand and organoclay (Aqua Technologies ET-I) sediment caps as well as that of laminated organoclay mats also placed at the site (CETCO PM-200). Although the depth of the sand cap at the site was a function of the contamination levels of the underlying sediment, and ranged from 3 to 5 ft throughout the site, the sand cap cores taken during this sampling event were all taken in areas where the sand cap measured 3 ft in thickness. The same consistency in cap thickness at core sampling locations was also found in the organoclay capped areas, but these caps were 1 ft thick at their respective locations. Ten cores were taken from bulk placement locations, and one core was taken from an uncapped area in Willamette Cove. The capped cores primarily came from two locations on the site, the Tank Farm Area (TFA) in the Willamette River, which supplied seven cores, and at the shore line in Willamette Cove (WC), which supplied three cores (see Figure 18 for core locations). A portion of the organoclay mat was also excavated from the pilot test area in the TFA in the Willamette River. This mat, produced by CETCO, was placed in the TFA area to capture any NAPL generated by gas ebullition from the underlying sediments. No mobile NAPL had been noted at this location beyond sheens produced by gas ebullition so the relatively small amount of organoclay in a mat (containing an equivalent cap thickness of 1 cm) was assumed sufficient. Since all cores were taken on either the shore line of the Willamette River or Willamette Cove, all the caps were subjected to tidal conditions and were usually exposed under low tide. See Table 12 for the names and core locations for all the samples taken during this sampling event. See Appendix F for detailed site maps of the McCormick & Baxter site containing exact sampling locations.

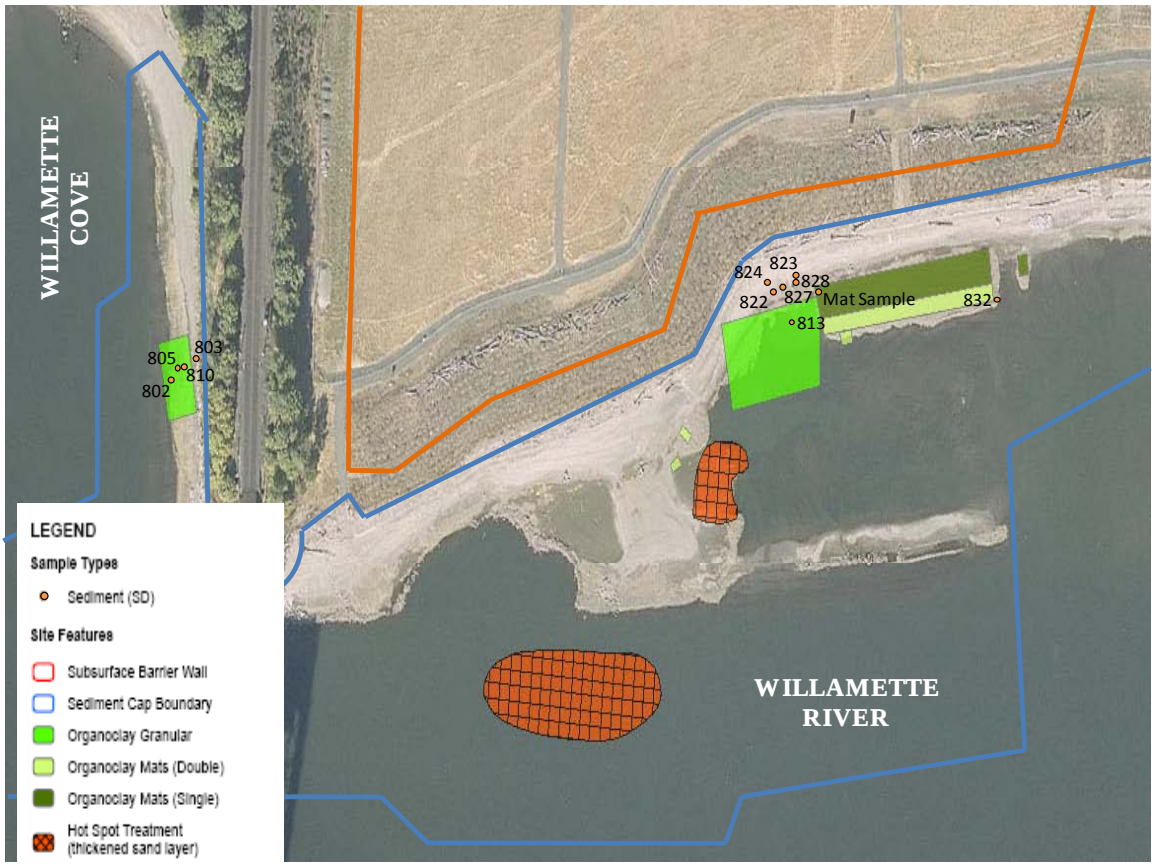

Figure 18: McCormick & Baxter Approximate Sampling Locations

Table 12: Core Name, Location and Capping Media at the McCormick & Baxter Site

Sample	Location	Sediment Cap
MBSDO802	Willamette Cove	Bulk OC
MBSDO803	Willamette Cove	NA*
MBSDO805	Willamette Cove	Bulk OC
MBSDO810	Willamette Cove	Bulk OC
MBSDO813	Willamette River (TFA)	Bulk Sand
MBSDO822	Willamette River (TFA)	Bulk Sand
MBSDO823	Willamette River (TFA)	Bulk Sand
MBSDO824	Willamette River (TFA)	Bulk Sand
MBSDO827	Willamette River (TFA)	Bulk Sand
MBSDO828	Willamette River (TFA)	Bulk Sand
MBSDO832	Willamette River (TFA)	Bulk Sand
CETCO Mat	Willamette River (TFA)	OC Mat

TFA - Tank Farm Area *Not Applicable

Each core was split into 2 to 3 inch segments. However, select samples were segmented to 4 or 6 inches. The organoclay from the mat was harvested and analyzed in bulk form. The samples from these cores and the mat were analyzed for water content and percent of hexane extractable material (% Dry HEM), while only a limited number of these samples were also analyzed for their PAH bulk content.

5.2.1 Results from Sampling at McCormick & Baxter

Before core samples taken in the field were subjected to hexane extraction, a standard was tested to ascertain the recovery the method would produce. A CETCO PM 199 organoclay was saturated with tap water for several hours and spiked with coal tar from a site in Ft. Wayne, IN (provided by Haley and Aldrich, Inc.) such that the organoclay contained 12% DNAPL by weight. The percentage of dry HEM recovered from the organoclay was equal to 79% of the NAPL weight used to spike the sample. Assuming similar recovery would be obtained in field samples, testing was commenced on the cores taken from the site. The % dry HEM results for core samples can be seen on the following page in Table 13.

Field samples showed low, but variable, amounts of % dry HEM. The highest % dry HEM recorded for a sample was 5.98% and was attained in a composite sample that was taken from the organoclay cap in Willamette Cove (WC). However even organoclay samples that were not in contact with the natural sediment and visually free of NAPL exhibited % dry HEM levels that ranged from 2-4%. These low levels of % dry HEM in organoclay samples could be attributed to several factors, including the presence of residual organic materials used during the production of organoclay and the possible sorption of natural dissolved organic matter (DOM) present in water at the site. In cap

evaluation studies conducted at the McCormick & Baxter Superfund Site by Lisa Moretti (2008), it was reported that fresh ET-1 organoclay at the site displayed an average % dry HEM of 2.1% and a maximum % dry HEM or 3.4%. These values were attained after fresh ET-1 organoclay was saturated at the site with Willamette River water for 7 days. Regardless of the location of organoclay core samples relative to the sediment-cap interface, the % dry HEM levels in all core samples spiked in the organoclay cap. This phenomenon can be seen in Figure 19. Ongoing studies of biological degradation at the McCormick & Baxter capping site (Blischke, personal communication) suggest that the organoclay placed in bulk (Aqua Technologies organoclay) is undergoing significant biological degradation, meaning organic matter may be relatively available (i.e. extractible by the HEM) and the available fraction may be increasing over time. Thus the HEM measurements in the bulk organoclay do not appear to be related to any sorbed NAPL but are reflective of the organoclay itself.

Table 13: Hexane Extractable Material (HEM) Core Analysis Results

Location	Sample	ID	Height Above Sediment Layer (in)	Media Layer	Water Content (% wt)	Average HEM (% Dry)
Willamette Cove	MBSDO802	1	15	Sand Cap	18.7%	0.03%
		2	12	Sand Cap	42.7%	3.84%
		3	11	Organoclay	45.9%	4.24%
		4	10	Organoclay	54.2%	5.42%
		5	8	Organoclay	51.8%	4.12%
		6	2	Organoclay	49.3%	1.32%
		7	0	Natural Sediment	24.6%	0.03%
	MBSDO803	1	-6	Natural Sediment	17.2%	0.02%
		2	-12	Natural Sediment	24.9%	0.01%
		3	-19.2	Natural Sediment	20.7%	0.02%
		4	-24	Natural Sediment	25.5%	0.01%
	MBSDO805	1	18.4	Sand Cap	18.0%	0.02%
		2	16.2	Sand Cap	26.2%	0.40%
		3	15	Organoclay	34.3%	2.07%
		4	12.8	Organoclay	45.5%	3.53%
		5	10.8	Organoclay	47.2%	4.10%
		6	7.2	Organoclay	48.8%	3.78%
		7	6.0	Organoclay	35.9%	2.40%
		8	0.0	Natural Sediment	18.6%	0.06%
	MBSDO810	1	18.8	Sand Cap	25.1%	0.10%
		2	14.8	Transition	21.2%	0.21%
		3	12.8	Organoclay	48.9%	4.61%
		4	10.8	Organoclay	54.1%	5.84%
		5	8.4	Organoclay	54.8%	5.98%
		6	4.8	Organoclay	48.4%	4.62%
		7	0	Natural Sediment	18.0%	0.24%
		8	-17.4	Natural Sediment	21.1%	0.16%
Tank Farm Area	MBSDO813	1	22.6	Sand Cap	19.3%	0.21%
		2	14.6	Sand Cap	23.0%	0.82%
		3	13.4	Organoclay	24.3%	1.12%
		4	12.2	Organoclay	31.5%	1.54%
		5	10.2	Organoclay	39.0%	3.00%
		6	4.8	Organoclay	33.1%	1.88%
		7	0	Natural Sediment	75.3%	0.78%
		8	-4.8	Natural Sediment	69.2%	0.92%
	MBSDO822	1	6	Sand Cap	46.9%	1.14%
		2	4.8	Sand Cap	28.9%	0.41%
		3	2.4	Sand Cap	23.1%	0.08%
		4	-4.2	Natural Sediment	22.7%	0.13%
	MBSDO823	1	4.5	Sand Cap	22.7%	0.02%
		2	0.0	Transition	20.8%	0.02%
		3	-4.5	Natural Sediment	22.2%	0.02%
		4	-12.3	Natural Sediment	16.4%	0.03%
	MBSDO824	1	16.8	Sand Cap	14.9%	0.01%
		2	8.4	Sand Cap	16.7%	0.04%
		3	0	Transition	44.1%	3.06%
		4	-2.2	Natural Sediment	19.9%	1.08%
	MBSDO827	1	13.2	Sand Cap	25.3%	0.35%
		2	3.0	Sand Cap	26.1%	0.70%
		3	1.2	Sand Cap	27.5%	0.31%
		4	-6	Natural Sediment	22.2%	0.34%
	MBSDO828	1	7.2	Sand Cap	21.9%	0.07%
		2	3.6	Sand Cap	21.5%	0.02%
		3	0	Natural Sediment	11.8%	0.02%
	MBSDO832	1	9.6	Sand Cap	25.0%	0.75%
		2	0.0	Natural Sediment	27.1%	0.79%
Tank Farm Area	Organoclay Mat	-	0.0	CETCO Organoclay	65.3%	1.25%
Controls	ET-1 Field Blank	-			-	2.1% (3.4% max)
	CETCO Blank	-			62.0%	1.25%
	Recovery	-			59.0%	10.98%

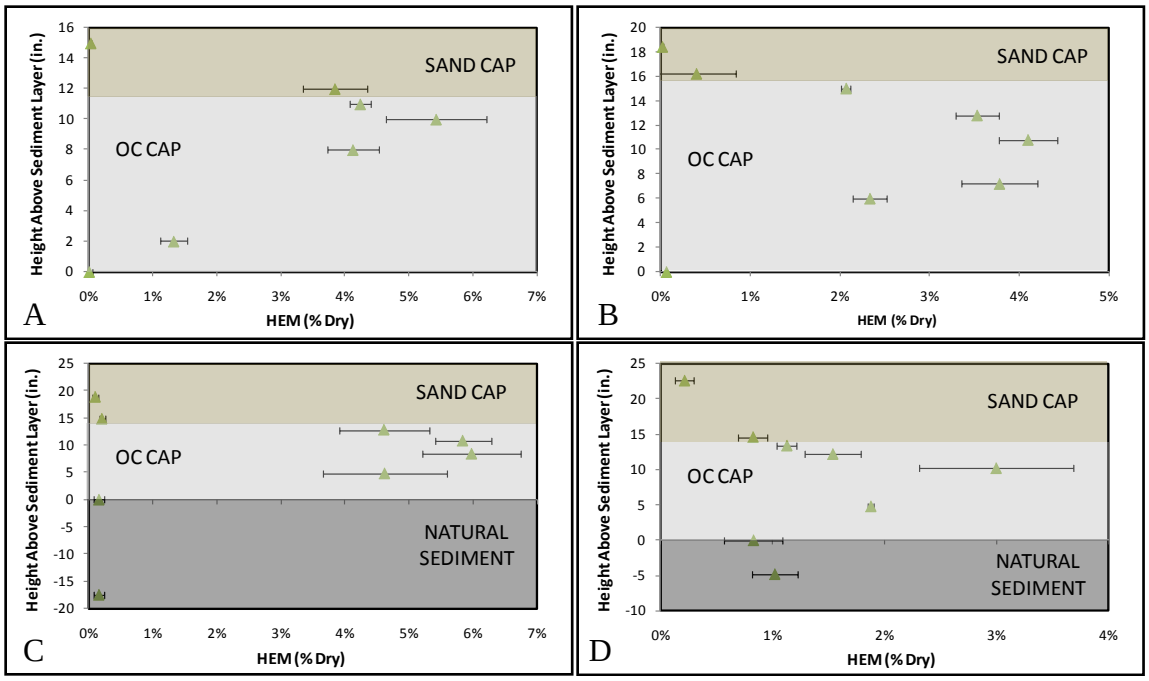

Figure 19: MBSDO813 HEM Profile (TFA)
(A) MBSDO802 Located in WC; (B) MBSDO805 Located in WC;
(C) MBSDO810 Located in WC; (D) MBSDO813 Located in TFA

The organoclay contained within the active mat (from CETCO, a different manufacturer) was harvested and exhibited a similar % dry HEM (1.25%) as to what was previously reported by Moretti (1.3%). The much lower values of HEM in the CETCO organoclay may suggest that it is more stable than the other organoclay.

This HEM data was also used previously by Moretti to determine the remaining sorption capacity of capping materials by conducting several batch tests with ET-1 (Aqua Technologies) Organoclay as gauges. The sorption capacity of the Aqua Technologies Organoclay is approximately 1 kg NAPL per kg of dry organoclay (Khanam 2006). Thus, HEM of approximately 50% would represent organoclay that is effectively saturated with NAPL. None of the HEM measurements showed organoclay approaching

NAPL saturation and due to the relatively high fraction of extractible materials from the ET-1 Organoclay, all of the organoclay samples may indicate effectively no NAPL present. Apparently, no significant NAPL migration is occurring in the cores samples, but the organoclay retains effectively full capacity to absorb NAPL if any were to migrate.

The HEM spike associated with organoclay cap was isolated to that particular capping material and was not observed in any of the cores taken in locations capped solely by sand (see Figure 20A). There were, however, two cores where the % dry HEM profile appeared to increase with increasing distance from the sediment-cap interface (i.e. toward the water column). The HEM profiles for these cores can be seen in Figure 20B. Both cores which generated these types of profiles, MBSDO822 and MBSDO827, were located in the TFA. However, field notes taken during the cores' extrusion noted the presence of a strong sheen and creosote odor in the natural sediment as well as pin sized globules of NAPL. MBSDO822 was also reported to contain fugitive organoclay in the sand cap that was speculated to have migrated over during the deployment of the bulk organoclay cap. These factors could have easily contributed to the elevated % dry HEM in these sampling locations. Field notes from sampling activities at the site can be seen in Appendix G.

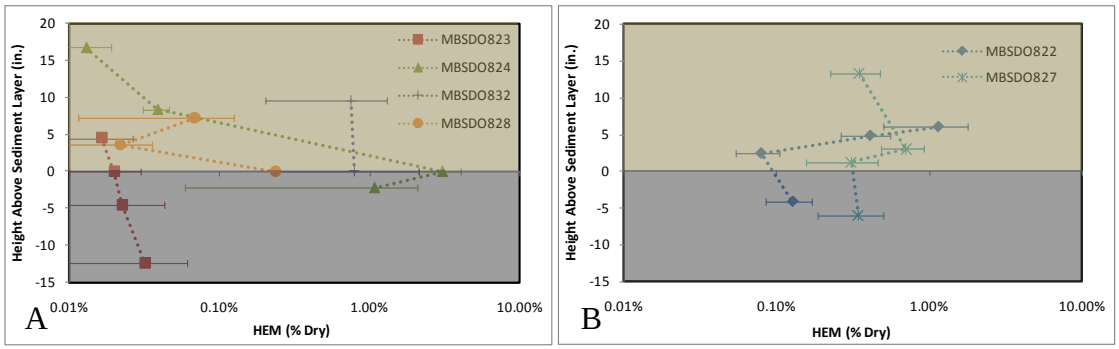

Figure 20: Sand Cap HEM Profiles (TFA)
(A) Sand Capped Cores with Decreasing HEM as samples approach the water column
(B) Sand Capped Cores with Increasing HEM as samples approach the water column

Although no evidence of NAPL migration was noted in the organoclay caps, dissolved contaminants would still be expected to migrate. The organoclay has the capability of sorbing dissolved organics, although the sorption capacity would be significantly less than for separate phase (on a weight basis) and related to dissolved phase concentration. Hexane extracted material from samples at the sediment-cap interface in cores taken where bulk organoclay had been deployed were also subjected to cleanup with silica gel and analyzed with HPLC for 14 PAHs. Samples were analyzed for naphthalene, fluorene, acenaphthene, phenanthrene, fluoranthene, pyrene, chrysene, benz[a]anthracene, benzo[b]fluoranthene, benzo[k]fluoranthene, benzo[a]pyrene, dibenz[a,h]anthracene, benzo[ghi]perylene, and indeno[1,2,3,-cd]pyrene. The chromatograms for benzo[ghi]perylene and indeno[1,2,3,-cd]pyrene did not separate very well and constantly showed up as a single peak. In order to salvage this data, these two PAHs were combined in analysis and a single bulk concentration reading for the two was taken, benzo[ghi]perylene+indeno[1,2,3,-cd]pyrene. Six of the samples that underwent this analysis were from cores taken in Willamette Cove, while two of the samples were derived from the TFA in the Willamette River. Figure 21 display bulk

concentrations for 14 PAHS in the natural sediment and the overlying organoclay cap at these locations. These results can also be seen in tabular for in Table 14.

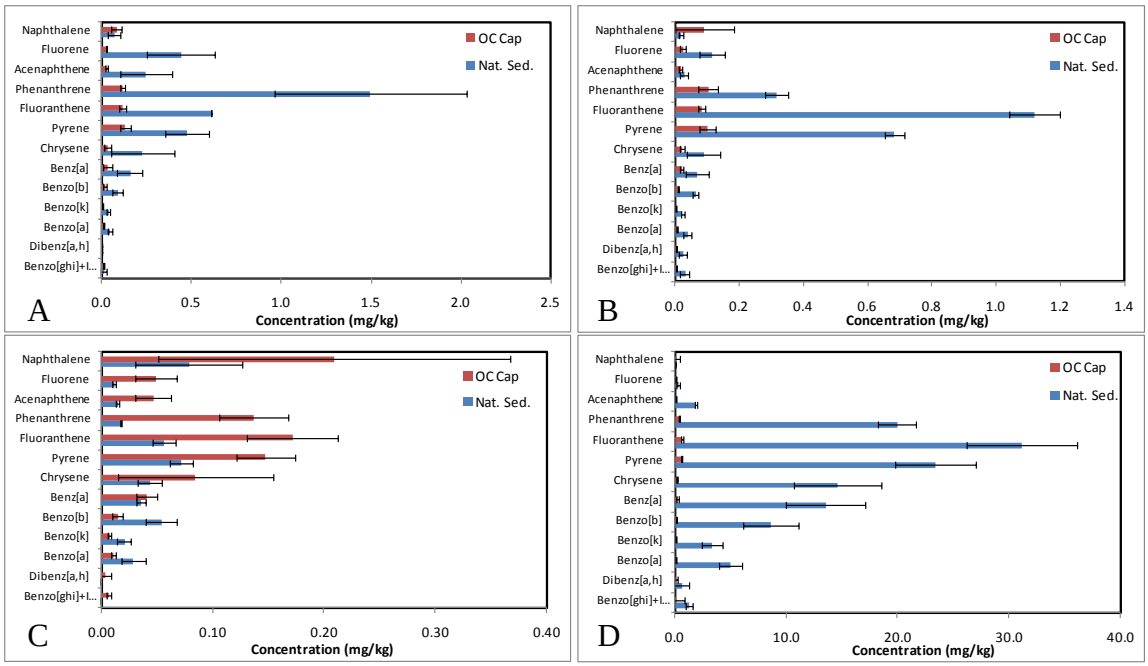

Figure 21: 14 PAH Bulk Concentrations at the Organoclay-Sediment Interface
(A) MBSDO802 Located in WC; (B) MBSDO805 Located in WC;
(C) MBSDO810 Located in WC; (D) MBSDO813 Located in TFA

Table 14: Bulk Concentration Summery Table for Samples at the Sediment-Cap Interface

PAH's	MSDO802 Conc. (mg/kg) Willamette Cove		MSDO805 Conc. (mg/kg) Willamette Cove		MSDO810 Conc. (mg/kg) Willamette Cove		MSDO813 Conc. (mg/kg) Willamette River (TFA)	
	Nat. Sed.	OC Cap	Nat. Sed.	OC Cap	Nat. Sed.	OC Cap	Nat. Sed.	OC Cap
Naphthalene	0.07	0.08	0.02	0.09	0.08	0.21	0.02	0.05
Fluorene	0.44	0.03	0.12	0.03	0.01	0.05	0.29	0.09
Acenaphthene	0.25	0.03	0.03	0.02	0.02	0.05	1.86	0.08
Phenanthrene	1.50	0.12	0.32	0.10	0.02	0.14	19.91	0.40
Fluoranthene	0.61	0.12	1.12	0.08	0.06	0.17	31.16	0.63
Pyrene	0.48	0.13	0.68	0.10	0.07	0.15	23.35	0.64
Chrysene	0.23	0.04	0.09	0.02	0.04	0.09	14.56	0.20
Benz[a]	0.16	0.03	0.07	0.02	0.04	0.04	13.54	0.19
Benzo[b]	0.09	0.02	0.07	0.01	0.05	0.02	8.62	0.13
Benzo[k]	0.04	0.01	0.02	0.00	0.02	0.01	3.32	0.06
Benzo[a]	0.05	0.01	0.04	0.01	0.03	0.01	4.99	0.07
Dibenz[a,h]	0.00	0.00	0.03	0.00	ND	0.00	0.58	0.01
Benzo[ghi]+Indeno[1	0.01	0.01	0.03	0.00	ND	0.01	1.29	0.01

The interface at two of the cores sampled at Willamette Cove (MBSDO802 & MBSDO805) demonstrated similar behavior, where the bulk concentration for the majority of the PAHs was much greater in the sediment than the cap. This would suggest that the PAHs in these locations are not migrating. In a third core (MBSDO810) from the cove, however, higher concentrations of PAHs were detected in the organoclay than in the sediment. This would be expected in a situation where PAHs were migrating in that the greater sorptive capacity of the organoclay would tend to concentrate the PAHs relative to the sediment. The greater sorption capacity of the organoclay would also retard the migration of the contaminants through the organoclay. This result is consistent with field notes taken during extrusion of the cores, which stated the presence of a slight creosote odor in the organoclay cap not mentioned in the other two cores. Furthermore, the underlying sediment at the location of this core was also noted to have a potent odor and sheen that was not present at the other two sampling locations.

The fourth core analyzed for PAH bulk concentration was extruded from the TFA and displayed a similar relationship as MBSDO802 and MBSDO805 in Willamette Cove (WC). In these cores, the natural sediment in the sample displayed a higher bulk concentration for a majority of the PAHs than the overlying organoclay, suggesting reduced contaminant mobility. Interestingly, the absolute concentrations of the sediment and organoclay were higher in these locations despite the conclusion of limited contaminant mobility.

Due to trend exhibited at MBSDO810, further analysis was deemed necessary to investigate migration of PAHs into and possibly through the organoclay cap. As a result, the complete bulk concentration profile of PAHs at this sampling location was generated. The concentration profile for the 14 PAHs of interest can be seen in tabular form in Table 15, as well as graphically in Figure 22 - Figure 24. The profiles show that the more

mobile PAHs (e.g. naphthalene through phenanthrene) have largely penetrated the entire layer of organoclay while the less mobile, more sorbing PAHs have not substantially penetrated the organoclay. Note that despite the movement of lighter PAHs throughout the organoclay layer, the organoclay remains capable of absorbing NAPL to the full extent.

Table 15: MBSDO810 PAH Bulk Concentration Profile

Core Sample Names and Average Height Above the Sediment-Cap Interface (in)		Average PAH Bulk Concentration (mg/kg)												
		Naph.	Fluor.	Acenaph.	Phen.	Fluoran.	Pyrene	Chrysene	Benz[a]	Benzo[b]	Benzo[k]	Benzo[a]	Dibenz [a,h]	Benzo[ghi] +Indeno
0.1 - 0.3' Above OC	18.8	0.21	0.01	0.01	0.02	0.01	0.00	0.00	0.00	0.00	0.00	0.00	0.00	0.00
0.1'-0.05 SC/OC Interface	14.8	0.40	0.02	0.02	0.05	0.00	0.01	0.00	0.00	0.00	0.00	0.00	0.00	0.00
0.05' - 0.2' Below Top of OC	12.8	0.34	0.04	0.05	0.11	0.01	0.01	0.00	0.01	0.00	0.00	0.00	0.00	0.00
0.2' - 0.3' Below Top of OC	10.8	0.46	0.05	0.06	0.10	0.00	0.00	0.01	0.01	0.01	0.00	0.00	0.00	0.00
0.3' -0.4' Into OC	8.4	0.11	0.04	0.04	0.06	0.00	0.01	0.01	0.01	0.00	0.00	0.00	0.00	0.00
0.0' - 0.4 Above Bottom of OC	4.8	0.21	0.05	0.05	0.14	0.17	0.15	0.09	0.04	0.02	0.01	0.01	0.00	0.01
0.65' Into Nat. Sed.	0	0.08	0.01	0.02	0.02	0.06	0.07	0.04	0.04	0.05	0.02	0.03	ND	ND
0.65' - 1.45' Below OC, Nat. Sed.	-17.4	0.02	0.01	0.01	0.01	0.02	0.00	0.03	0.00	0.01	0.00	0.01	0.00	0.01

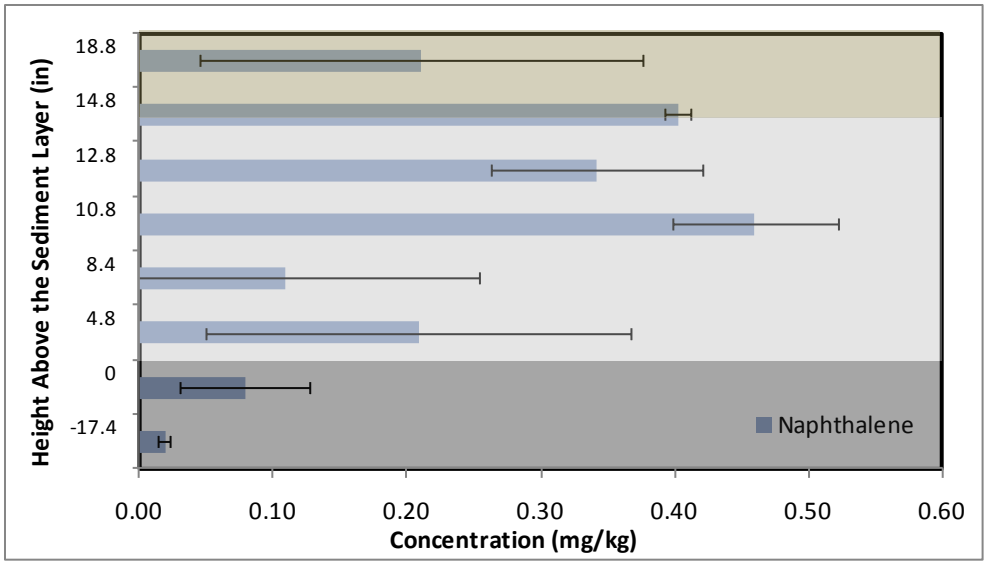

Figure 22: MBSDO810 Naphthalene Bulk Concentration Profile

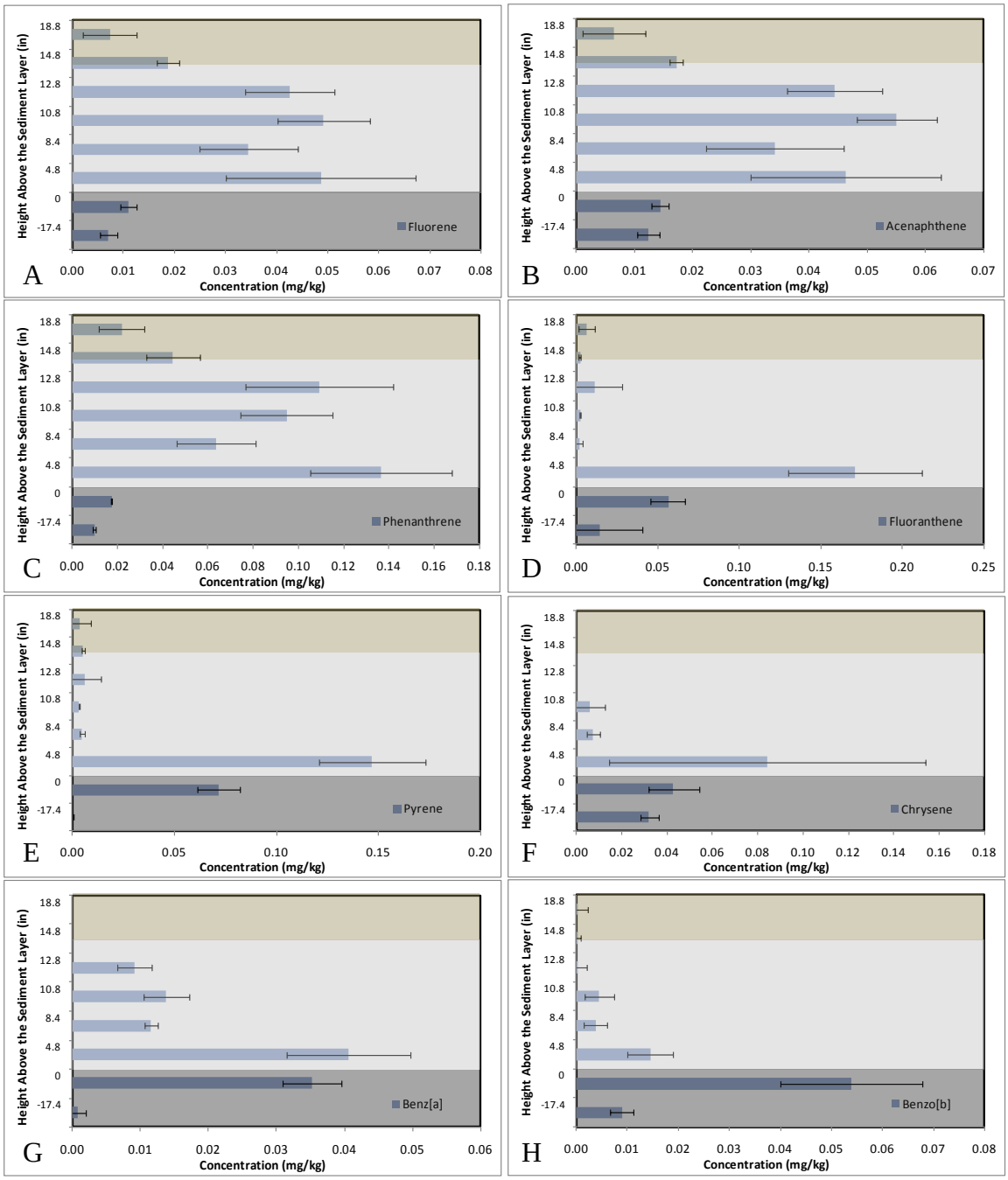

Figure 23: MBSDO810 PAH Bulk Concentration Profiles (Fluorene to Benzo[b]fluoranthene)

(A) Fluorene; (B) Acenaphthene; (C) Phenanthrene; (D) Fluoranthene; (E) Pyrene; (F) Chrysene; (G) Benz[a]anthracene; (H) Benzo[b]fluoranthene

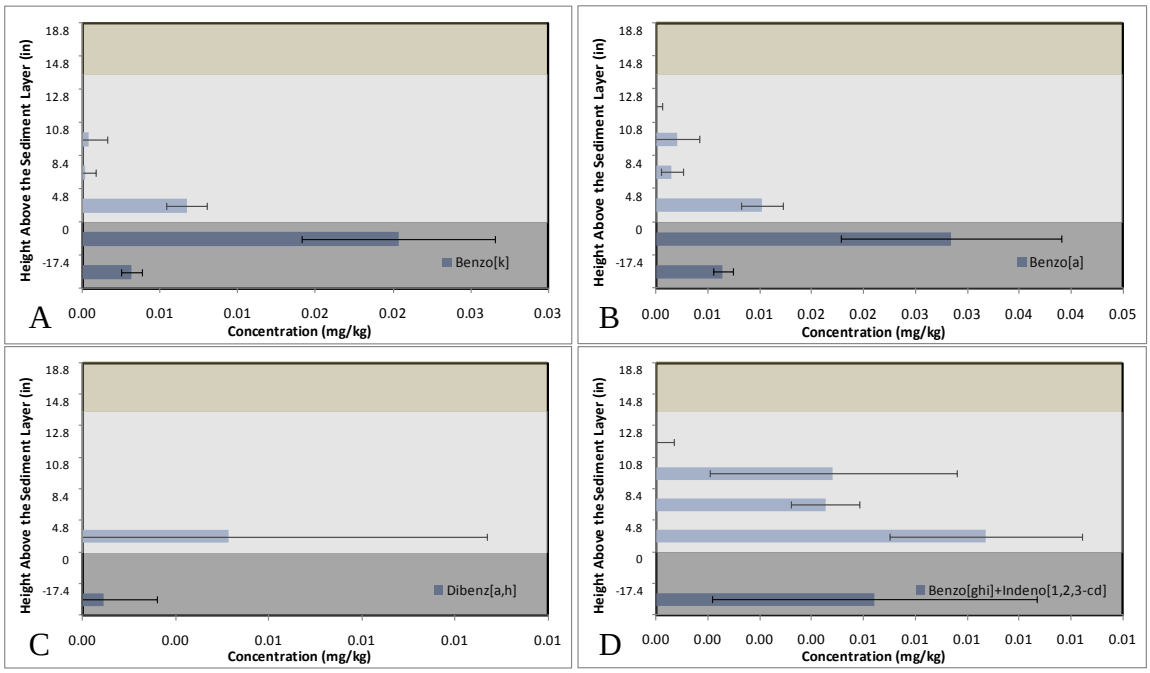

Figure 24: MBSDO810 PAH Bulk Concentration Profiles (Benzo[k]fluoranthene to Benzo[ghi]perylene)
(A) Benzo[k]fluoranthene; (B) Benzo[a]pyrene; (C) Dibenz[a,h]anthracene;
(D) Benzo[ghi]perylene + Indeno[1,2,3,-cd]pyrene

5.3 ACTIVATED CARBON GEOTEXTILE VS. BULK ORGANOCLAY CAP

Once partitioning coefficients could be estimated for the active material in Huesker's Filtermat 200 and the organoclay sediment caps at the McCormick & Baxter site were evaluated, the operational life of both materials were assessed under conditions present at the site. Partitioning coefficients under equilibrium conditions for naphthalene, phenanthrene, and pyrene were estimated for activated carbon using Walters' and Luthy's Langmuir or Freundlich models depending on which provided the best fit (based on their reported r^2), while linear equilibrium partitioning coefficients for CETCO PM 199 Organoclay were used as representative surrogates for Aqua Technology's ET-1 Organoclay (for whom fresh material to directly measure sorption was unavailable).

Both materials' behavior was simulated under conditions that have been or could have been experienced at the site using the same advection-dispersion transport model (Van Genuchten 1981) discussed above.

Since the performance of the two active materials was sought to be compared, several assumptions were made regarding the physical properties of two capping materials that could only be measured conducting column experiments. Given that the organoclay cap deployed at the site was a foot thick (30.48 cm), it was decided that this would remain constant in the simulations so as to make a direct comparison to activities in the field. Likewise, initial simulations were conducted using the previously measured properties of the Huesker Filtermat, such as is porosity, bulk density, dispersivity, and thickness (0.50, 0.1 kg/L, 0.0025 cm, & 0.2 cm). Simulations were conducted using a 30.48 cm long theoretical column, at a representative Darcy velocity of 1 cm/day (GSI 2005). Physical properties for the PM 199 CETCO Organoclay were obtained from the Master's thesis of Dufreche (2008). Her work provided values for porosity (0.50), dispersivity (0.33), and linear equilibrium partitioning coefficients that were used as inputs in the advection-dispersion transport model.

Because the organoclay exhibited linear equilibrium, its partitioning coefficients were constant, and this held true for all aqueous concentrations. This is not the case in general with activated carbon, which sorption behaves non-linearly. Walters and Luthy's High C_e Langmuir Model was used to estimate concentration specific partitioning coefficients for naphthalene and pyrene, while their Freundlich Model was used to predict sorption of phenanthrene. Although the reported sorption is nonlinear, for purposes of simulation, linear sorption with the effective linear partition coefficient at the cap influent concentration was employed. The influent concentrations used in generating these partitioning coefficients and subsequently used in simulations were the historical

maximum naphthalene, phenanthrene, and pyrene concentrations that have observed in groundwater at the site (GSI 2005), as can be seen in Table 16, along with several input parameters used in the simulations.

Table 16: Comparative Transport Model Input Parameters

Media	Porosity	Dispersivity (cm)	Bulk Density (kg/L)	Conc., C_0 (mg/L)			Partitiong Coefficients (L/kg)		
				Naph	Phen	Pyr	Naph	Phen	Pyr
Activated Carbon	0.500	0.003	0.100	9.180	0.084	0.021	60,280	1,189,000	3,613,000
Organoclay		0.330	0.750				3,284	68,020	104,900

Models were run to their breakthrough time, which with these simulations was defined as the time when $C/C_0 = 0.05$. Despite having partitioning coefficients that were at least an order of magnitude larger than those of organoclay, activated carbon from Huesker's Filtermat 200 consistently had quicker break through times than the 1 ft thick bulk organoclay cap. Even with retardation factors (the ratio of water flow velocity and contaminant migration velocity) double that of organoclay, the thin layer of activated carbon could not maintain its integrity as long as the 1 ft thick organoclay cap could. In fact, it would take more than sixty 0.2 cm thick activated carbon mats to achieve equivalent of that observed in the 1 ft organoclay cap. Figure 25 contain concentration profiles for the three PAHs at various times generated by the simulations.

The primary purpose of active cap, however, is to achieve a given degree of protectiveness with a thinner cap than might otherwise be necessary. The thickness of cap required to achieve a certain sorption capacity is proportional to the effective partition coefficient of the contaminant. Thus the activated carbon is 17 (for naphthalene) to 34 (for pyrene) times more sorbing than the organoclay caps. Thus the effectiveness of the 30 cm thick organoclay layer at McCormick & Baxter (loading of 225 kg/m^2) could be met with a loading of 6.7 to 13 g/m^2 of activated carbon. This could

be accomplished with a bulk layer of bulk layer of activated carbon 1.65-3.3 cm thick (assuming a dry density of activated carbon of 0.4 g/cm^3 in bulk).

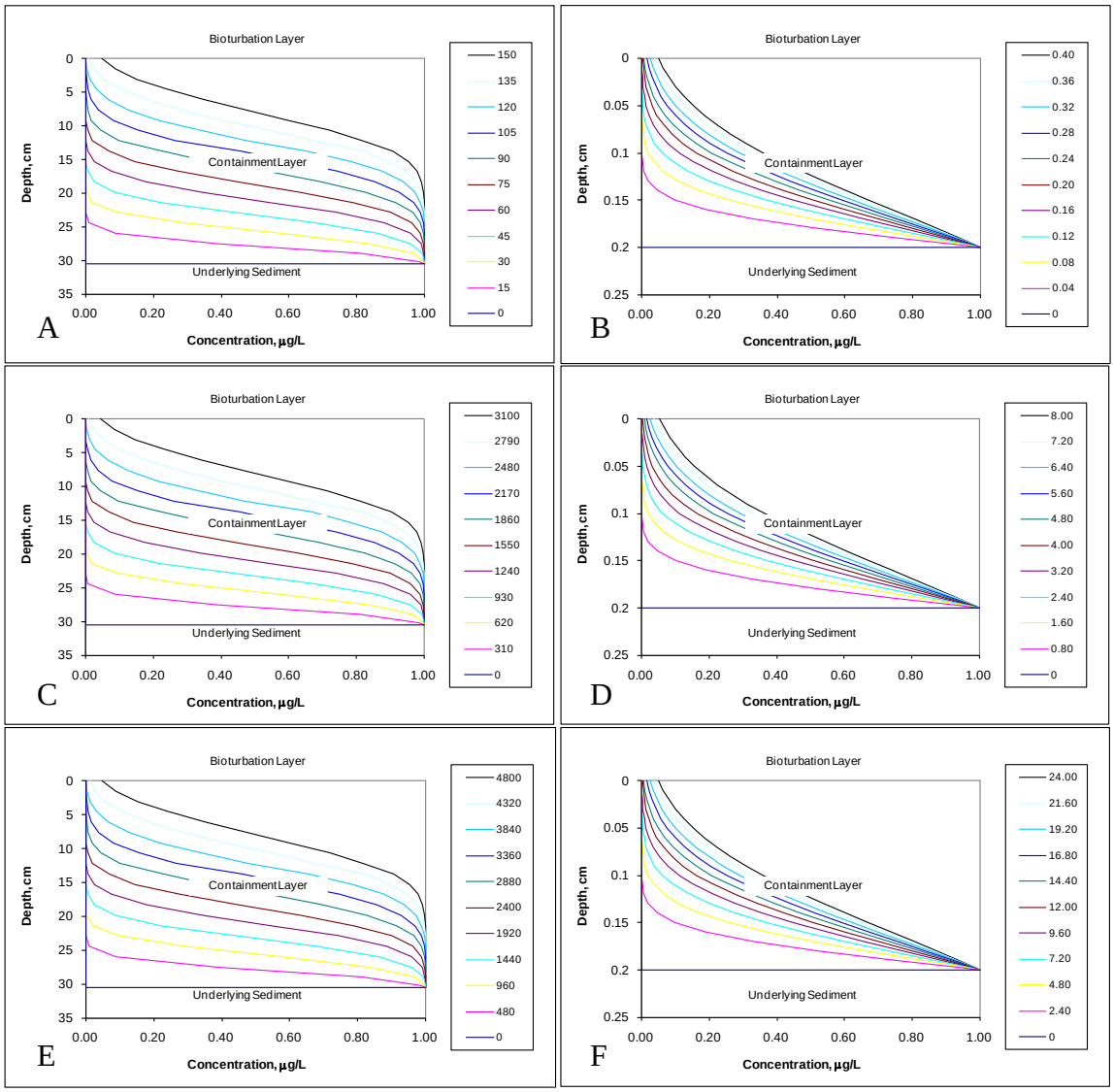

Figure 25: Organoclay vs. Activated Carbon Field Simulations
(A) Organoclay Naphthalene Model; (B) Activated Carbon Naphthalene Model;
(C) Organoclay Phenanthrene Model; (D) Activated Carbon Phenanthrene Model;
(C) Organoclay Pyrene Model; (D) Activated Carbon Pyrene Model
NOTE: Plots correspond to concentration profiles in the cap at different times (years)

Chapter 6: Conclusions

In this research, two active capping methods were evaluated for their effectiveness, capacity, and life when in the presence of dissolved and separate phase contaminants. The two principle materials of interest in this study were Aqua Technology's ET-1 Organoclay, which was deployed in bulk at the McCormick & Baxter Superfund Site in Portland, OR, and a powdered activated carbon impregnated geotextile produced by Huesker, Inc.

Based on data from this round of cap evaluation studies and coupling those results with previous evaluations of caps at the McCormick & Baxter site, it can be concluded that the sediment caps at the site have retained a significant portion of their sorption capacity. Assuming the samples analyzed are representative of the current conditions throughout the capped areas, the sand cap seems to be performing well at isolating NAPL and preventing its migration. Cores taken in the sand capped TFA, which had reported residual NAPL contamination in sediments at the time of cap deployment, nearly all exhibited a decreasing dry percentage of HEM with decreasing distance to the water column. Since HEM is used as a surrogate for free-phase, NAPL contamination, it can be said that the sand caps are effectively isolating any residual NAPL in sediments. Their performance indicates that although active caps can be very effective at sites, their use is not always necessitated.

The hexane extractible material test was not as effective at indicating the performance of the organoclay. The organoclay exhibited elevated levels of HEM that were apparently not associated with NAPL. The Aqua Technologies ET-1 Organoclay appears to have a significant fraction of extractible organic matter compared to the CETCO PM-199. The relatively high levels of HEM, however, are still far below the

HEM of NAPL saturated organoclay, indicating that the organoclay retains significant capacity to absorb NAPL.

The HEM extract from four cores were analyzed for PAHs at the sediment-cap interface. Most displayed a similar trend in which higher bulk concentrations were recorded in the underlying natural sediment than in the organoclay cap. This suggests that NAPL and dissolved contaminants are not migrating significantly, in that contaminated organoclay would be expected to display higher bulk solid concentrations than the less sorbing underlying sediment. Core MBSDO810, which was located no more than 30 ft away from the other two cores taken in Willamette Cove, however, exhibited higher concentrations in the organoclay layer than in the underlying sediment suggesting contaminant migration. The organoclay concentrations were very low suggesting that the PAHs, though apparently mobile, are not present in high enough concentrations to cause concern. Evaluation of all PAH concentrations above the sediment organoclay interface in this core also showed that the low molecular weight PAHs were relatively uniform throughout the organoclay layer whereas high molecular weight PAHs only influenced the bottom layers of organoclay. This again indicates that the PAHs in this core were mobile but that the low molecular weight PAHs have achieved near steady state concentrations below levels of concern. Overall, the McCormick & Baxter caps are performing as expected and have continued to isolate residual NAPL in sediments, as well as control its seepage.

In column tests conducted on Huesker's NAPL and activated carbon geotextile mats, both types of materials showed qualities that would lend them to be used in sediment capping applications. While the NAPL mat is designed to sorb free-phase contaminants, it also displayed some capacity to sorb dissolved-phase contaminants. However, its sequestration capacity is not sufficient to merit its sole use as a barrier

against dissolved HOC's. Batch tests did however demonstrate the mat's sorptive capacity, which was on par with that of PM 199 CETCO Organoclay. This ability lends the NAPL mat to applications where it is meant to provide an effective barrier versus NAPL contaminated sediment, especially when used to protect against residual NAPL migration or sheen generation. Since the mat has a finite sorptive capacity, its use is not recommended when contaminant releases have yet been controlled at a site. However, its application is acceptable to prevent sheens in the water column and when used in concert with other active materials which are superior sorbents of HOCs.

Similar experiments were conducted for Huesker's Filtermat 200 activated carbon geotextile and bulk activated carbon extracted from said mat, which produced effective partitioning coefficients for the same PAHs studied in the NAPL mat studies. The major difference in this batch of column studies and those which analyzed the NAPL mat is, although columns of similar geometries were used for the bulk activated carbon studies, a different shaped column was used to test the Filtermat. Since unrealistically fast upwelling velocities were used to expedite the test, the experiments conducted for the bulk activated carbon, in the 2.54 cm diameter columns proved to be compromised, as approximately half the sorption took place in these columns as what was exhibited in the column testing the intact Filtermat. The Filtermat column, ACMS, was tested at a velocity about an order of magnitude slower than the other columns, but was still at a velocity an order of magnitude above what one would expect to see in the field. The column's threefold increase of residence time per unit mass of activated carbon, as compared to the bulk activated carbon columns, provided a kinetically favorable environment which fostered sorption to proceed to equilibrium.

Due to the enhanced hydrophobicity of phenanthrene and pyrene, significant effluent concentrations were never observed for these PAHs in the activated carbon

columns. Naphthalene, however, was measured in the effluent, allowing an estimation of the in-situ sorption capacity. Initial analysis of effluent data was normalized by the concentration in the reservoirs which supplied water to the systems, but questions were raised as to the validity of the assumption that the concentration in the reservoirs was the actual concentration reaching the active materials. Testing conducted after the conclusion of the column studies showed this to be the case, which gave credence to using the column's steady state effluent concentration as their influent concentration, C_0, in analysis. Using dispersivities acquired from inert tracer tests, breakthrough models were fit to experimental data, based on sorption within the column and the material's effective partitioning coefficient.

Data and models for the ACB columns with both deionized water and natural site water were effectively identical, indicating that dissolved organic matter and other site specific matrix effects were not important. As discussed above, these columns were not allowed to reach equilibrium due to the high velocity used in the studies. However, the effective sorption capacity of the activated carbon appeared to be approaching of that measured by Walters and Luthy (1983). This led to the assumption used in the comparative modeling aspect of this work, in which the Walter's and Luthy's data for sorption of PAHs onto activated carbon were used to provide estimates for PAH sorption onto Huesker's activated carbon under conditions expected to allow the achievement of equilibrium.

Models were run to predict the lives of both the bulk organoclay cap and activated carbon Filtermat under conditions present at the McCormick & Baxter site. Parameters for the bulk activated carbon were either acquired from previous work, or estimated to be similar to that of other organoclay. In this comparison, bulk organoclay was modeled as

deployed in the field, at a thickness of 1 ft, while the Filtermat was modeled as if it had been deployed in the field.

Despite possessing significantly greater specific sorption capacities, Huesker's Filtermat could not offer the same protection for the extended period of time that the 1 ft thick organoclay cap granted. As great as the specific sorption capacity is for the activated carbon in Huesker's Filtermat 200 is, its significantly smaller mass per unit area make fair comparisons to a 1 ft thick organoclay cap hard to make. In order to provide the same sorptive capacity as the 1 ft organoclay cap, over 60 Huesker mats would have to be stacked on top of one another, creating an effective thickness of 12 cm. The lack of any measurable NAPL migration into the organoclay cap cores, however, suggests that the full 30 cm of organoclay is unneeded at the site, and it may be that a thin layer of activated carbon would provide adequate containment of dissolved phase organics. It must be noted though, that activated carbon is not designed for containing NAPLs, and any contact with them will foul the carbon.

In conclusion, the evaluation of emerging materials used for contaminated sediment applications is critical to the effectiveness, capacity, and life of the capping materials. A versatile material which can be used effectively against both organic and inorganic contaminants has not been found or yet developed, and remains elusive to researchers who aspire to find this "silver bullet" for contaminated sediment. Until then, the claims of manufactures that produce innovative active capping materials must be verified through experimental investigations. Also, due to the limited time available to analyze new materials in an independent lab setting, materials must continually be monitored once deployed in the field to ensure their continued effectiveness and integrity. The intelligent and efficient implantation of these materials will only enhance remedial

strategies, which will undoubtedly reduce the risks associated with hazardous waste sites, such as the McCormick & Baxter Superfund Site in Portland, OR.

APPENDIX A:

Term Definitions of Advection-Dispersion Model

C = Effluent Concentration (mg/L)

C_e = Influent Concentration (mg/L)

P_e = Peclet Number

$$P_e = \frac{Uh_{cap}}{D_1}$$

U = Darcy Velocity (cm/yr)

h_{cap} = Cap Thickness (cm)

D_{eff} = Diffusion-Dispersion Coefficient = $\alpha U + D_w \varepsilon^{4/3}$ (cm^2/yr)

α = Dispersivity (cm)

D_w = Diffusion Coefficient (cm^2/sec)

$$u = \sqrt{\frac{P_e^{\,2}}{4} + \frac{\varepsilon \lambda h_{cap}^2}{D_{eff}}}$$

ε = Porosity

λ = Decay Rate (yr^{-1})

$$\zeta = \frac{h_{cap} - z}{h_{cap}}$$

$$\tau = \frac{D_{eff} t}{R_f h_{cap}^2}$$

t = time (min)

$$R_f = Retardation\ Factor = \epsilon + \rho K_D$$

P = Bulk Density (kg/L)

K_D = Partitioning Coefficient (L/kg)

APPENDIX B:

NM Data and Models normalized by the
Steady State concentrations achieved in the columns

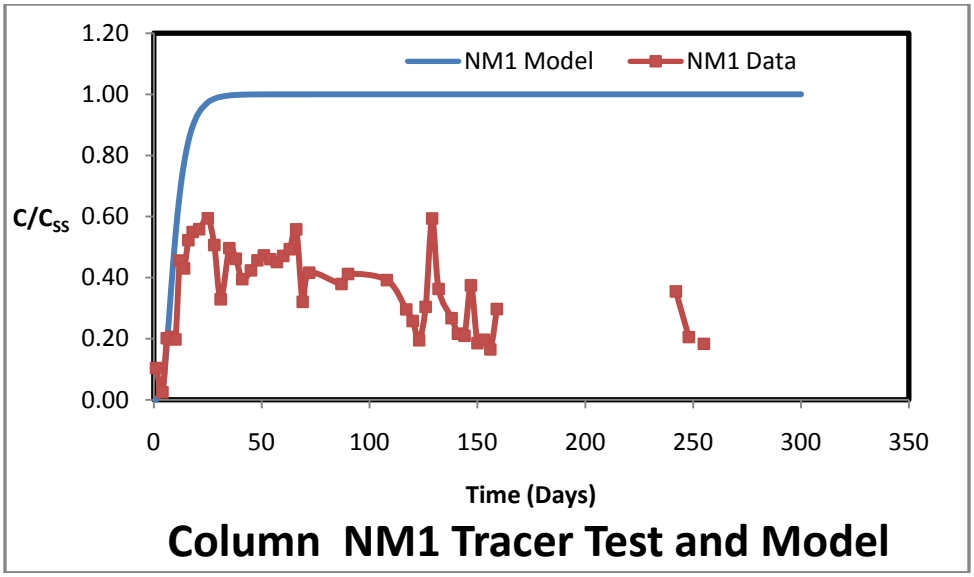
1.20
1.00
0.80
0.60
0.40
0.20
0.00
C/Css
NM1 Model
NM1 Data
0
50
100
150
200
250
300
350
Time (Days)
Column NM1 Tracer Test and Model

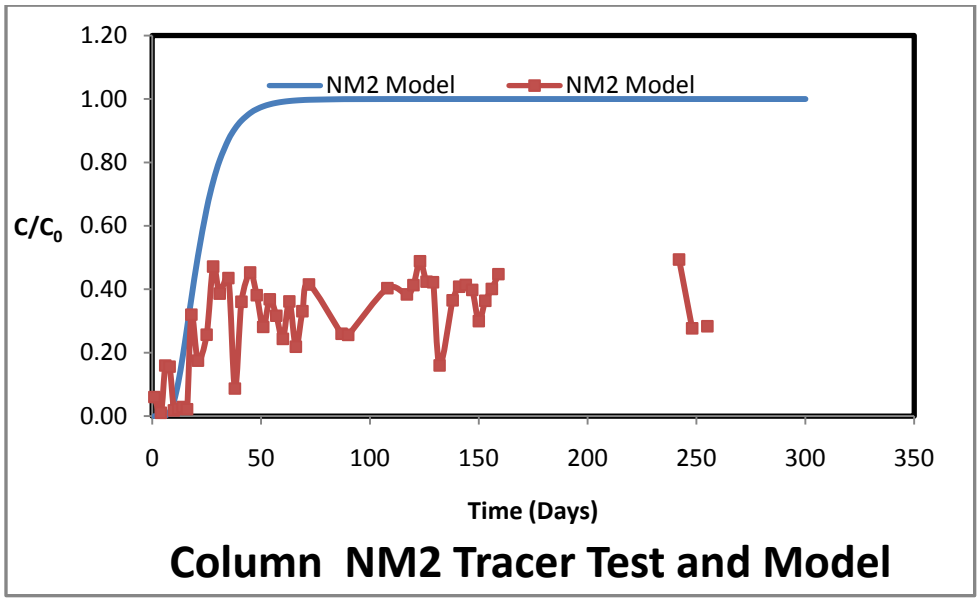
1.20
1.00
0.80
0.60
0.40
0.20
0.00
C/C0
NM2 Model
NM2 Model
0
50
100
150
200
250
300
350
Time (Days)
Column NM2 Tracer Test and Model

APPENDIX C:

Column Studies Raw Data
(Effluent Data Normalized by Measured Influent Data, C/C_0)

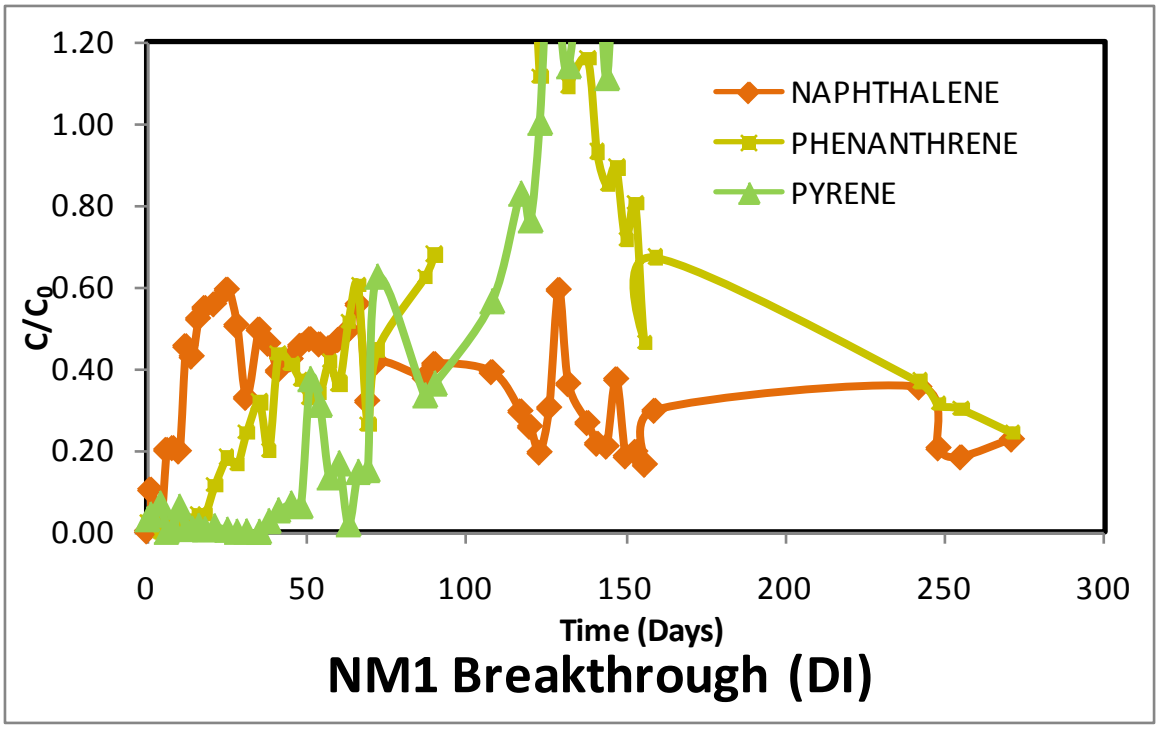
1.20
1.00
0.80
0.60
0.40
0.20
0.00
C/C0
0
50
100
150
200
250
300
Time (Days)
NAPHTHALENE
PHENANTHRENE
PYRENE
NM1 Breakthrough (DI)

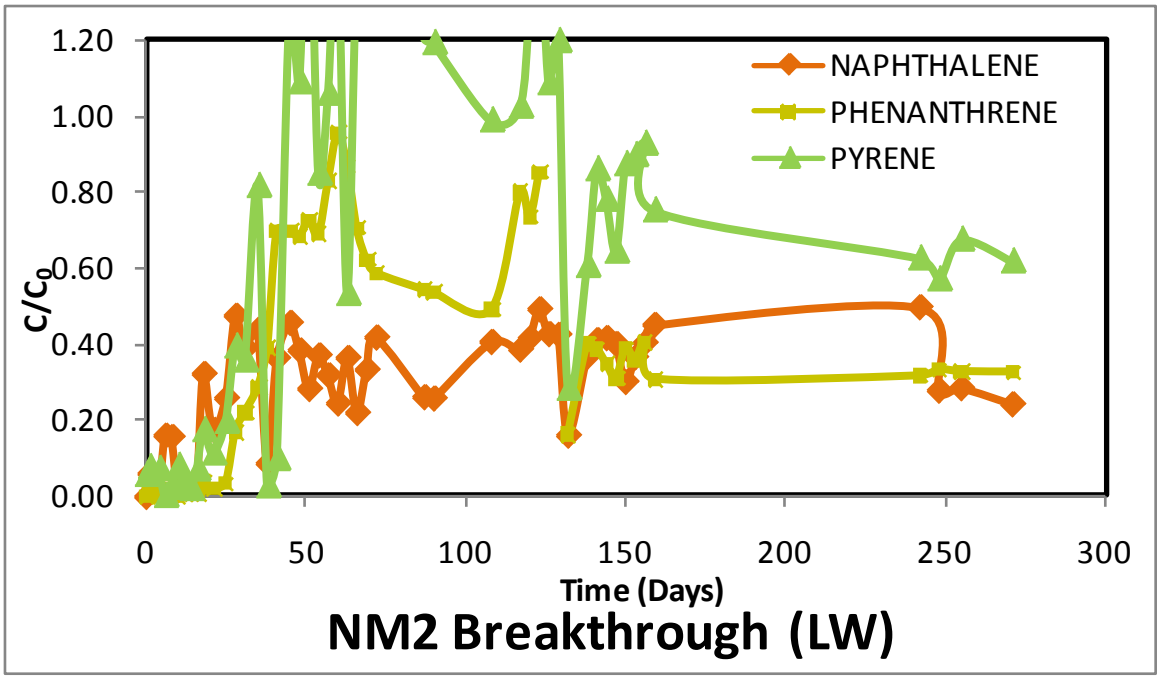
1.20
1.00
0.80
0.60
0.40
0.20
0.00
C/C0
0
50
100
150
200
250
300
Time (Days)
NAPHTHALENE
PHENANTHRENE
PYRENE
NM2 Breakthrough (LW)

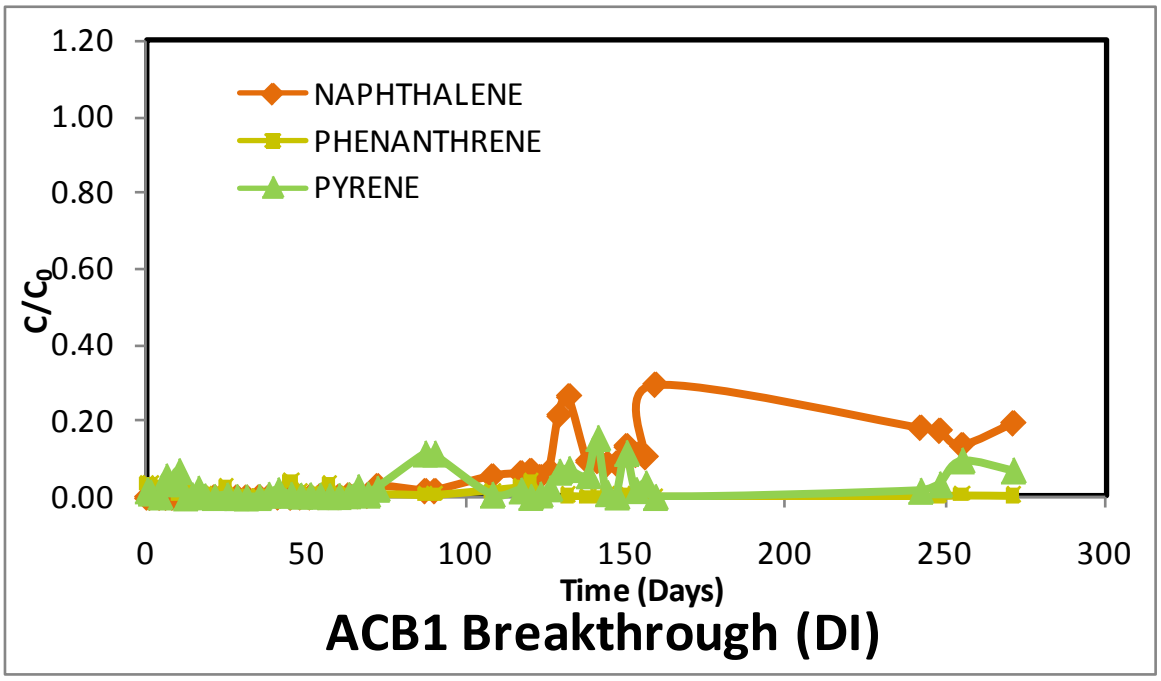
1.20
1.00
0.80
0.60
0.40
0.20
0.00
C/C0
NAPHTHALENE
PHENANTHRENE
PYRENE
0
50
100
150
200
250
300
Time (Days)
ACB1 Breakthrough (DI)

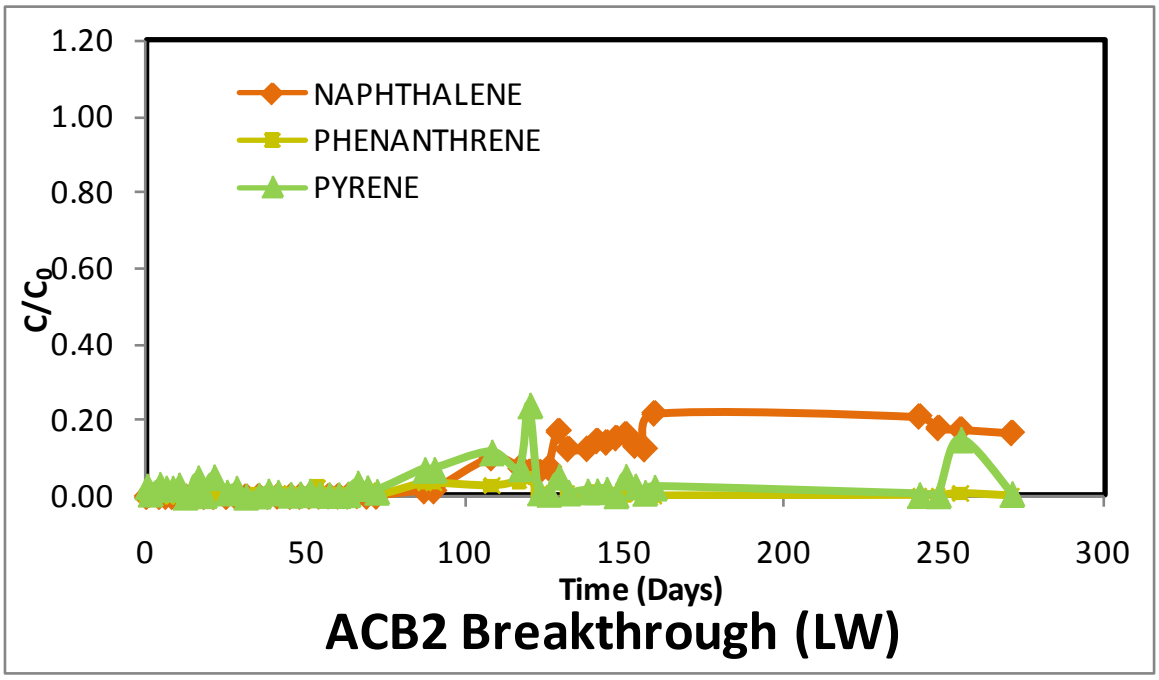
1.20
1.00
0.80
0.60
0.40
0.20
0.00
C/C0
NAPHTHALENE
PHENANTHRENE
PYRENE
0
50
100
150
200
250
300
Time (Days)
ACB2 Breakthrough (LW)

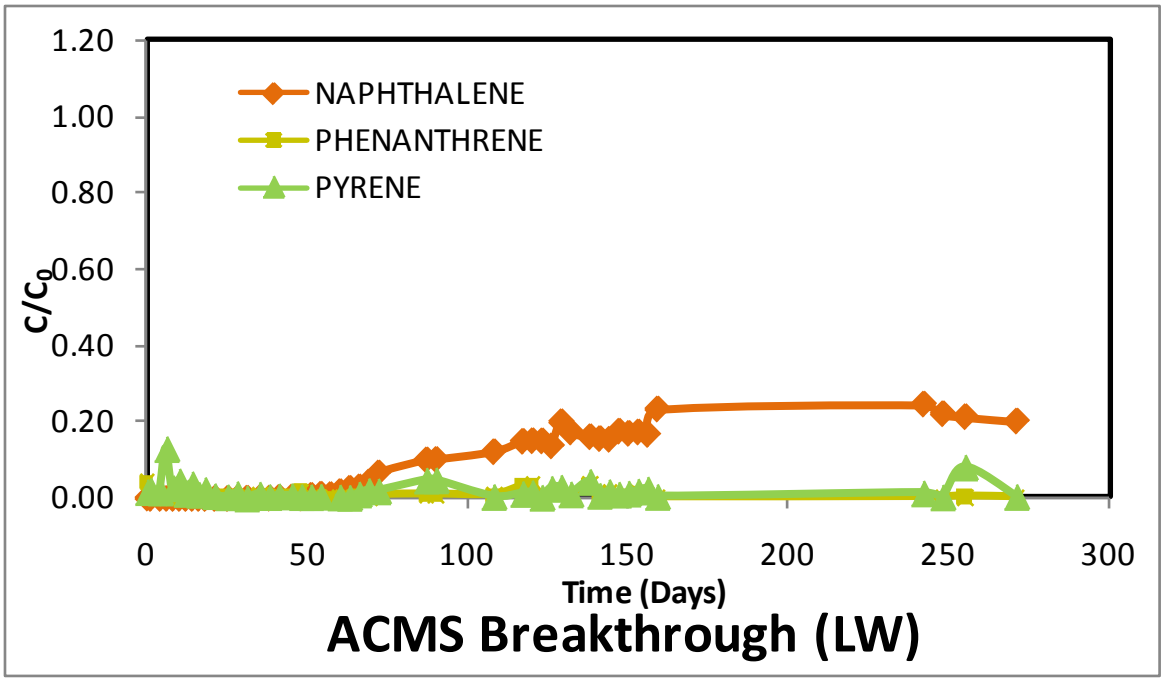
1.20
1.00
0.80
0.60
0.40
0.20
0.00
C/C0
NAPHTHALENE
PHENANTHRENE
PYRENE
0
50
100
150
200
250
300
Time (Days)
ACMS Breakthrough (LW)

Day	NAPHTHALENE									
	NM1		NM2		ACB1		ACB2		ACMS	
	Conc. (ppb)	C/Co	Conc. (ppb)	C/Co	Conc. (ppb)	C/Co	Conc. (ppb)	C/Co	Conc. (ppb)	C/Co
0	27.11	0.00	4.55	0.00	7.86	0.00	2.99	0.00	17.95	0.00
1	1,650.60	0.10	970.12	0.06	2.10	0.00	89.01	0.01	1.05	0.00
4	390.20	0.02	166.68	0.01	1.40	0.00	0.21	0.00	2.94	0.00
6	3,197.50	0.20	2,571.72	0.16	1.82	0.00	1.47	0.00	2.97	0.00
8	3,267.87	0.21	2,515.30	0.16	0.49	0.00	0.31	0.00	0.87	0.00
10	3,134.63	0.20	290.51	0.02	0.63	0.00	5.49	0.00	1.50	0.00
12	7,235.79	0.46	367.45	0.02	0.42	0.00	0.07	0.00	0.16	0.00
14	6,827.40	0.43	465.35	0.03	1.99	0.00	1.26	0.00	1.36	0.00
16	8,298.55	0.52	350.54	0.02	2.41	0.00	2.80	0.00	2.13	0.00
18	8,722.72	0.55	5,160.95	0.32	0.91	0.00	0.17	0.00	0.09	0.00
21	8,865.02	0.56	2,818.62	0.18	2.58	0.00	0.06	0.00	1.13	0.00
25	9,434.59	0.59	4,140.13	0.26	1.35	0.00	0.13	0.00	0.83	0.00
28	8,042.97	0.51	7,603.93	0.47	0.01	0.00	0.01	0.00	0.04	0.00
31	5,222.81	0.33	6,231.66	0.39	0.04	0.00	0.03	0.00	11.50	0.00
35	7,882.33	0.50	7,018.33	0.44	7.96	0.00	1.21	0.00	21.35	0.00
38	7,329.25	0.46	1,400.27	0.09	3.11	0.00	6.42	0.00	13.95	0.00
41	6,268.20	0.39	5,816.45	0.36	11.49	0.00	15.06	0.00	44.71	0.00
45	6,724.30	0.42	7,306.62	0.45	2.34	0.00	5.14	0.00	64.10	0.00
48	7,249.93	0.46	6,151.78	0.38	13.82	0.00	7.77	0.00	25.28	0.00
51	7,508.61	0.47	4,533.57	0.28	14.59	0.00	14.89	0.00	130.94	0.01
54	7,306.54	0.46	5,941.78	0.37	30.92	0.00	15.69	0.00	177.12	0.01
57	7,157.44	0.45	5,104.73	0.32	34.32	0.00	21.31	0.00	161.55	0.01
60	7,479.74	0.47	3,925.15	0.24	29.83	0.00	16.51	0.00	286.66	0.02
63	7,828.52	0.49	5,832.58	0.36	90.42	0.01	16.29	0.00	423.19	0.03
66	8,859.30	0.56	3,526.21	0.22	66.43	0.00	36.48	0.00	480.82	0.03
69	5,090.88	0.32	5,334.42	0.33	79.60	0.01	10.82	0.00	682.60	0.04
72	6,607.76	0.42	6,693.12	0.42	475.47	0.03	10.52	0.00	1,060.31	0.07
87	6,018.67	0.38	4,189.33	0.26	269.35	0.02	231.95	0.01	1,603.51	0.10
90	6,539.90	0.41	4,132.15	0.26	269.11	0.02	232.85	0.01	1,621.46	0.10
108	6,224.10	0.39	6,506.72	0.40	877.93	0.06	1,608.49	0.10	1,943.03	0.12
117	4,696.66	0.30	6,187.99	0.38	1,008.73	0.06	1,216.11	0.08	2,375.90	0.15
120	4,095.61	0.26	6,659.83	0.41	1,102.95	0.07	1,038.85	0.06	2,400.09	0.15
123	3,092.59	0.19	7,879.12	0.49	849.31	0.05	1,022.93	0.06	2,394.24	0.15
126	4,829.95	0.30	6,836.58	0.42	1,086.67	0.07	1,205.12	0.07	2,186.83	0.14
129	9,423.96	0.59	6,806.27	0.42	3,412.88	0.21	2,730.06	0.17	3,189.91	0.20
132	5,761.17	0.36	2,576.83	0.16	4,203.27	0.26	1,985.24	0.12	2,762.06	0.17
138	4,244.16	0.27	5,888.54	0.37	1,511.93	0.10	1,993.49	0.12	2,567.22	0.16
141	3,437.29	0.22	6,583.34	0.41	1,520.97	0.10	2,318.95	0.14	2,489.28	0.15
144	3,323.95	0.21	6,670.50	0.41	1,383.34	0.09	2,258.16	0.14	2,460.34	0.15
147	5,945.49	0.37	6,419.44	0.40	1,418.78	0.09	2,439.54	0.15	2,797.77	0.17
150	2,944.56	0.19	4,829.56	0.30	2,133.50	0.13	2,596.99	0.16	2,706.92	0.17
153	3,119.85	0.20	5,862.47	0.36	1,775.26	0.11	2,127.91	0.13	2,764.01	0.17
156	2,616.03	0.16	6,464.72	0.40	1,678.04	0.11	1,979.93	0.12	2,661.28	0.17
159	4,719.18	0.30	7,220.45	0.45	4,681.98	0.29	3,468.03	0.22	3,718.51	0.23
242	5,629.94	0.35	7,965.37	0.49	2,897.08	0.18	3,340.45	0.21	3,923.34	0.24
248	3,258.54	0.21	4,464.69	0.28	2,772.12	0.17	2,860.70	0.18	3,523.66	0.22
255	2,907.45	0.18	4,569.46	0.28	2,174.05	0.14	2,798.62	0.17	3,400.35	0.21
271	3,599.77	0.23	3,890.32	0.24	3,081.27	0.19	2,652.39	0.16	3,219.33	0.20

Day	PHENANTHRENE									
	NM1		NM2		ACB1		ACB2		ACMS	
	Conc. (ppb)	C/Co	Conc. (ppb)	C/Co	Conc. (ppb)	C/Co	Conc. (ppb)	C/Co	Conc. (ppb)	C/Co
0	9.09	0.02	0.21	0.00	13.78	0.04	0.53	0.00	16.14	0.04
1	8.79	0.02	1.98	0.01	13.93	0.04	0.66	0.00	1.30	0.00
4	0.19	0.00	0.07	0.00	9.26	0.02	0.43	0.00	0.04	0.00
6	8.71	0.02	6.40	0.02	8.02	0.02	0.29	0.00	0.06	0.00
8	8.17	0.02	7.22	0.02	7.04	0.02	0.14	0.00	1.58	0.00
10	3.70	0.01	0.37	0.00	2.43	0.01	0.05	0.00	0.99	0.00
12	9.22	0.02	1.58	0.00	3.99	0.01	0.76	0.00	1.27	0.00
14	11.69	0.03	2.44	0.01	3.37	0.01	0.53	0.00	0.32	0.00
16	16.78	0.05	2.96	0.01	1.98	0.01	1.31	0.00	1.20	0.00
18	16.78	0.05	14.27	0.04	1.80	0.00	1.17	0.00	1.20	0.00
21	42.89	0.12	7.68	0.02	1.39	0.00	0.05	0.00	0.53	0.00
25	68.37	0.18	13.10	0.03	9.55	0.03	0.37	0.00	1.14	0.00
28	61.25	0.17	63.77	0.17	0.54	0.00	0.15	0.00	1.35	0.00
31	79.97	0.24	83.01	0.22	0.54	0.00	0.68	0.00	0.76	0.00
35	104.26	0.32	107.98	0.29	0.55	0.00	1.95	0.01	2.39	0.01
38	65.83	0.20	147.32	0.39	0.60	0.00	0.60	0.00	2.02	0.01
41	142.75	0.44	263.30	0.70	0.62	0.00	2.09	0.01	0.42	0.00
45	134.86	0.41	262.89	0.70	15.90	0.04	1.06	0.00	2.01	0.01
48	121.66	0.37	257.50	0.68	6.08	0.02	1.76	0.00	6.60	0.02
51	107.82	0.33	273.56	0.73	3.09	0.01	2.81	0.01	0.47	0.00
54	111.23	0.34	259.46	0.69	3.02	0.01	9.18	0.02	1.09	0.00
57	136.50	0.42	312.19	0.83	13.29	0.04	1.15	0.00	0.95	0.00
60	118.73	0.36	359.99	0.96	0.17	0.00	0.76	0.00	0.59	0.00
63	168.97	0.52	327.30	0.87	1.53	0.00	1.45	0.00	0.38	0.00
66	197.27	0.60	265.52	0.70	1.08	0.00	2.79	0.01	2.24	0.01
69	86.86	0.27	234.91	0.62	0.87	0.00	5.28	0.01	0.64	0.00
72	146.19	0.45	221.50	0.59	2.91	0.01	0.22	0.00	2.88	0.01
87	204.68	0.63	204.62	0.54	1.98	0.01	12.63	0.03	3.48	0.01
90	222.40	0.68	201.83	0.54	1.98	0.01	12.68	0.03	3.51	0.01
108			184.93	0.49	6.38	0.02	9.83	0.03	3.14	0.01
117			301.37	0.80	9.33	0.03	14.19	0.04	12.27	0.03
120	585.82	1.58	276.08	0.73	14.86	0.04	18.13	0.05	13.54	0.04
123	413.44	1.11	321.22	0.85	0.90	0.00	2.10	0.01	2.65	0.01
126										
129										
132	405.47	1.09	61.45	0.16	1.26	0.00	2.83	0.01	0.59	0.00
138	430.10	1.16	150.89	0.40	0.54	0.00	1.89	0.01	14.43	0.04
141	345.90	0.93	146.13	0.39	0.79	0.00	4.01	0.01	4.12	0.01
144	316.18	0.85	131.21	0.35	2.18	0.01	0.42	0.00	5.09	0.01
147	331.38	0.89	116.91	0.31	1.13	0.00	3.05	0.01	1.11	0.00
150	265.95	0.72	146.74	0.39	1.77	0.00	1.37	0.00	1.78	0.00
153	298.39	0.80	135.46	0.36	1.68	0.00	2.71	0.01	6.49	0.02
156	172.62	0.47	152.33	0.40	2.81	0.01	0.62	0.00	2.95	0.01
159	250.01	0.67	116.30	0.31	0.60	0.00	0.20	0.00	0.28	0.00
242	137.18	0.37	119.44	0.32	0.44	0.00	0.72	0.00	0.60	0.00
248	116.29	0.31	125.62	0.33	0.90	0.00	0.36	0.00	0.35	0.00
255	112.65	0.30	123.66	0.33	1.67	0.00	2.48	0.01	1.24	0.00
271	91.32	0.25	123.27	0.33	1.29	0.00	0.23	0.00	0.37	0.00

Day	PYRENE									
	NM1		NM2		ACB1		ACB2		ACMS	
	Conc. (ppb)	C/Co	Conc. (ppb)	C/Co	Conc. (ppb)	C/Co	Conc. (ppb)	C/Co	Conc. (ppb)	C/Co
0	0.64	0.03	1.13	0.06	0.38	0.02	0.53	0.03	0.33	0.02
1	0.86	0.04	1.52	0.08	0.26	0.01	0.16	0.01	0.39	0.02
4	1.42	0.07	1.43	0.07	0.06	0.00	0.61	0.03	0.31	0.02
6	0.01	0.00	0.04	0.00	1.11	0.05	0.42	0.02	2.53	0.13
8	0.19	0.01	0.56	0.03	0.75	0.04	0.42	0.02	0.53	0.03
10	1.26	0.06	1.59	0.08	1.39	0.07	0.58	0.03	0.88	0.04
12	0.15	0.01	0.44	0.02	0.01	0.00	0.01	0.00	0.24	0.01
14	0.15	0.01	0.39	0.02	0.12	0.01	0.22	0.01	0.73	0.04
16	0.30	0.01	1.41	0.07	0.47	0.02	0.95	0.05	0.19	0.01
18	0.13	0.01	3.45	0.17	0.06	0.00	0.08	0.00	0.44	0.02
21	0.28	0.01	2.23	0.11	0.03	0.00	1.00	0.05	0.12	0.01
25	0.11	0.01	3.87	0.20	0.11	0.01	0.22	0.01	0.07	0.00
28	0.01	0.00	7.78	0.39	0.03	0.00	0.42	0.02	0.23	0.01
31	0.02	0.00	7.05	0.36	0.01	0.00	0.00	0.00	0.00	0.00
35	0.00	0.00	16.09	0.82	0.03	0.00	0.07	0.00	0.20	0.01
38	0.54	0.03	0.53	0.03	0.14	0.01	0.28	0.01	0.08	0.00
41	1.08	0.05	1.95	0.10	0.39	0.02	0.21	0.01	0.11	0.01
45	1.42	0.07	25.26	1.28	0.14	0.01	0.10	0.01	0.12	0.01
48	1.29	0.06	21.46	1.09	0.10	0.00	0.13	0.01	0.08	0.00
51	7.66	0.37	33.49	1.70	0.12	0.01	0.27	0.01	0.07	0.00
54	6.37	0.31	16.72	0.85	0.10	0.00	0.12	0.01	0.09	0.00
57	2.73	0.13	20.86	1.06	0.07	0.00	0.09	0.00	27.04	
60	3.44	0.17	29.02	1.47	0.08	0.00	0.09	0.00	0.06	0.00
63	0.38	0.02	10.50	0.53	0.12	0.01	0.13	0.01	0.04	0.00
66	3.00	0.15	27.06	1.37	0.55	0.03	0.68	0.03	0.21	0.01
69	3.10	0.15	26.21	1.33	0.15	0.01	0.44	0.02	0.39	0.02
72	12.79	0.62	30.61	1.55	0.46	0.02	0.25	0.01	0.37	0.02
87	6.84	0.33	23.81	1.21	2.31	0.11	1.37	0.07	0.92	0.05
90	7.44	0.36	23.49	1.19	2.31	0.11	1.38	0.07	0.93	0.05
108	11.56	0.56	19.49	0.99	0.15	0.01	2.26	0.11	0.08	0.00
117	16.95	0.83	20.19	1.03	0.37	0.02	1.45	0.07	0.24	0.01
120	15.62	0.76	25.00	1.27	0.03	0.00	4.66	0.24	0.28	0.01
123	20.50	1.00	29.71	1.51	0.16	0.01	0.22	0.01	0.04	0.00
126	29.11	1.42	21.41	1.09	0.49	0.02	0.15	0.01	0.50	0.03
129	26.13	1.28	23.59	1.20	1.36	0.07	1.02	0.05	0.56	0.03
132	23.34	1.14	5.59	0.28	1.50	0.07	0.22	0.01	0.21	0.01
138	31.37	1.53	11.95	0.61	1.17	0.06	0.28	0.01	0.85	0.04
141	30.20	1.47	16.96	0.86	3.13	0.15	0.28	0.01	0.14	0.01
144	22.75	1.11	15.37	0.78	0.23	0.01	0.36	0.02	0.33	0.02
147	31.39	1.53	12.69	0.64	0.06	0.00	0.08	0.00	0.20	0.01
150	35.26	1.72	17.22	0.87	2.34	0.11	1.02	0.05	0.25	0.01
153	34.88	1.70	17.69	0.90	0.39	0.02	0.53	0.03	0.36	0.02
156	30.15	1.47	18.28	0.93	0.74	0.04	0.20	0.01	0.46	0.02
159	27.68	1.35	14.83	0.75	0.03	0.00	0.47	0.02	0.09	0.00
242	41.99	2.05	12.34	0.63	0.35	0.02	0.09	0.00	0.26	0.01
248	45.66	2.23	11.25	0.57	0.70	0.03	0.07	0.00	0.06	0.00
255	45.40	2.22	13.31	0.68	1.95	0.10	2.92	0.15	1.59	0.08
271	42.96	2.10	12.18	0.62	1.42	0.07	0.14	0.01	0.08	0.00

APPENDIX D:

Column Studies Data
(Effluent Data Normalized by Steady State Effluent Data, C/C_{SS})

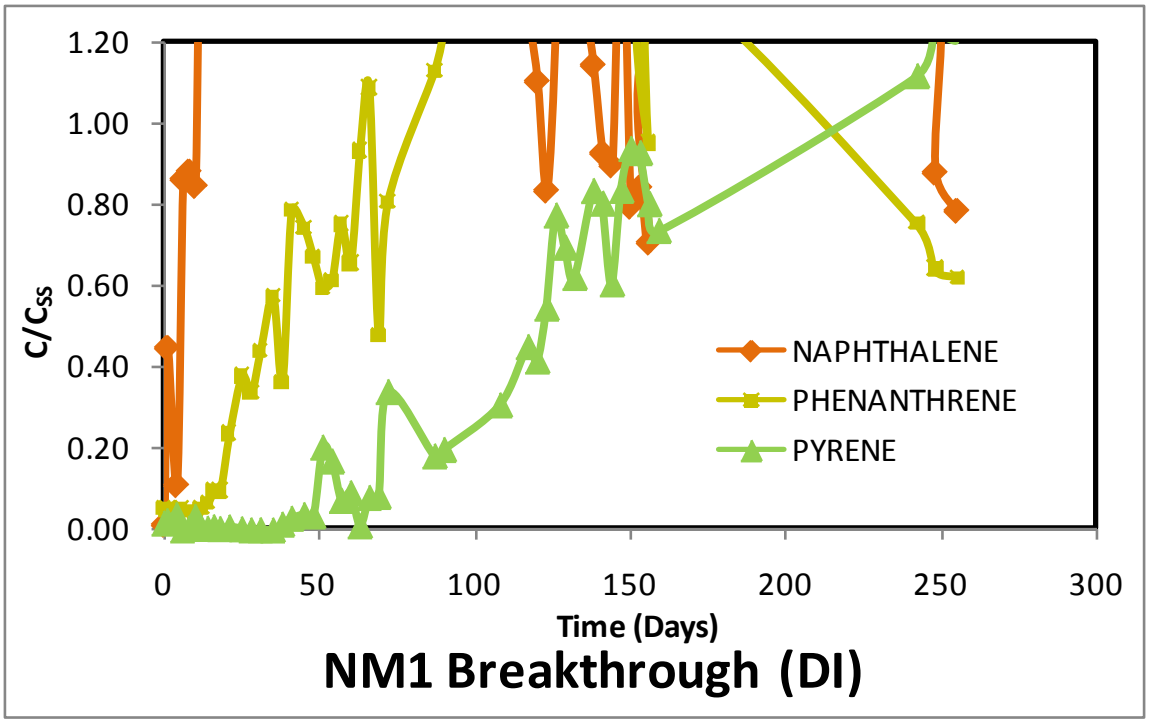
1.20
1.00
0.80
0.60
0.40
0.20
0.00
C/Css
0
50
100
150
200
250
300
Time (Days)
NAPHTHALENE
PHENANTHRENE
PYRENE
NM1 Breakthrough (DI)

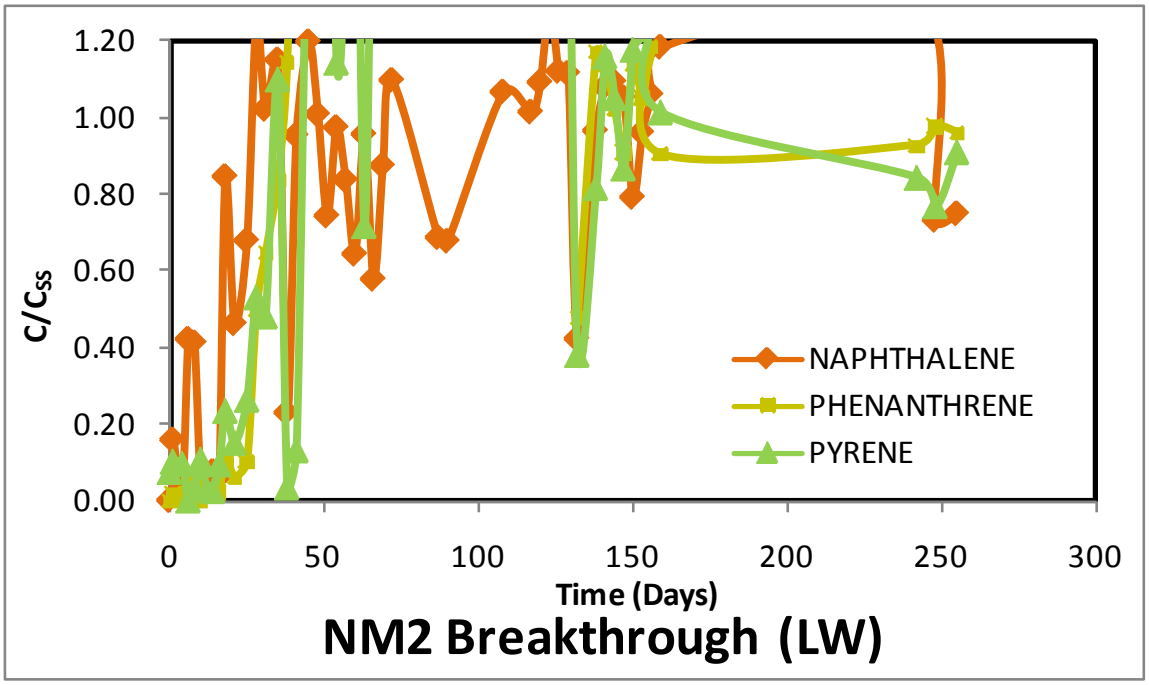
1.20
1.00
0.80
0.60
0.40
0.20
0.00
C/Css
0
50
100
150
200
250
300
Time (Days)
NAPHTHALENE
PHENANTHRENE
PYRENE
NM2 Breakthrough (LW)

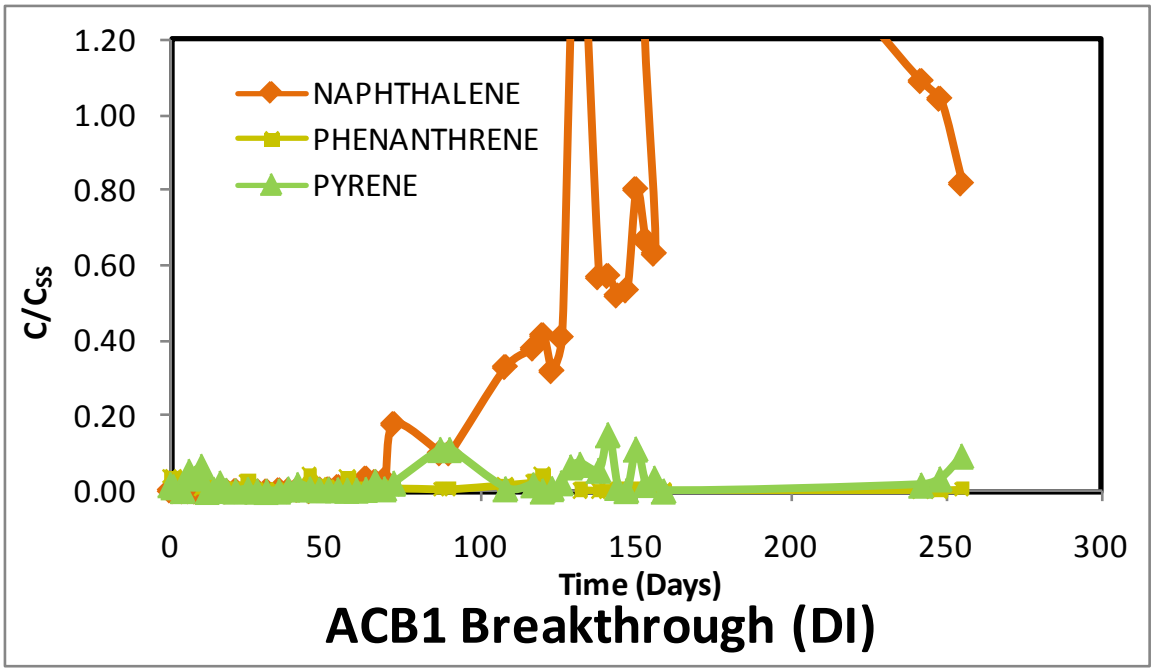
1.20
1.00
0.80
0.60
0.40
0.20
0.00
C/Css
NAPHTHALENE
PHENANTHRENE
PYRENE
0
50
100
150
200
250
300
Time (Days)
ACB1 Breakthrough (DI)

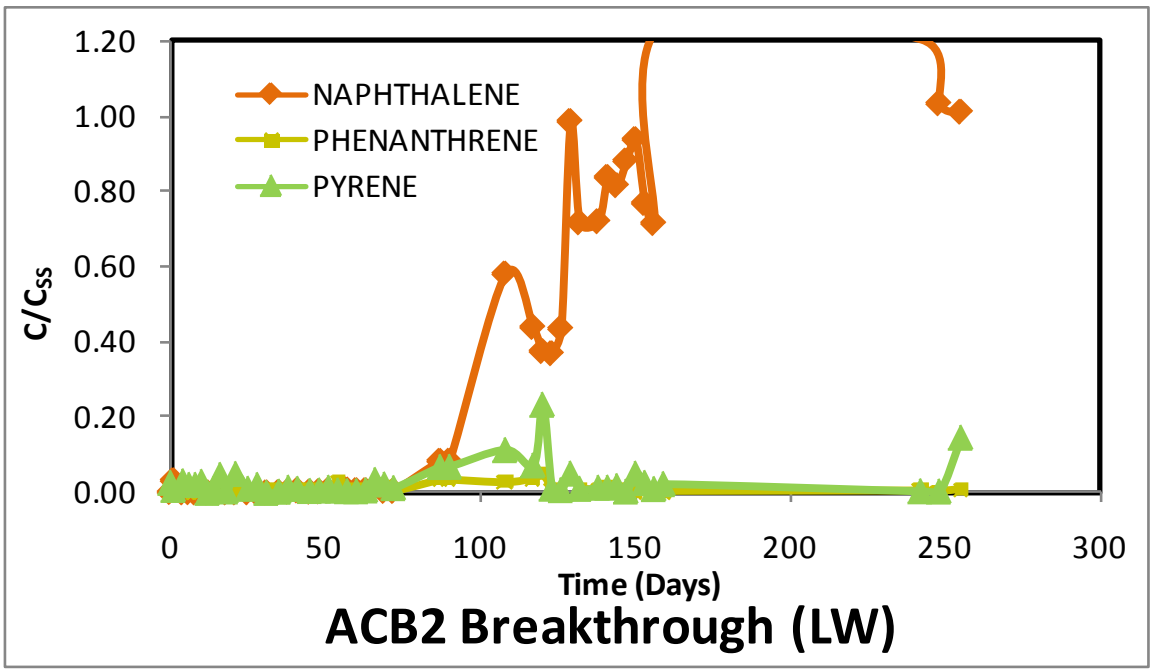
1.20
1.00
0.80
0.60
0.40
0.20
0.00
C/Css
NAPHTHALENE
PHENANTHRENE
PYRENE
0
50
100
150
200
250
300
Time (Days)
ACB2 Breakthrough (LW)

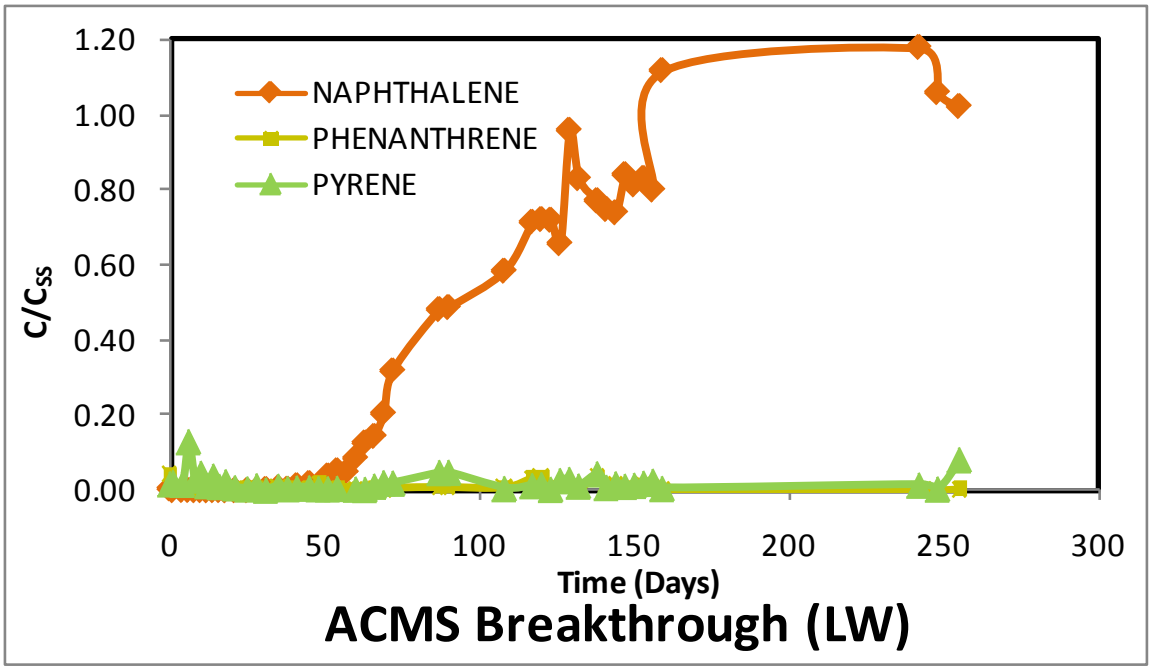
1.20
1.00
0.80
0.60
0.40
0.20
0.00
C/Css
NAPHTHALENE
PHENANTHRENE
PYRENE
0
50
100
150
200
250
300
Time (Days)
ACMS Breakthrough (LW)

Day	NAPHTHALENE									
	NM1		NM2		ACB1		ACB2		ACMS	
	Conc. (ppb)	C/C_{ss}	Conc. (ppb)	C/C_{ss}	Conc. (ppb)	C/C_{ss}	Conc. (ppb)	C/C_{ss}	Conc. (ppb)	C/C_{ss}
0	27.11	0.01	4.55	0.00	7.86	0.00	2.99	0.00	17.95	0.01
1	1,650.60	0.45	970.12	0.16	2.10	0.00	89.01	0.03	1.05	0.00
4	390.20	0.11	166.68	0.03	1.40	0.00	0.21	0.00	2.94	0.00
6	3,197.50	0.86	2,571.72	0.42	1.82	0.00	1.47	0.00	2.97	0.00
8	3,267.87	0.88	2,515.30	0.41	0.49	0.00	0.31	0.00	0.87	0.00
10	3,134.63	0.85	290.51	0.05	0.63	0.00	5.49	0.00	1.50	0.00
12	7,235.79	1.95	367.45	0.06	0.42	0.00	0.07	0.00	0.16	0.00
14	6,827.40	1.84	465.35	0.08	1.99	0.00	1.26	0.00	1.36	0.00
16	8,298.55	2.24	350.54	0.06	2.41	0.00	2.80	0.00	2.13	0.00
18	8,722.72	2.35	5,160.95	0.85	0.91	0.00	0.17	0.00	0.09	0.00
21	8,865.02	2.39	2,818.62	0.46	2.58	0.00	0.06	0.00	1.13	0.00
25	9,434.59	2.54	4,140.13	0.68	1.35	0.00	0.13	0.00	0.83	0.00
28	8,042.97	2.17	7,603.93	1.25	0.01	0.00	0.01	0.00	0.04	0.00
31	5,222.81	1.41	6,231.66	1.02	0.04	0.00	0.03	0.00	11.50	0.00
35	7,882.33	2.13	7,018.33	1.15	7.96	0.00	1.21	0.00	21.35	0.01
38	7,329.25	1.98	1,400.27	0.23	3.11	0.00	6.42	0.00	13.95	0.00
41	6,268.20	1.69	5,816.45	0.95	11.49	0.00	15.06	0.01	44.71	0.01
45	6,724.30	1.81	7,306.62	1.20	2.34	0.00	5.14	0.00	64.10	0.02
48	7,249.93	1.95	6,151.78	1.01	13.82	0.01	7.77	0.00	25.28	0.01
51	7,508.61	2.02	4,533.57	0.74	14.59	0.01	14.89	0.01	130.94	0.04
54	7,306.54	1.97	5,941.78	0.98	30.92	0.01	15.69	0.01	177.12	0.05
57	7,157.44	1.93	5,104.73	0.84	34.32	0.01	21.31	0.01	161.55	0.05
60	7,479.74	2.02	3,925.15	0.64	29.83	0.01	16.51	0.01	286.66	0.09
63	7,828.52	2.11	5,832.58	0.96	90.42	0.03	16.29	0.01	423.19	0.13
66	8,859.30	2.39	3,526.21	0.58	66.43	0.02	36.48	0.01	480.82	0.14
69	5,090.88	1.37	5,334.42	0.88	79.60	0.03	10.82	0.00	682.60	0.20
72	6,607.76	1.78	6,693.12	1.10	475.47	0.18	10.52	0.00	1,060.31	0.32
87	6,018.67	1.62	4,189.33	0.69	269.35	0.10	231.95	0.08	1,603.51	0.48
90	6,539.90	1.76	4,132.15	0.68	269.11	0.10	232.85	0.08	1,621.46	0.49
108	6,224.10	1.68	6,506.72	1.07	877.93	0.33	1,608.49	0.58	1,943.03	0.58
117	4,696.66	1.27	6,187.99	1.02	1,008.73	0.38	1,216.11	0.44	2,375.90	0.71
120	4,095.61	1.10	6,659.83	1.09	1,102.95	0.41	1,038.85	0.38	2,400.09	0.72
123	3,092.59	0.83	7,879.12	1.29	849.31	0.32	1,022.93	0.37	2,394.24	0.72
126	4,829.95	1.30	6,836.58	1.12	1,086.67	0.41	1,205.12	0.44	2,186.83	0.66
129	9,423.96	2.54	6,806.27	1.12	3,412.88	1.28	2,730.06	0.99	3,189.91	0.96
132	5,761.17	1.55	2,576.83	0.42	4,203.27	1.58	1,985.24	0.72	2,762.06	0.83
138	4,244.16	1.14	5,888.54	0.97	1,511.93	0.57	1,993.49	0.72	2,567.22	0.77
141	3,437.29	0.93	6,583.34	1.08	1,520.97	0.57	2,318.95	0.84	2,489.28	0.75
144	3,323.95	0.90	6,670.50	1.10	1,383.34	0.52	2,258.16	0.82	2,460.34	0.74
147	5,945.49	1.60	6,419.44	1.05	1,418.78	0.53	2,439.54	0.88	2,797.77	0.84
150	2,944.56	0.79	4,829.56	0.79	2,133.50	0.80	2,596.99	0.94	2,706.92	0.81
153	3,119.85	0.84	5,862.47	0.96	1,775.26	0.67	2,127.91	0.77	2,764.01	0.83
156	2,616.03	0.71	6,464.72	1.06	1,678.04	0.63	1,979.93	0.72	2,661.28	0.80
159	4,719.18	1.27	7,220.45	1.19	4,681.98	1.76	3,468.03	1.26	3,718.51	1.12
242	5,629.94	1.52	7,965.37	1.31	2,897.08	1.09	3,340.45	1.21	3,923.34	1.18
248	3,258.54	0.88	4,464.69	0.73	2,772.12	1.04	2,860.70	1.04	3,523.66	1.06
255	2,907.45	0.78	4,569.46	0.75	2,174.05	0.82	2,798.62	1.01	3,400.35	1.02
C_{ss}	3,708.50		6,091.19		2,663.09		2,762.61		3,331.86	

Day	PHENANTHRENE									
	NM1		NM2		ACB1		ACB2		ACMS	
	Conc. (ppb)	C/C_{ss}	Conc. (ppb)	C/C_{ss}	Conc. (ppb)	C/C_{ss}	Conc. (ppb)	C/C_{ss}	Conc. (ppb)	C/C_{ss}
0	9.09	0.05	0.21	0.00	13.78	0.04	0.53	0.00	16.14	0.04
1	8.79	0.05	1.98	0.02	13.93	0.04	0.66	0.00	1.30	0.00
4	0.19	0.00	0.07	0.00	9.26	0.02	0.43	0.00	0.04	0.00
6	8.71	0.05	6.40	0.05	8.02	0.02	0.29	0.00	0.06	0.00
8	8.17	0.05	7.22	0.06	7.04	0.02	0.14	0.00	1.58	0.00
10	3.70	0.02	0.37	0.00	2.43	0.01	0.05	0.00	0.99	0.00
12	9.22	0.05	1.58	0.01	3.99	0.01	0.76	0.00	1.27	0.00
14	11.69	0.06	2.44	0.02	3.37	0.01	0.53	0.00	0.32	0.00
16	16.78	0.09	2.96	0.02	1.98	0.01	1.31	0.00	1.20	0.00
18	16.78	0.09	14.27	0.11	1.80	0.00	1.17	0.00	1.20	0.00
21	42.89	0.24	7.68	0.06	1.39	0.00	0.05	0.00	0.53	0.00
25	68.37	0.38	13.10	0.10	9.55	0.03	0.37	0.00	1.14	0.00
28	61.25	0.34	63.77	0.50	0.54	0.00	0.15	0.00	1.35	0.00
31	79.97	0.44	83.01	0.64	0.54	0.00	0.68	0.00	0.76	0.00
35	104.26	0.58	107.98	0.84	0.55	0.00	1.95	0.01	2.39	0.01
38	65.83	0.36	147.32	1.14	0.60	0.00	0.60	0.00	2.02	0.01
41	142.75	0.79	263.30	2.04	0.62	0.00	2.09	0.01	0.42	0.00
45	134.86	0.74	262.89	2.04	15.90	0.04	1.06	0.00	2.01	0.01
48	121.66	0.67	257.50	2.00	6.08	0.02	1.76	0.00	6.60	0.02
51	107.82	0.60	273.56	2.12	3.09	0.01	2.81	0.01	0.47	0.00
54	111.23	0.61	259.46	2.01	3.02	0.01	9.18	0.02	1.09	0.00
57	136.50	0.75	312.19	2.42	13.29	0.04	1.15	0.00	0.95	0.00
60	118.73	0.66	359.99	2.79	0.17	0.00	0.76	0.00	0.59	0.00
63	168.97	0.93	327.30	2.54	1.53	0.00	1.45	0.00	0.38	0.00
66	197.27	1.09	265.52	2.06	1.08	0.00	2.79	0.01	2.24	0.01
69	86.86	0.48	234.91	1.82	0.87	0.00	5.28	0.01	0.64	0.00
72	146.19	0.81	221.50	1.72	2.91	0.01	0.22	0.00	2.88	0.01
87	204.68	1.13	204.62	1.59	1.98	0.01	12.63	0.03	3.48	0.01
90	222.40	1.23	201.83	1.57	1.98	0.01	12.68	0.03	3.51	0.01
108			184.93	1.44	6.38	0.02	9.83	0.03	3.14	0.01
117			301.37	2.34	9.33	0.02	14.19	0.04	12.27	0.03
120	585.82	3.23	276.08	2.14	14.86	0.04	18.13	0.05	13.54	0.04
123	413.44	2.28	321.22	2.49	0.90	0.00	2.10	0.01	2.65	0.01
126										
129										
132	405.47	2.24	61.45	0.48	1.26	0.00	2.83	0.01	0.59	0.00
138	430.10	2.37	150.89	1.17	0.54	0.00	1.89	0.00	14.43	0.04
141	345.90	1.91	146.13	1.13	0.79	0.00	4.01	0.01	4.12	0.01
144	316.18	1.75	131.21	1.02	2.18	0.01	0.42	0.00	5.09	0.01
147	331.38	1.83	116.91	0.91	1.13	0.00	3.05	0.01	1.11	0.00
150	265.95	1.47	146.74	1.14	1.77	0.00	1.37	0.00	1.78	0.00
153	298.39	1.65	135.46	1.05	1.68	0.00	2.71	0.01	6.49	0.02
156	172.62	0.95	152.33	1.18	2.81	0.01	0.62	0.00	2.95	0.01
159	250.01	1.38	116.30	0.90	0.60	0.00	0.20	0.00	0.28	0.00
242	137.18	0.76	119.44	0.93	0.44	0.00	0.72	0.00	0.60	0.00
248	116.29	0.64	125.62	0.98	0.90	0.00	0.36	0.00	0.35	0.00
255	112.65	0.62	123.66	0.96	1.67	0.00	2.48	0.01	1.24	0.00
C_{ss}	181.19		128.80							

Day	PYRENE									
	NM1		NM2		ACB1		ACB2		ACMS	
	Conc. (ppb)	C/C_{ss}	Conc. (ppb)	C/C_{ss}	Conc. (ppb)	C/C_{ss}	Conc. (ppb)	C/C_{ss}	Conc. (ppb)	C/C_{ss}
0	0.64	0.02	1.13	0.08	0.38	0.02	0.53	0.03	0.33	0.02
1	0.86	0.02	1.52	0.10	0.26	0.01	0.16	0.01	0.39	0.02
4	1.42	0.04	1.43	0.10	0.06	0.00	0.61	0.03	0.31	0.02
6	0.01	0.00	0.04	0.00	1.11	0.05	0.42	0.02	2.53	0.13
8	0.19	0.01	0.56	0.04	0.75	0.04	0.42	0.02	0.53	0.03
10	1.26	0.03	1.59	0.11	1.39	0.07	0.58	0.03	0.88	0.04
12	0.15	0.00	0.44	0.03	0.01	0.00	0.01	0.00	0.24	0.01
14	0.15	0.00	0.39	0.03	0.12	0.01	0.22	0.01	0.73	0.04
16	0.30	0.01	1.41	0.10	0.47	0.02	0.95	0.05	0.19	0.01
18	0.13	0.00	3.45	0.24	0.06	0.00	0.08	0.00	0.44	0.02
21	0.28	0.01	2.23	0.15	0.03	0.00	1.00	0.05	0.12	0.01
25	0.11	0.00	3.87	0.27	0.11	0.01	0.22	0.01	0.07	0.00
28	0.01	0.00	7.78	0.53	0.03	0.00	0.42	0.02	0.23	0.01
31	0.02	0.00	7.05	0.48	0.01	0.00	0.00	0.00	0.00	0.00
35	0.00	0.00	16.09	1.10	0.03	0.00	0.07	0.00	0.20	0.01
38	0.54	0.01	0.53	0.04	0.14	0.01	0.28	0.01	0.08	0.00
41	1.08	0.03	1.95	0.13	0.39	0.02	0.21	0.01	0.11	0.01
45	1.42	0.04	25.26	1.73	0.14	0.01	0.10	0.01	0.12	0.01
48	1.29	0.03	21.46	1.47	0.10	0.00	0.13	0.01	0.08	0.00
51	7.66	0.20	33.49	2.29	0.12	0.01	0.27	0.01	0.07	0.00
54	6.37	0.17	16.72	1.14	0.10	0.00	0.12	0.01	0.09	0.00
57	2.73	0.07	20.86	1.43	0.07	0.00	0.09	0.00	~~27.04~~	~~X~~
60	3.44	0.09	29.02	1.99	0.08	0.00	0.09	0.00	0.06	0.00
63	0.38	0.01	10.50	0.72	0.12	0.01	0.13	0.01	0.04	0.00
66	3.00	0.08	27.06	1.85	0.55	0.03	0.68	0.03	0.21	0.01
69	3.10	0.08	26.21	1.79	0.15	0.01	0.44	0.02	0.39	0.02
72	12.79	0.34	30.61	2.09	0.46	0.02	0.25	0.01	0.37	0.02
87	6.84	0.18	23.81	1.63	2.31	0.11	1.37	0.07	0.92	0.05
90	7.44	0.20	23.49	1.61	2.31	0.11	1.38	0.07	0.93	0.05
108	11.56	0.31	19.49	1.33	0.15	0.01	2.26	0.11	0.08	0.00
117	16.95	0.45	20.19	1.38	0.37	0.02	1.45	0.07	0.24	0.01
120	15.62	0.42	25.00	1.71	0.03	0.00	4.66	0.23	0.28	0.01
123	20.50	0.54	29.71	2.03	0.16	0.01	0.22	0.01	0.04	0.00
126	29.11	0.77	21.41	1.47	0.49	0.02	0.15	0.01	0.50	0.03
129	26.13	0.69	23.59	1.61	1.36	0.07	1.02	0.05	0.56	0.03
132	23.34	0.62	5.59	0.38	1.50	0.07	0.22	0.01	0.21	0.01
138	31.37	0.83	11.95	0.82	1.17	0.06	0.28	0.01	0.85	0.04
141	30.20	0.80	16.96	1.16	3.13	0.15	0.28	0.01	0.14	0.01
144	22.75	0.60	15.37	1.05	0.23	0.01	0.36	0.02	0.33	0.02
147	31.39	0.83	12.69	0.87	0.06	0.00	0.08	0.00	0.20	0.01
150	35.26	0.94	17.22	1.18	2.34	0.11	1.02	0.05	0.25	0.01
153	34.88	0.93	17.69	1.21	0.39	0.02	0.53	0.03	0.36	0.02
156	30.15	0.80	18.28	1.25	0.74	0.04	0.20	0.01	0.46	0.02
159	27.68	0.74	14.83	1.01	0.03	0.00	0.47	0.02	0.09	0.00
242	41.99	1.12	12.34	0.84	0.35	0.02	0.09	0.00	0.26	0.01
248	45.66	1.21	11.25	0.77	0.70	0.03	0.07	0.00	0.06	0.00
255	45.40	1.21	13.31	0.91	1.95	0.09	2.92	0.15	1.59	0.08
C_{ss}	37.63		14.61							

APPENDIX E:

Influent Sample Losses

Unflitered Sample Concentrations taken at the Influent Sampling Port / Reservoir Concentration

PAH	DI	LW
Naph	45%	42%
Phen	61%	69%
Pyr	11941%	182%

APPENDIX F:

McCormick & Baxter Site Maps

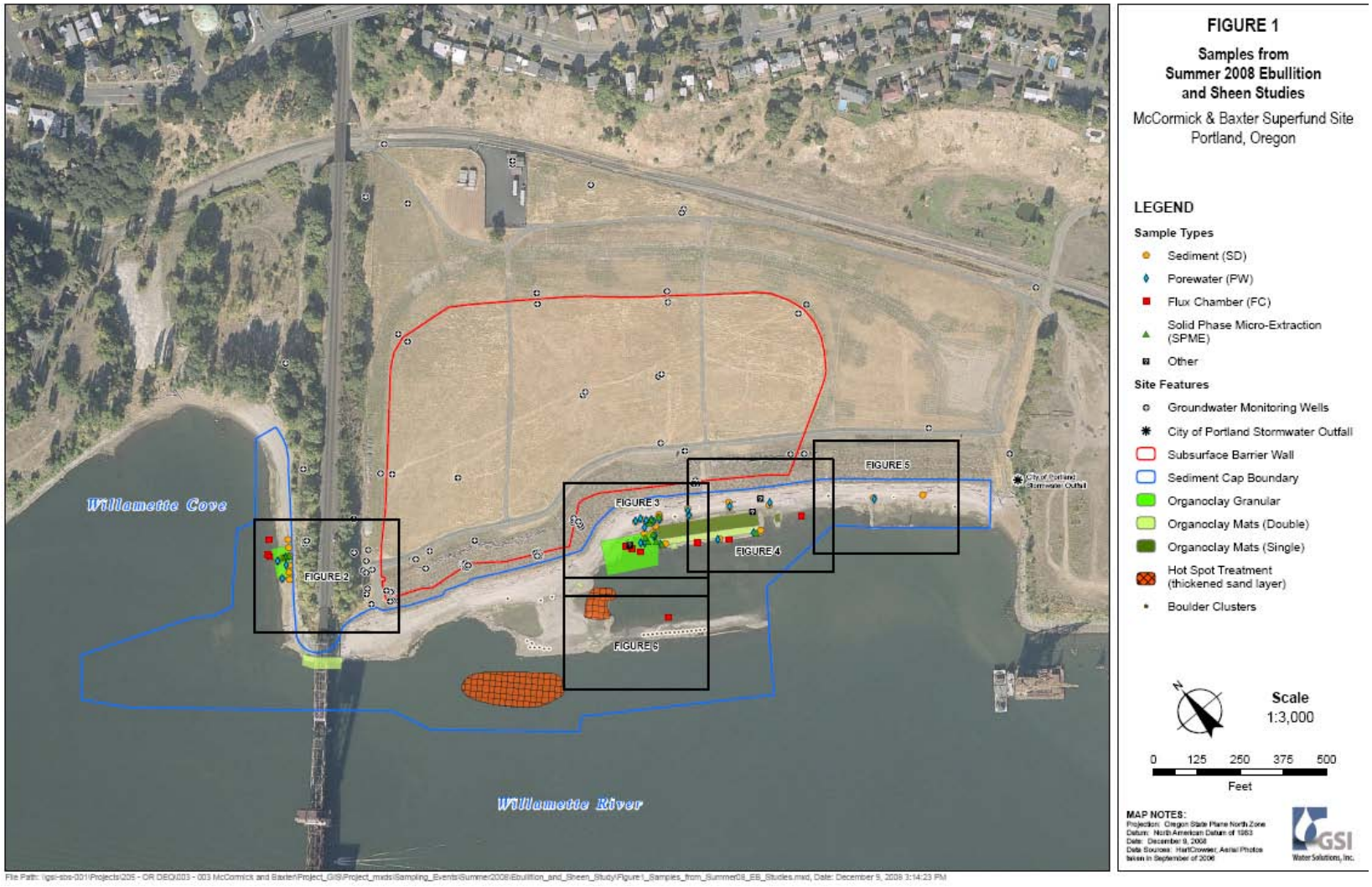

File Path: \\gsi-sbs-001\Projects\205 - OR DEQ\003 - 003 McCormick and Baxter\Project_GIS\Project_mxds\Sampling_Events\Summer2008\Ebullition_and_Sheen_Study\Figure1_Samples_from_Summer08_EB_Studies.mxd, Date: December 9, 2008 3:14:23 PM


WCFC-1
SD0808
MW-58s
MW-58i
MW-58d
SD0809
MW-Ds
EW-3s
WCFC-2
WCFC-3
SPME-WC-1
SPME-WC-2
SPME-WC-3
SD0803
PW0810
A
A'
SD0802
PW0802
EW-2s
SD0804
PW0804
MW-20i
MW-60d
MW-Gs
SD0807
SD0801
PW0801
SD0806
MW-34i
MW-36s
MW-36i
EW-10s
MW-37s
EW-15s
FIGURE 2
Willamette Cove Sampling Area
Summer 2008 Ebullition
and Sheen Studies
McCormick & Baxter Superfund Site
Portland, Oregon
LEGEND
Sample Types
Sediment (SD)
Porewater (PW)
Flux Chamber (FC)
Solid Phase Micro-Extraction (SPME)
Site Features
Groundwater Monitoring Well
Cross Section A-A'
Subsurface Barrier Wall
Sediment Cap Boundary
Organoclay Granular
Scale
1:360
0
15
30
45
60
Feet
MAP NOTES:
Projection: Oregon State Plane North Zone
Datum: North American Datum of 1983
Date: December 9, 2008
Data Sources: HartCrowser, Aerial Photos taken in September of 2006
GSI
Water Solutions, Inc.
File Path: \\gsi-sbs-001\Projects\205 - OR DEQ\003 - 003 McCormick and Baxter\Project_GIS\Project_mxds\Sampling_Events\Summer2008\Ebullition_and_Sheen_Study\Figure2_Samples_In_WC_Sampling_Area.mxd, Date: December 9, 2008 2:24:04 PM

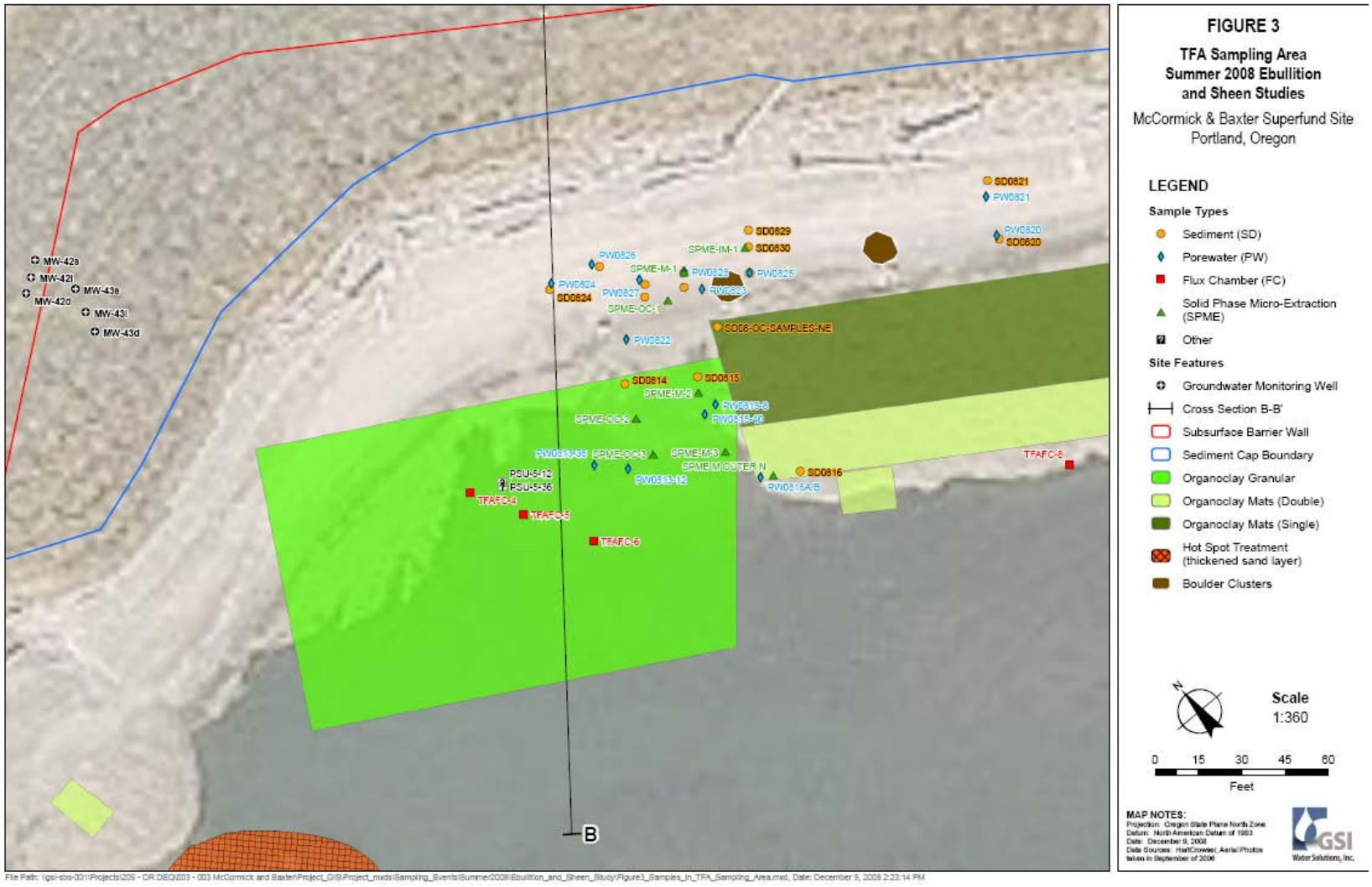
MW-42s
MW-42i
MW-42d
MW-43s
MW-43i
MW-43d
SD0821
PW0821
PW0820
SD0620
SD0829
SD0830
SPME-IM-1
PW0826
SPME-M-1
PW0828
PW0825
PW0824
SD0824
PW0827
PW0823
SPME-OC-1
SD06-OC-SAMPLES-NE
PW0822
SD0814
SD0815
SPME-M-2
PW0813-3
PW0813-40
SPME-OC-2
PW0813-35
SPME-OC-3
SPME-M-3
SPME M OUTER N
PW0813-12
SD0816
PW0816A/B
TFAFC-8
PSU-5-12
PSU-5-36
TFAFC-4
TFAFC-5
TFAFC-6
B
FIGURE 3
TFA Sampling Area
Summer 2008 Ebullition
and Sheen Studies
McCormick & Baxter Superfund Site
Portland, Oregon
LEGEND
Sample Types
Sediment (SD)
Porewater (PW)
Flux Chamber (FC)
Solid Phase Micro-Extraction (SPME)
Other
Site Features
Groundwater Monitoring Well
Cross Section B-B'
Subsurface Barrier Wall
Sediment Cap Boundary
Organoclay Granular
Organoclay Mats (Double)
Organoclay Mats (Single)
Hot Spot Treatment (thickened sand layer)
Boulder Clusters
N
Scale
1:360
0
15
30
45
60
Feet
MAP NOTES:
Projection: Oregon State Plane North Zone
Datum: North American Datum of 1983
Date: December 9, 2008
Data Sources: HartCrowser, Aerial Photos taken in September of 2006
GSI
Water Solutions, Inc.
File Path: \\gsi-sbs-001\Projects\205 - OR DEQ\003 - 003 McCormick and Baxter\Project_GIS\Project_mxds\Sampling_Events\Summer2008\Ebullition_and_Sheen_Study\Figure3_Samples_In_TFA_Sampling_Area.mxd, Date: December 9, 2008 2:23:14 PM

File Path: \\gsi-sbs-001\Projects\205 - OR DEQ\003 - 003 McCormick and Baxter\Project_GIS\Project_mxds\Sampling_Events\Summer2008\Ebullition_and_Sheen_Study\Figure4_Samples_In_TFA_Sampling_Area.mxd, Date: December 9, 2008 2:34:51 PM

FIGURE 5

TFA Sampling Area
Summer 2008 Ebullition and Sheen Studies

McCormick & Baxter Superfund Site
Portland, Oregon

LEGEND

Sample Types
- Sediment (SD)
- Porewater (PW)

Site Features
- Sediment Cap Boundary
- Boulder Clusters

N

Scale
1:360

0 15 30 45 60
Feet

MAP NOTES:
Projection: Oregon State Plane North Zone
Datum: North American Datum of 1983
Date: December 9, 2008
Data Sources: HartCrowser, Aerial Photos taken in September of 2006

GSI Water Solutions, Inc.

File Path: \\gsi-sbs-001\Projects\205 - OR DEQ\003 - 003 McCormick and Baxter\Project_GIS\Project_mxds\Sampling_Events\Summer2008\Ebullition_and_Sheen_Study\FigureS_Samples_In_TFA_Sampling_Area.mxd, Date: December 9, 2008 2:48:18 PM


B
TFAFC07
FIGURE 6
TFA Sampling Area
Summer 2008 Ebullition
and Sheen Studies
McCormick & Baxter Superfund Site
Portland, Oregon
LEGEND
Sample Types
Flux Chamber (FC)
Site Features
Cross Section B-B'
Organoclay Mats (Double)
Hot Spot Treatment
(thickened sand layer)
Boulder Clusters
N
Scale
1:360
0 15 30 45 60
Feet
MAP NOTES:
Projection: Oregon State Plane North Zone
Datum: North American Datum of 1983
Date: December 9, 2008
Data Sources: HartCrowser, Aerial Photos
taken in September of 2006
GSI
Water Solutions, Inc.
File Path: \\gsi-sbs-001\Projects\205 - OR DEQ\003 - 003 McCormick and Baxter\Project_GIS\Project_mxds\Sampling_Events\Summer2008\Ebullition_and_Sheen_Study\Figure6_Samples_In_TFA_Sampling_Area.mxd, Date: December 9, 2008 2:54:26 PM

APPENDIX G:

McCormick & Baxter Field Notes from Core Extrusions

Willamette Cove

MBSD0802 - Core through organoclay
Pore water sample collected - no SPME.

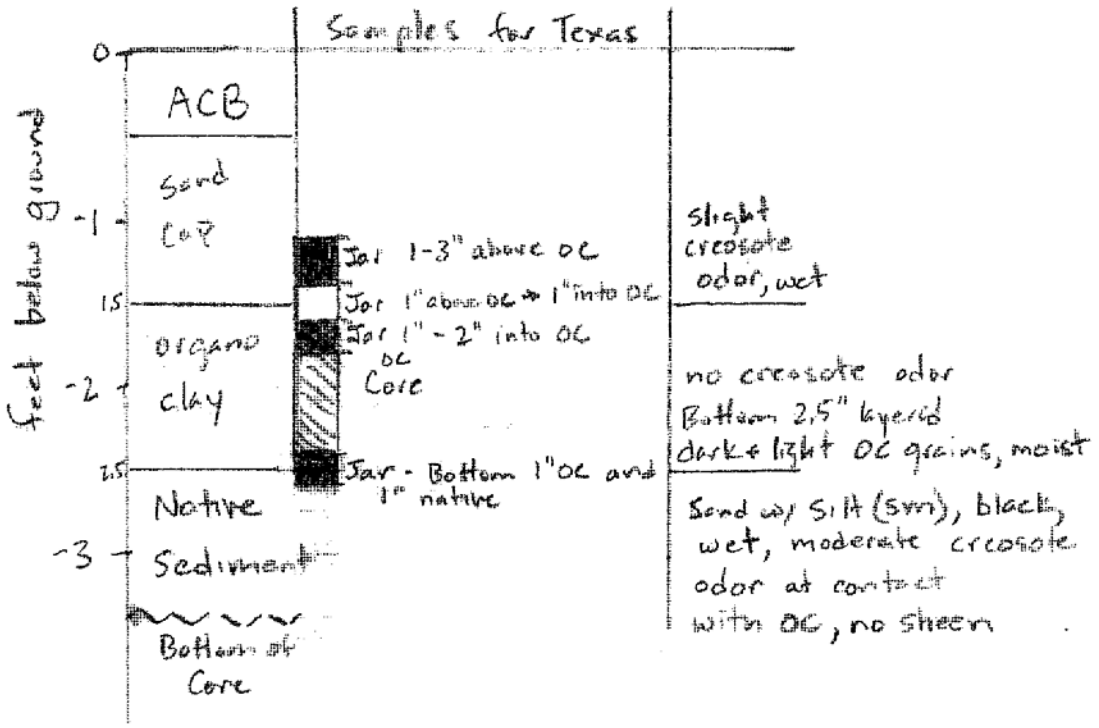

Note: Not a sharp boundary between OC and native sediment

Willamette Cove

In Native Sediment - MBSD0803(b)

- No Core
- Co-located w/ SPME-WC-1 (nearest bank outside of granular organoclay; SPME appeared to be placed in bentonite from Core abandonment)

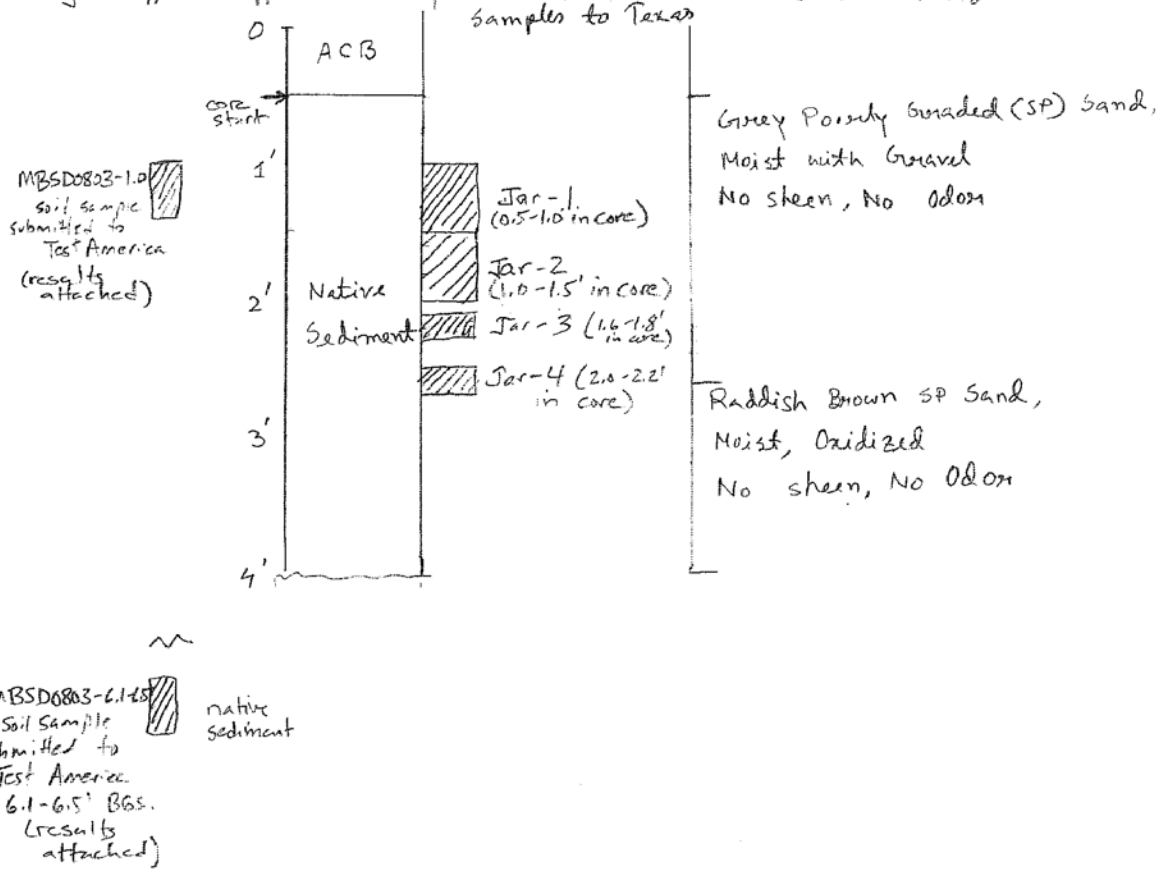

Willamette Cove

In organoclay; co-located MBSD080% with SPME-WC-3.

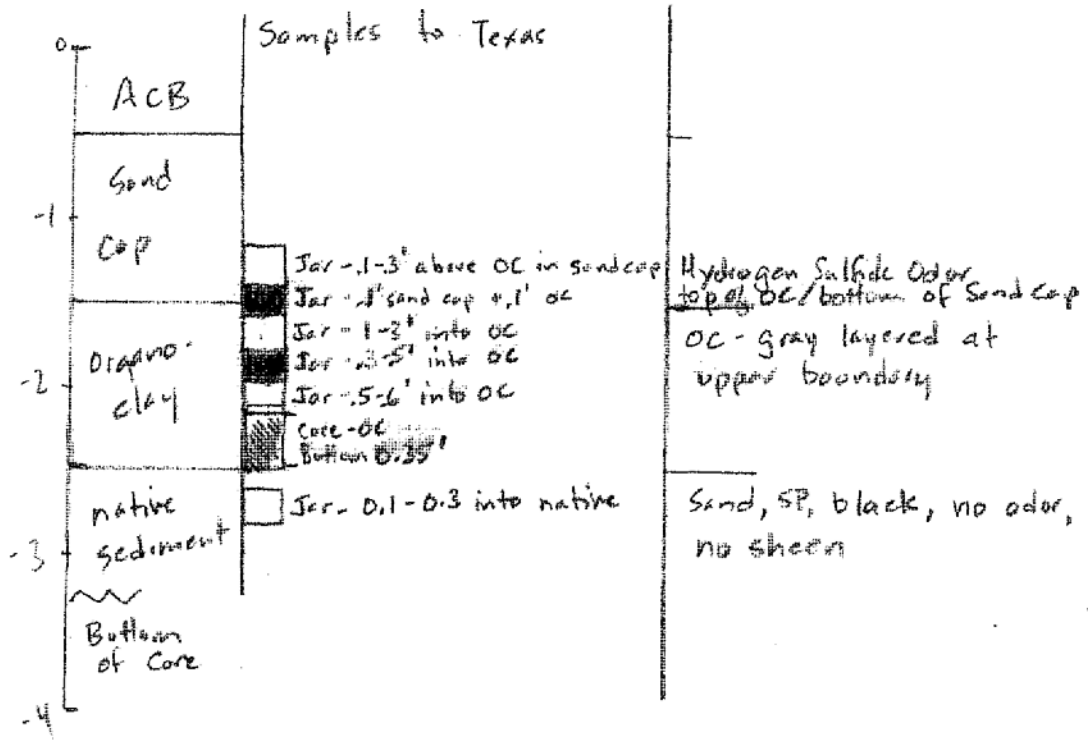

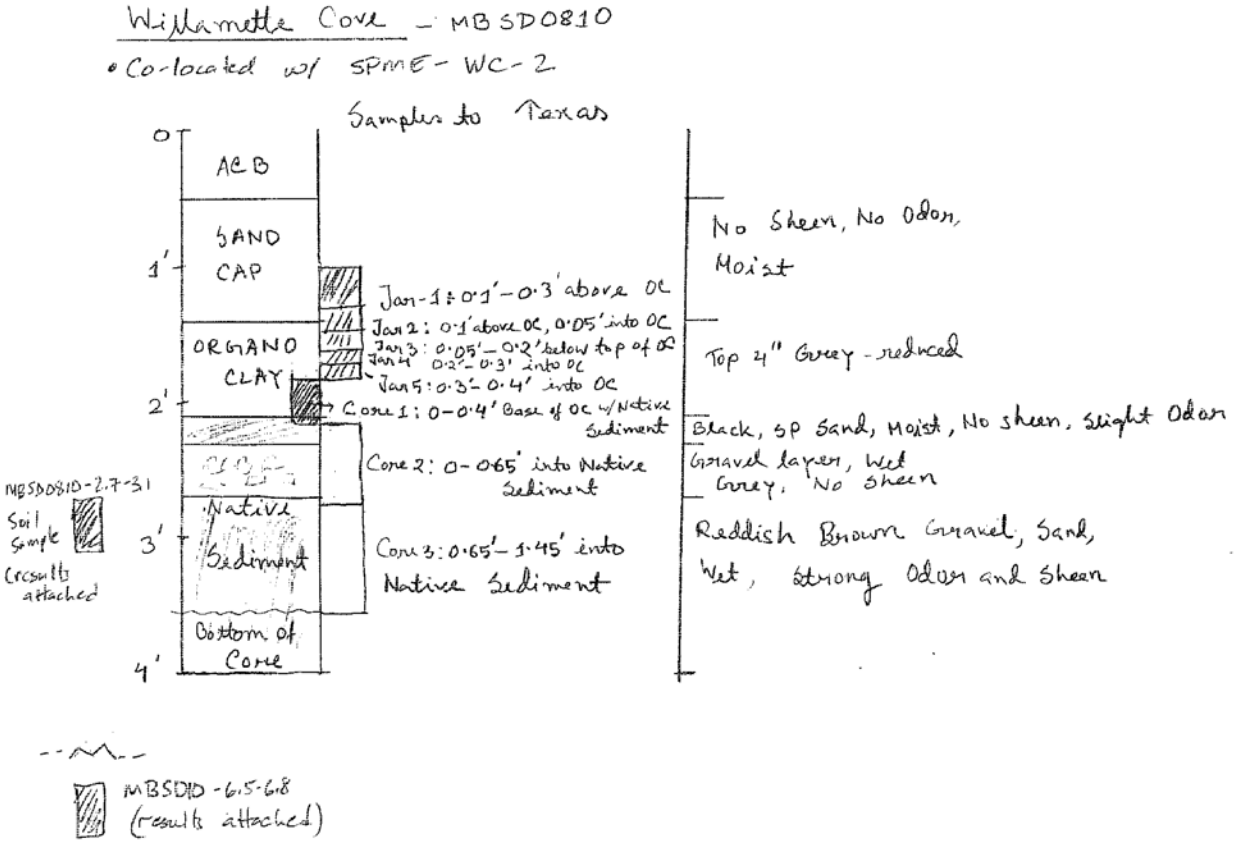
Willamette Cove – MBSD0810
• Co-located w/ SPME-WC-2
Samples to Texas
0
ACB
1'
SAND CAP
ORGANO CLAY
2'
3'
Native Sediment
Bottom of Core
4'
Jan-1: 0.1'–0.3' above OC
Jan 2: 0.1' above OC, 0.05' into OC
Jan 3: 0.05'–0.2' below top of OC
Jan 4 0.2'–0.3' into OC
Jan 5: 0.3'–0.4' into OC
Core 1: 0–0.4' Base of OC w/ Native Sediment
Core 2: 0–0.65' into Native Sediment
Core 3: 0.65'–1.45' into Native Sediment
No Sheen, No Odor, Moist
Top 4" Grey - reduced
Black, SP Sand, Moist, No sheen, slight Odor
Gravel layer, Wet
Grey, No Sheen
Reddish Brown Gravel, Sand, Wet, Strong Odor and Sheen
MBSD0810-2.7-3.1
Soil Sample
Results attached
MBSD10-6.5-6.8
(results attached)

Tank Farm Area (TFA)
Willamette River – MBSD0813

- Near SPME-OC-Z

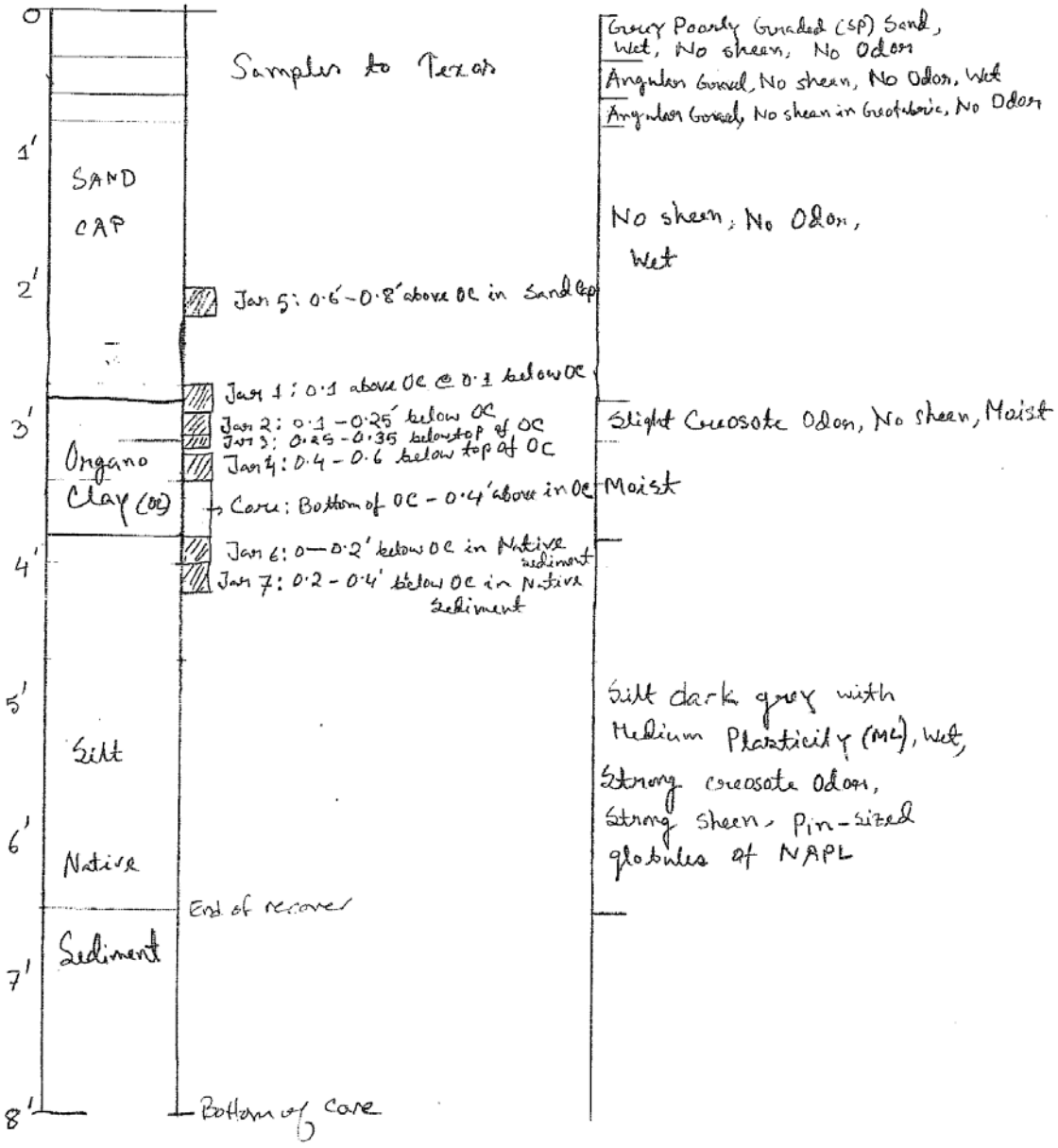

Willamette River

MBSD0822

Core advanced in trench (ie. rock + sand cap mostly removed). Co-located w/ SPME-OC-1 - however, SPME placed in rock + sand sediment cap adjacent to trench.

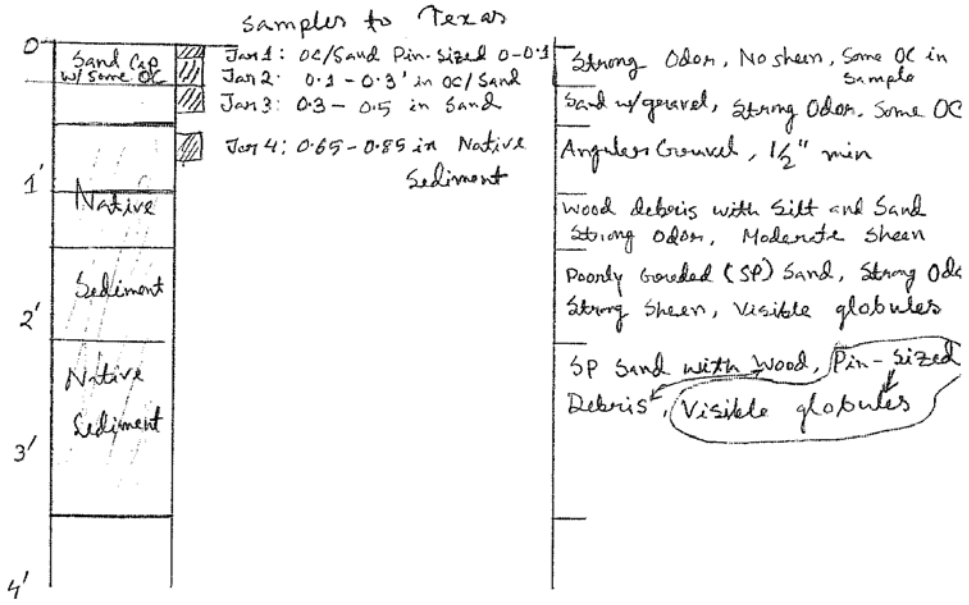

Notes: Organoclay not placed in top 3" of Sand cap, it (may have) floated into the sand cap layer. (during OC placement.)

Willamette River - Tank Farm Area

MBSD0823

10 feet riverward of (SPME-M-1) (which is co-located w/ MBSD0828)

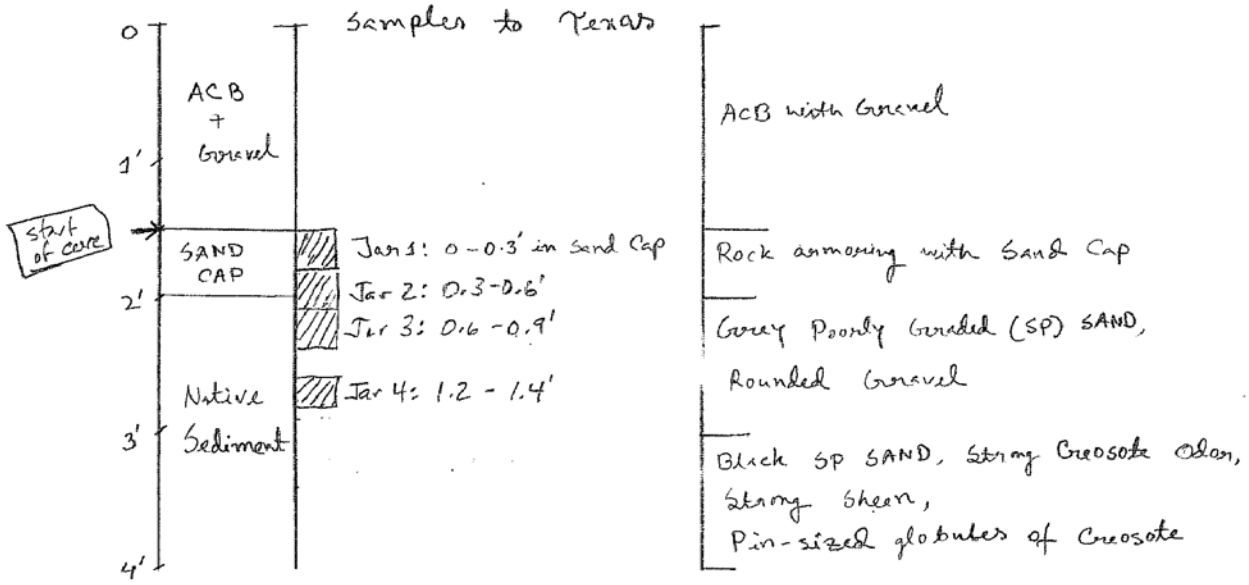

Notes: Boulder cluster near sampling location

Willamette River - MBSD0824

TFA - Not near an SPME. Shore ward of granular OC. Please analyze even though not assoc. w/ other Tx samples.

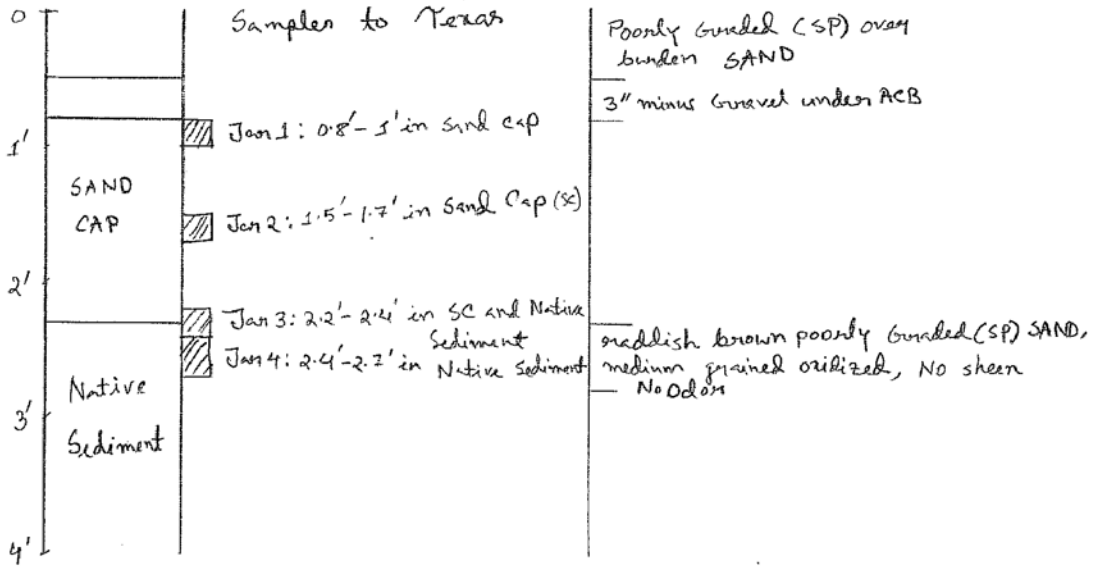

Willamette River - Tank Farm Area

MBSD0827 - Uppermost core of the OC transect, ~10' shoreward of SPME-OC-1 which is co-located with MBSD0822.

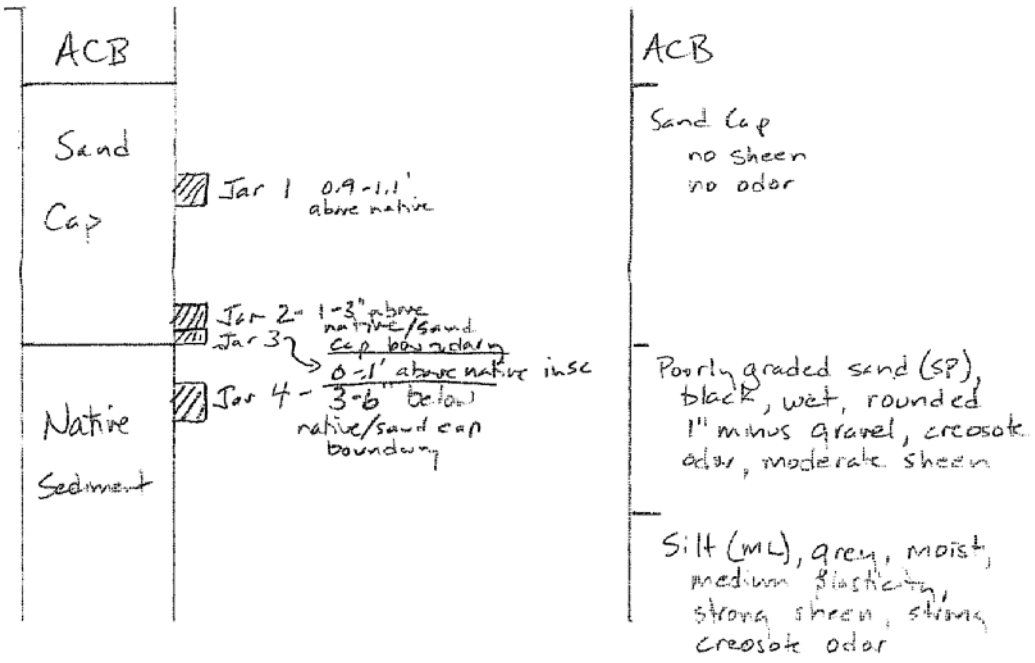

Willamette River, Tank Farm Area

MBSD0828 co-located w/ SPME-M-1

Uppermost core in transect adjacent to OC mat #2.

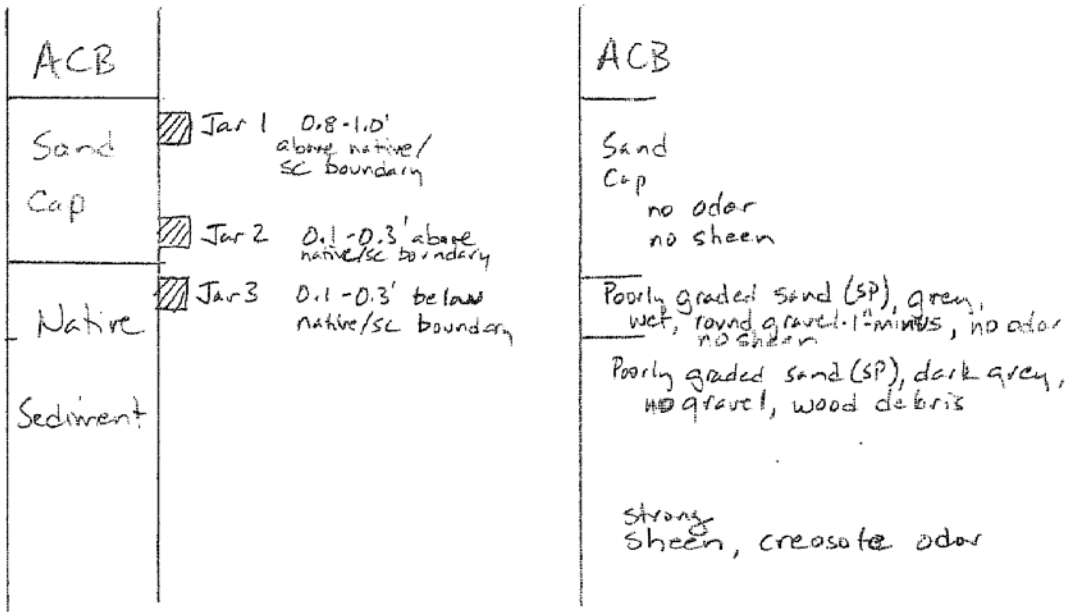

Willamette River - Tank Farm Area

MBSD0832 - SW corner of Mat #2

co-located w/ SPME-outer mat-S

(At 8/27/08 12:50 PM 3' below River Level)

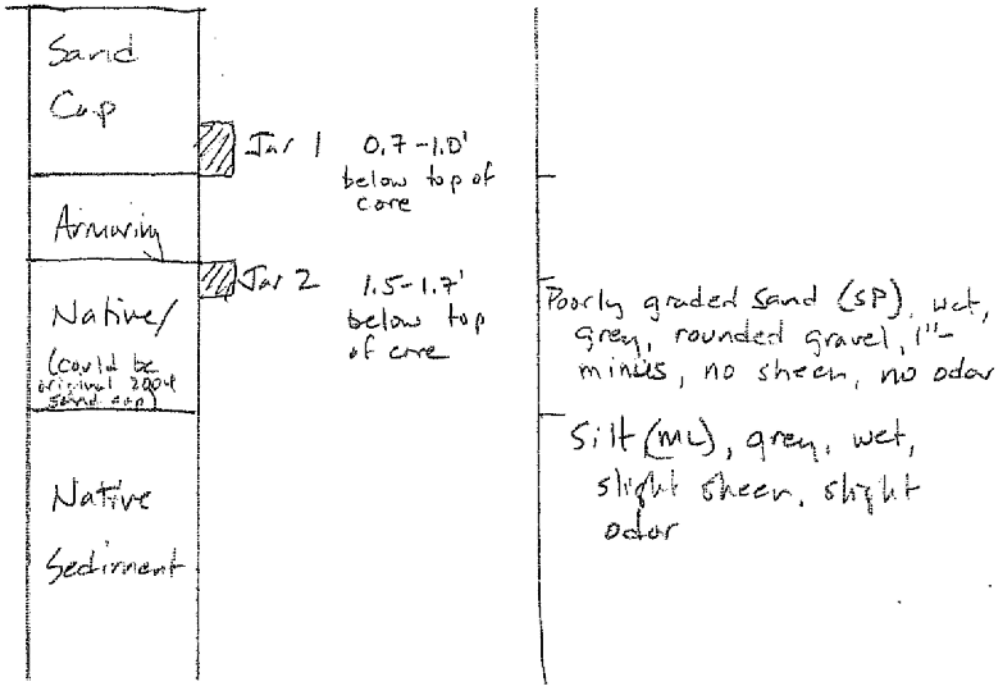

APPENDIX H:

Column Studies Raw Data
(Effluent Data Normalized by Measured Influent Data, C/C_0)

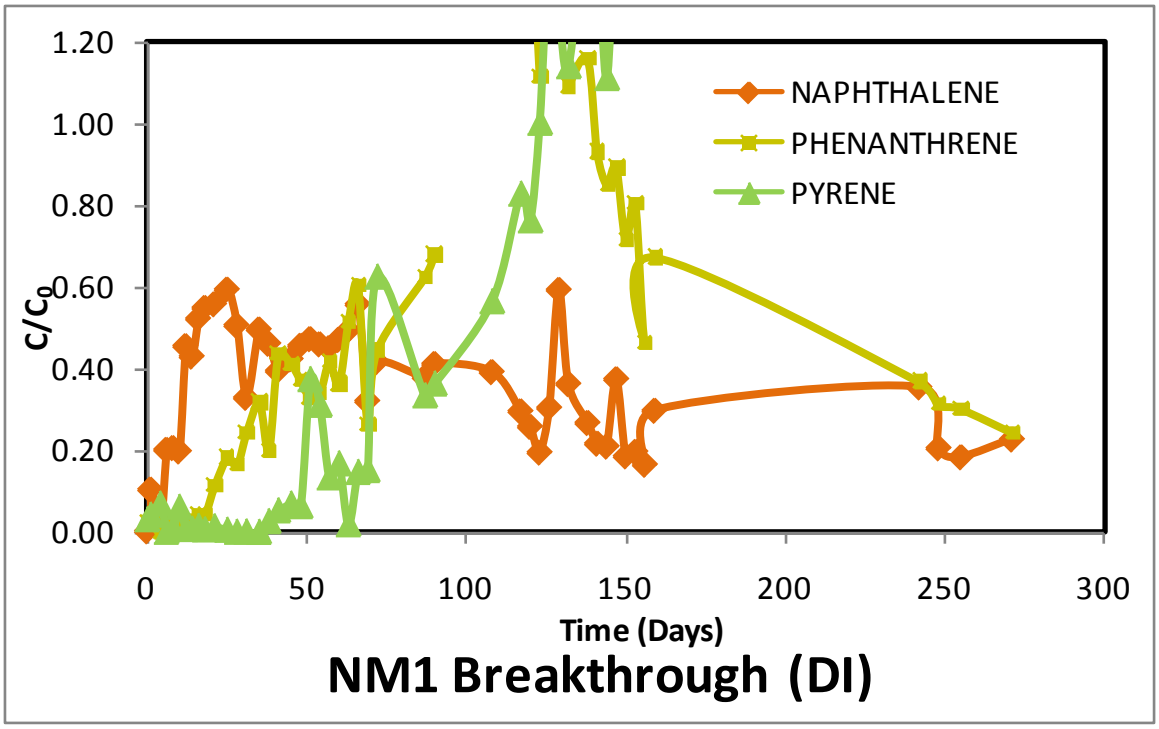
1.20
1.00
0.80
0.60
0.40
0.20
0.00
C/C0
0
50
100
150
200
250
300
Time (Days)
NAPHTHALENE
PHENANTHRENE
PYRENE
NM1 Breakthrough (DI)

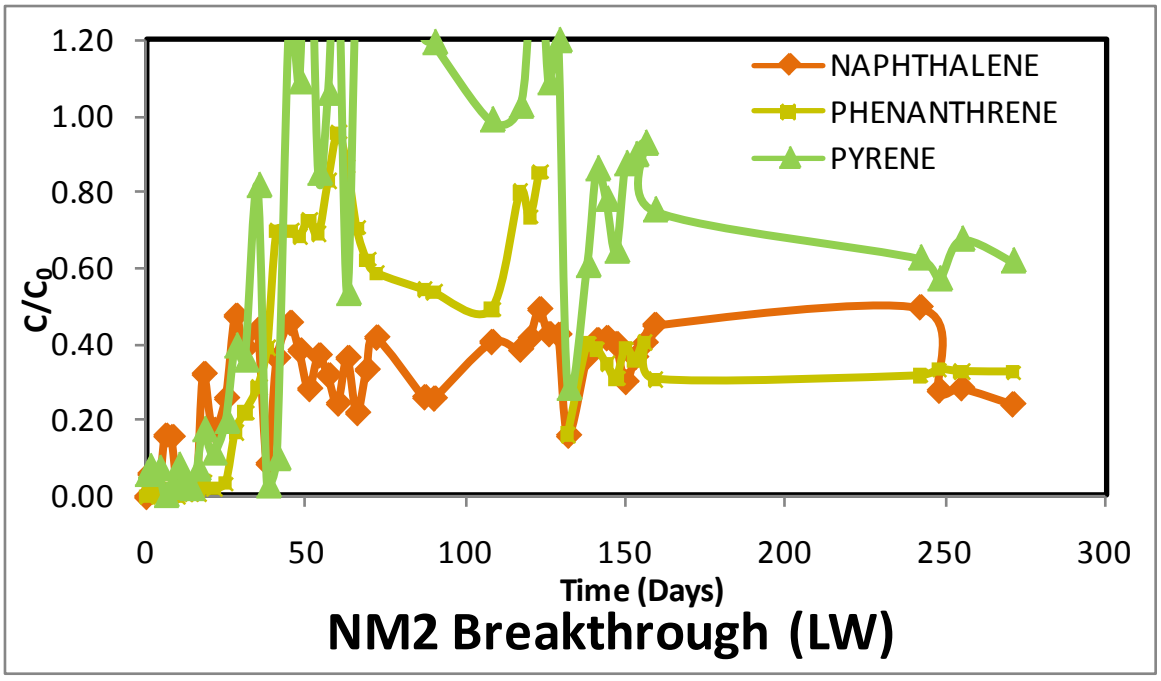
1.20
1.00
0.80
0.60
0.40
0.20
0.00
C/C0
0
50
100
150
200
250
300
Time (Days)
NAPHTHALENE
PHENANTHRENE
PYRENE
NM2 Breakthrough (LW)

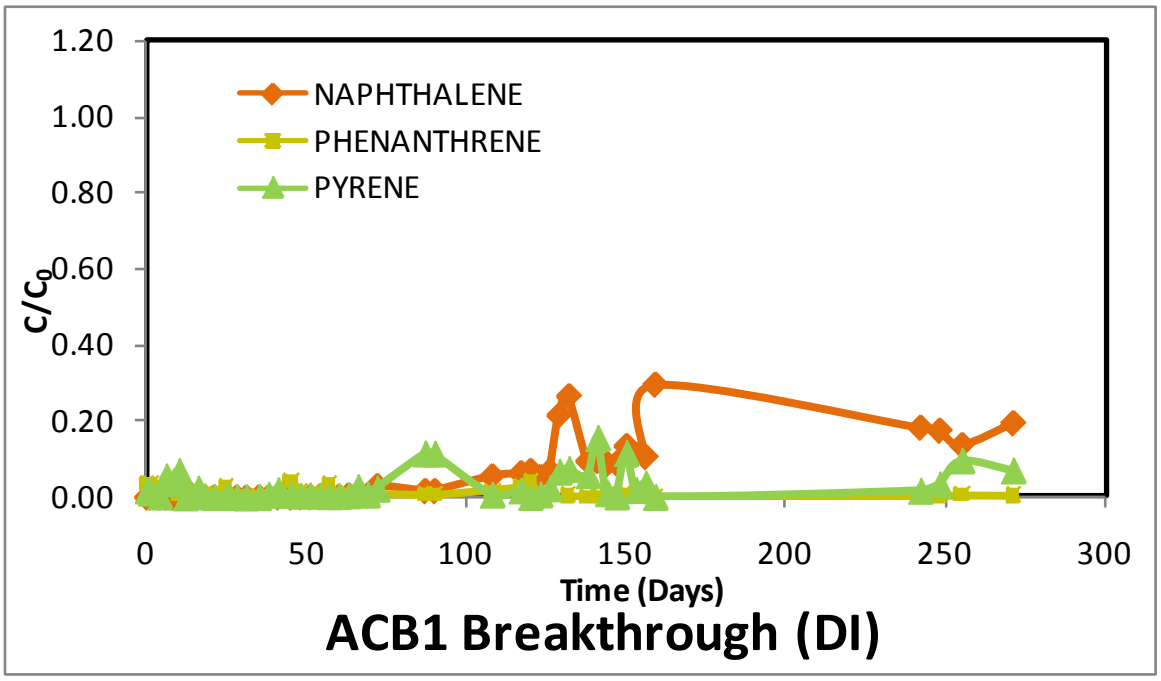
1.20
1.00
0.80
0.60
0.40
0.20
0.00
C/C0
NAPHTHALENE
PHENANTHRENE
PYRENE
0
50
100
150
200
250
300
Time (Days)
ACB1 Breakthrough (DI)

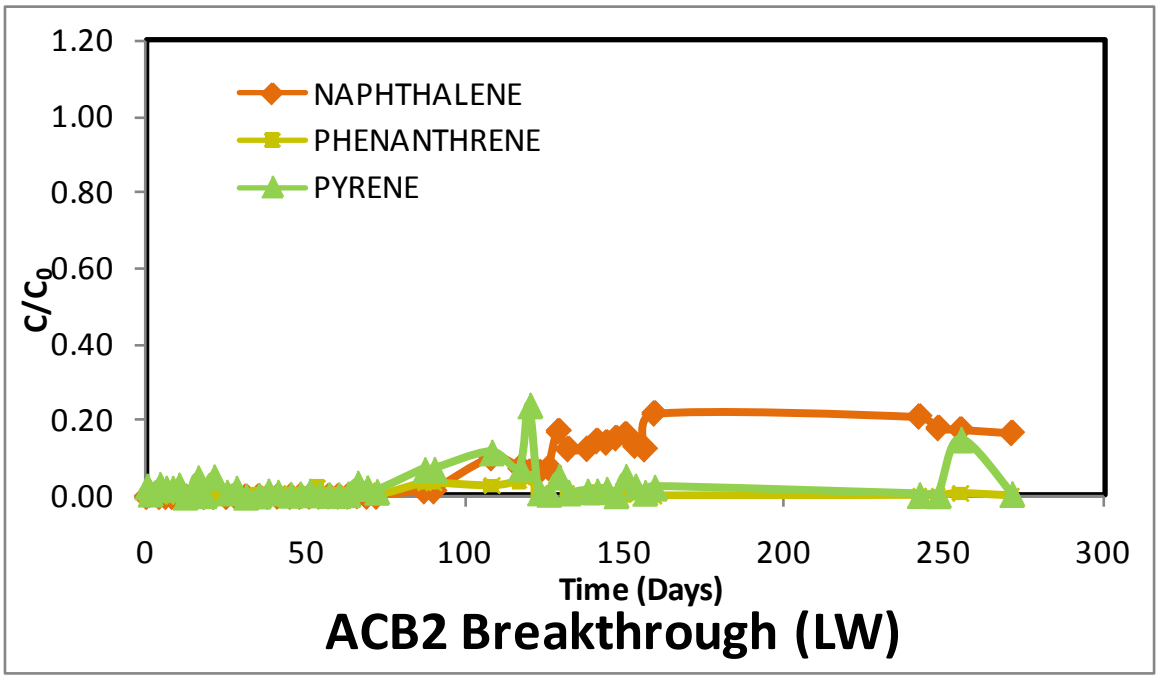
1.20
1.00
0.80
0.60
0.40
0.20
0.00
C/C0
NAPHTHALENE
PHENANTHRENE
PYRENE
0
50
100
150
200
250
300
Time (Days)
ACB2 Breakthrough (LW)

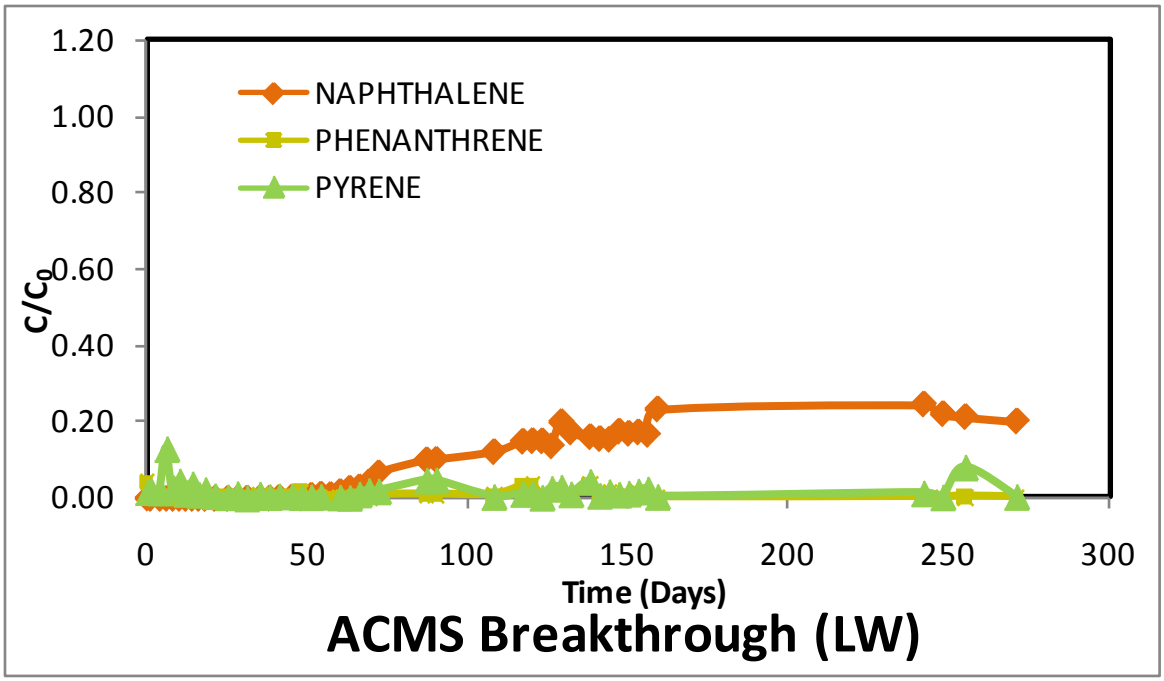
1.20
1.00
0.80
0.60
0.40
0.20
0.00
C/C0
NAPHTHALENE
PHENANTHRENE
PYRENE
0
50
100
150
200
250
300
Time (Days)
ACMS Breakthrough (LW)

Day	NAPHTHALENE									
	NM1		NM2		ACB1		ACB2		ACMS	
	Conc. (ppb)	C/Co	Conc. (ppb)	C/Co	Conc. (ppb)	C/Co	Conc. (ppb)	C/Co	Conc. (ppb)	C/Co
0	27.11	0.00	4.55	0.00	7.86	0.00	2.99	0.00	17.95	0.00
1	1,650.60	0.10	970.12	0.06	2.10	0.00	89.01	0.01	1.05	0.00
4	390.20	0.02	166.68	0.01	1.40	0.00	0.21	0.00	2.94	0.00
6	3,197.50	0.20	2,571.72	0.16	1.82	0.00	1.47	0.00	2.97	0.00
8	3,267.87	0.21	2,515.30	0.16	0.49	0.00	0.31	0.00	0.87	0.00
10	3,134.63	0.20	290.51	0.02	0.63	0.00	5.49	0.00	1.50	0.00
12	7,235.79	0.46	367.45	0.02	0.42	0.00	0.07	0.00	0.16	0.00
14	6,827.40	0.43	465.35	0.03	1.99	0.00	1.26	0.00	1.36	0.00
16	8,298.55	0.52	350.54	0.02	2.41	0.00	2.80	0.00	2.13	0.00
18	8,722.72	0.55	5,160.95	0.32	0.91	0.00	0.17	0.00	0.09	0.00
21	8,865.02	0.56	2,818.62	0.18	2.58	0.00	0.06	0.00	1.13	0.00
25	9,434.59	0.59	4,140.13	0.26	1.35	0.00	0.13	0.00	0.83	0.00
28	8,042.97	0.51	7,603.93	0.47	0.01	0.00	0.01	0.00	0.04	0.00
31	5,222.81	0.33	6,231.66	0.39	0.04	0.00	0.03	0.00	11.50	0.00
35	7,882.33	0.50	7,018.33	0.44	7.96	0.00	1.21	0.00	21.35	0.00
38	7,329.25	0.46	1,400.27	0.09	3.11	0.00	6.42	0.00	13.95	0.00
41	6,268.20	0.39	5,816.45	0.36	11.49	0.00	15.06	0.00	44.71	0.00
45	6,724.30	0.42	7,306.62	0.45	2.34	0.00	5.14	0.00	64.10	0.00
48	7,249.93	0.46	6,151.78	0.38	13.82	0.00	7.77	0.00	25.28	0.00
51	7,508.61	0.47	4,533.57	0.28	14.59	0.00	14.89	0.00	130.94	0.01
54	7,306.54	0.46	5,941.78	0.37	30.92	0.00	15.69	0.00	177.12	0.01
57	7,157.44	0.45	5,104.73	0.32	34.32	0.00	21.31	0.00	161.55	0.01
60	7,479.74	0.47	3,925.15	0.24	29.83	0.00	16.51	0.00	286.66	0.02
63	7,828.52	0.49	5,832.58	0.36	90.42	0.01	16.29	0.00	423.19	0.03
66	8,859.30	0.56	3,526.21	0.22	66.43	0.00	36.48	0.00	480.82	0.03
69	5,090.88	0.32	5,334.42	0.33	79.60	0.01	10.82	0.00	682.60	0.04
72	6,607.76	0.42	6,693.12	0.42	475.47	0.03	10.52	0.00	1,060.31	0.07
87	6,018.67	0.38	4,189.33	0.26	269.35	0.02	231.95	0.01	1,603.51	0.10
90	6,539.90	0.41	4,132.15	0.26	269.11	0.02	232.85	0.01	1,621.46	0.10
108	6,224.10	0.39	6,506.72	0.40	877.93	0.06	1,608.49	0.10	1,943.03	0.12
117	4,696.66	0.30	6,187.99	0.38	1,008.73	0.06	1,216.11	0.08	2,375.90	0.15
120	4,095.61	0.26	6,659.83	0.41	1,102.95	0.07	1,038.85	0.06	2,400.09	0.15
123	3,092.59	0.19	7,879.12	0.49	849.31	0.05	1,022.93	0.06	2,394.24	0.15
126	4,829.95	0.30	6,836.58	0.42	1,086.67	0.07	1,205.12	0.07	2,186.83	0.14
129	9,423.96	0.59	6,806.27	0.42	3,412.88	0.21	2,730.06	0.17	3,189.91	0.20
132	5,761.17	0.36	2,576.83	0.16	4,203.27	0.26	1,985.24	0.12	2,762.06	0.17
138	4,244.16	0.27	5,888.54	0.37	1,511.93	0.10	1,993.49	0.12	2,567.22	0.16
141	3,437.29	0.22	6,583.34	0.41	1,520.97	0.10	2,318.95	0.14	2,489.28	0.15
144	3,323.95	0.21	6,670.50	0.41	1,383.34	0.09	2,258.16	0.14	2,460.34	0.15
147	5,945.49	0.37	6,419.44	0.40	1,418.78	0.09	2,439.54	0.15	2,797.77	0.17
150	2,944.56	0.19	4,829.56	0.30	2,133.50	0.13	2,596.99	0.16	2,706.92	0.17
153	3,119.85	0.20	5,862.47	0.36	1,775.26	0.11	2,127.91	0.13	2,764.01	0.17
156	2,616.03	0.16	6,464.72	0.40	1,678.04	0.11	1,979.93	0.12	2,661.28	0.17
159	4,719.18	0.30	7,220.45	0.45	4,681.98	0.29	3,468.03	0.22	3,718.51	0.23
242	5,629.94	0.35	7,965.37	0.49	2,897.08	0.18	3,340.45	0.21	3,923.34	0.24
248	3,258.54	0.21	4,464.69	0.28	2,772.12	0.17	2,860.70	0.18	3,523.66	0.22
255	2,907.45	0.18	4,569.46	0.28	2,174.05	0.14	2,798.62	0.17	3,400.35	0.21
271	3,599.77	0.23	3,890.32	0.24	3,081.27	0.19	2,652.39	0.16	3,219.33	0.20

Day	PHENANTHRENE									
	NM1		NM2		ACB1		ACB2		ACMS	
	Conc. (ppb)	C/Co	Conc. (ppb)	C/Co	Conc. (ppb)	C/Co	Conc. (ppb)	C/Co	Conc. (ppb)	C/Co
0	9.09	0.02	0.21	0.00	13.78	0.04	0.53	0.00	16.14	0.04
1	8.79	0.02	1.98	0.01	13.93	0.04	0.66	0.00	1.30	0.00
4	0.19	0.00	0.07	0.00	9.26	0.02	0.43	0.00	0.04	0.00
6	8.71	0.02	6.40	0.02	8.02	0.02	0.29	0.00	0.06	0.00
8	8.17	0.02	7.22	0.02	7.04	0.02	0.14	0.00	1.58	0.00
10	3.70	0.01	0.37	0.00	2.43	0.01	0.05	0.00	0.99	0.00
12	9.22	0.02	1.58	0.00	3.99	0.01	0.76	0.00	1.27	0.00
14	11.69	0.03	2.44	0.01	3.37	0.01	0.53	0.00	0.32	0.00
16	16.78	0.05	2.96	0.01	1.98	0.01	1.31	0.00	1.20	0.00
18	16.78	0.05	14.27	0.04	1.80	0.00	1.17	0.00	1.20	0.00
21	42.89	0.12	7.68	0.02	1.39	0.00	0.05	0.00	0.53	0.00
25	68.37	0.18	13.10	0.03	9.55	0.03	0.37	0.00	1.14	0.00
28	61.25	0.17	63.77	0.17	0.54	0.00	0.15	0.00	1.35	0.00
31	79.97	0.24	83.01	0.22	0.54	0.00	0.68	0.00	0.76	0.00
35	104.26	0.32	107.98	0.29	0.55	0.00	1.95	0.01	2.39	0.01
38	65.83	0.20	147.32	0.39	0.60	0.00	0.60	0.00	2.02	0.01
41	142.75	0.44	263.30	0.70	0.62	0.00	2.09	0.01	0.42	0.00
45	134.86	0.41	262.89	0.70	15.90	0.04	1.06	0.00	2.01	0.01
48	121.66	0.37	257.50	0.68	6.08	0.02	1.76	0.00	6.60	0.02
51	107.82	0.33	273.56	0.73	3.09	0.01	2.81	0.01	0.47	0.00
54	111.23	0.34	259.46	0.69	3.02	0.01	9.18	0.02	1.09	0.00
57	136.50	0.42	312.19	0.83	13.29	0.04	1.15	0.00	0.95	0.00
60	118.73	0.36	359.99	0.96	0.17	0.00	0.76	0.00	0.59	0.00
63	168.97	0.52	327.30	0.87	1.53	0.00	1.45	0.00	0.38	0.00
66	197.27	0.60	265.52	0.70	1.08	0.00	2.79	0.01	2.24	0.01
69	86.86	0.27	234.91	0.62	0.87	0.00	5.28	0.01	0.64	0.00
72	146.19	0.45	221.50	0.59	2.91	0.01	0.22	0.00	2.88	0.01
87	204.68	0.63	204.62	0.54	1.98	0.01	12.63	0.03	3.48	0.01
90	222.40	0.68	201.83	0.54	1.98	0.01	12.68	0.03	3.51	0.01
108			184.93	0.49	6.38	0.02	9.83	0.03	3.14	0.01
117			301.37	0.80	9.33	0.03	14.19	0.04	12.27	0.03
120	585.82	1.58	276.08	0.73	14.86	0.04	18.13	0.05	13.54	0.04
123	413.44	1.11	321.22	0.85	0.90	0.00	2.10	0.01	2.65	0.01
126										
129										
132	405.47	1.09	61.45	0.16	1.26	0.00	2.83	0.01	0.59	0.00
138	430.10	1.16	150.89	0.40	0.54	0.00	1.89	0.01	14.43	0.04
141	345.90	0.93	146.13	0.39	0.79	0.00	4.01	0.01	4.12	0.01
144	316.18	0.85	131.21	0.35	2.18	0.01	0.42	0.00	5.09	0.01
147	331.38	0.89	116.91	0.31	1.13	0.00	3.05	0.01	1.11	0.00
150	265.95	0.72	146.74	0.39	1.77	0.00	1.37	0.00	1.78	0.00
153	298.39	0.80	135.46	0.36	1.68	0.00	2.71	0.01	6.49	0.02
156	172.62	0.47	152.33	0.40	2.81	0.01	0.62	0.00	2.95	0.01
159	250.01	0.67	116.30	0.31	0.60	0.00	0.20	0.00	0.28	0.00
242	137.18	0.37	119.44	0.32	0.44	0.00	0.72	0.00	0.60	0.00
248	116.29	0.31	125.62	0.33	0.90	0.00	0.36	0.00	0.35	0.00
255	112.65	0.30	123.66	0.33	1.67	0.00	2.48	0.01	1.24	0.00
271	91.32	0.25	123.27	0.33	1.29	0.00	0.23	0.00	0.37	0.00

Day	PYRENE									
	NM1		NM2		ACB1		ACB2		ACMS	
	Conc. (ppb)	C/Co	Conc. (ppb)	C/Co	Conc. (ppb)	C/Co	Conc. (ppb)	C/Co	Conc. (ppb)	C/Co
0	0.64	0.03	1.13	0.06	0.38	0.02	0.53	0.03	0.33	0.02
1	0.86	0.04	1.52	0.08	0.26	0.01	0.16	0.01	0.39	0.02
4	1.42	0.07	1.43	0.07	0.06	0.00	0.61	0.03	0.31	0.02
6	0.01	0.00	0.04	0.00	1.11	0.05	0.42	0.02	2.53	0.13
8	0.19	0.01	0.56	0.03	0.75	0.04	0.42	0.02	0.53	0.03
10	1.26	0.06	1.59	0.08	1.39	0.07	0.58	0.03	0.88	0.04
12	0.15	0.01	0.44	0.02	0.01	0.00	0.01	0.00	0.24	0.01
14	0.15	0.01	0.39	0.02	0.12	0.01	0.22	0.01	0.73	0.04
16	0.30	0.01	1.41	0.07	0.47	0.02	0.95	0.05	0.19	0.01
18	0.13	0.01	3.45	0.17	0.06	0.00	0.08	0.00	0.44	0.02
21	0.28	0.01	2.23	0.11	0.03	0.00	1.00	0.05	0.12	0.01
25	0.11	0.01	3.87	0.20	0.11	0.01	0.22	0.01	0.07	0.00
28	0.01	0.00	7.78	0.39	0.03	0.00	0.42	0.02	0.23	0.01
31	0.02	0.00	7.05	0.36	0.01	0.00	0.00	0.00	0.00	0.00
35	0.00	0.00	16.09	0.82	0.03	0.00	0.07	0.00	0.20	0.01
38	0.54	0.03	0.53	0.03	0.14	0.01	0.28	0.01	0.08	0.00
41	1.08	0.05	1.95	0.10	0.39	0.02	0.21	0.01	0.11	0.01
45	1.42	0.07	25.26	1.28	0.14	0.01	0.10	0.01	0.12	0.01
48	1.29	0.06	21.46	1.09	0.10	0.00	0.13	0.01	0.08	0.00
51	7.66	0.37	33.49	1.70	0.12	0.01	0.27	0.01	0.07	0.00
54	6.37	0.31	16.72	0.85	0.10	0.00	0.12	0.01	0.09	0.00
57	2.73	0.13	20.86	1.06	0.07	0.00	0.09	0.00	27.04	
60	3.44	0.17	29.02	1.47	0.08	0.00	0.09	0.00	0.06	0.00
63	0.38	0.02	10.50	0.53	0.12	0.01	0.13	0.01	0.04	0.00
66	3.00	0.15	27.06	1.37	0.55	0.03	0.68	0.03	0.21	0.01
69	3.10	0.15	26.21	1.33	0.15	0.01	0.44	0.02	0.39	0.02
72	12.79	0.62	30.61	1.55	0.46	0.02	0.25	0.01	0.37	0.02
87	6.84	0.33	23.81	1.21	2.31	0.11	1.37	0.07	0.92	0.05
90	7.44	0.36	23.49	1.19	2.31	0.11	1.38	0.07	0.93	0.05
108	11.56	0.56	19.49	0.99	0.15	0.01	2.26	0.11	0.08	0.00
117	16.95	0.83	20.19	1.03	0.37	0.02	1.45	0.07	0.24	0.01
120	15.62	0.76	25.00	1.27	0.03	0.00	4.66	0.24	0.28	0.01
123	20.50	1.00	29.71	1.51	0.16	0.01	0.22	0.01	0.04	0.00
126	29.11	1.42	21.41	1.09	0.49	0.02	0.15	0.01	0.50	0.03
129	26.13	1.28	23.59	1.20	1.36	0.07	1.02	0.05	0.56	0.03
132	23.34	1.14	5.59	0.28	1.50	0.07	0.22	0.01	0.21	0.01
138	31.37	1.53	11.95	0.61	1.17	0.06	0.28	0.01	0.85	0.04
141	30.20	1.47	16.96	0.86	3.13	0.15	0.28	0.01	0.14	0.01
144	22.75	1.11	15.37	0.78	0.23	0.01	0.36	0.02	0.33	0.02
147	31.39	1.53	12.69	0.64	0.06	0.00	0.08	0.00	0.20	0.01
150	35.26	1.72	17.22	0.87	2.34	0.11	1.02	0.05	0.25	0.01
153	34.88	1.70	17.69	0.90	0.39	0.02	0.53	0.03	0.36	0.02
156	30.15	1.47	18.28	0.93	0.74	0.04	0.20	0.01	0.46	0.02
159	27.68	1.35	14.83	0.75	0.03	0.00	0.47	0.02	0.09	0.00
242	41.99	2.05	12.34	0.63	0.35	0.02	0.09	0.00	0.26	0.01
248	45.66	2.23	11.25	0.57	0.70	0.03	0.07	0.00	0.06	0.00
255	45.40	2.22	13.31	0.68	1.95	0.10	2.92	0.15	1.59	0.08
271	42.96	2.10	12.18	0.62	1.42	0.07	0.14	0.01	0.08	0.00

APPENDIX I:

Column Studies Influent Data

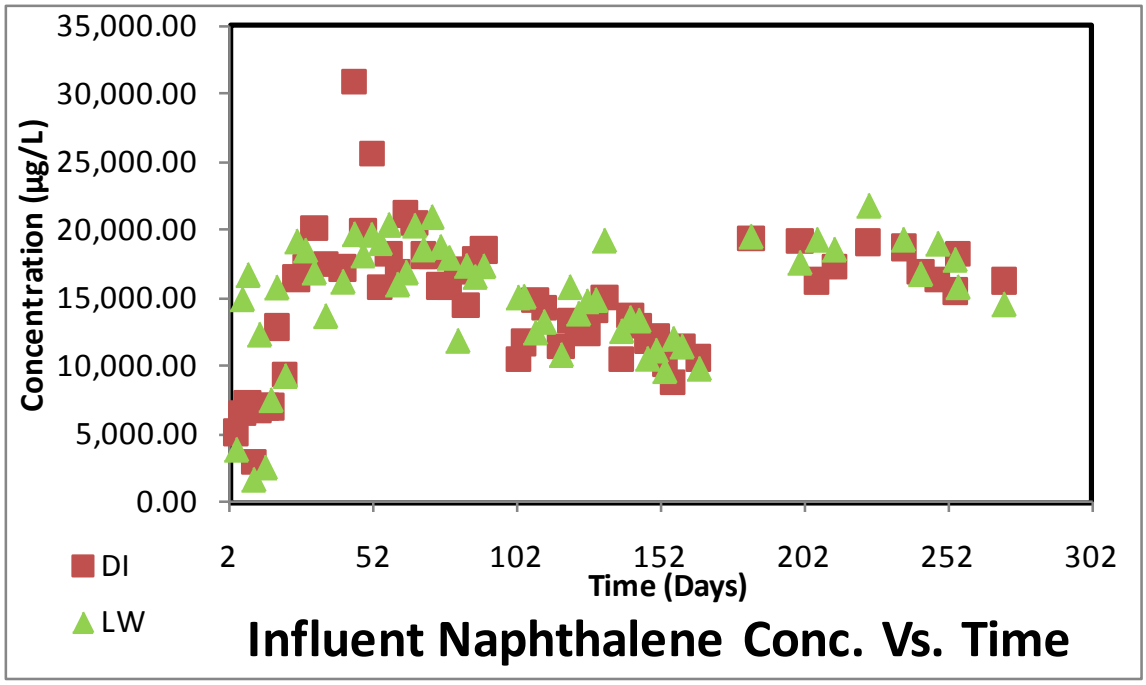
35,000.00
30,000.00
25,000.00
20,000.00
15,000.00
10,000.00
5,000.00
0.00
Concentration (µg/L)
2
52
102
152
202
252
302
Time (Days)
DI
LW
Influent Naphthalene Conc. Vs. Time

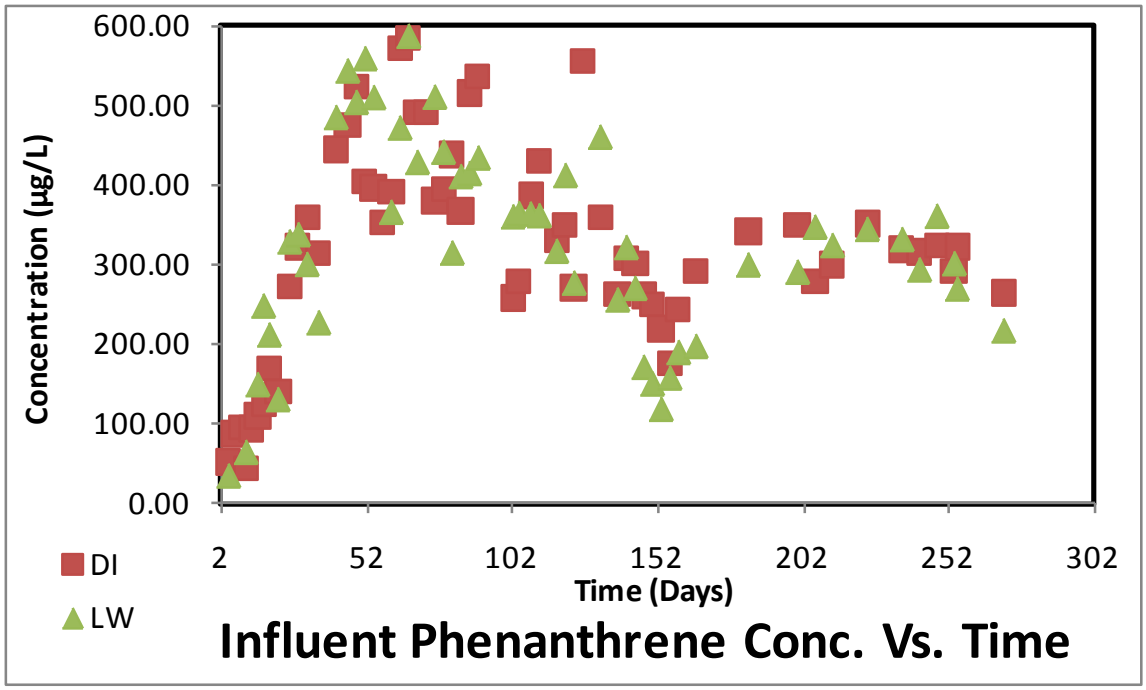
600.00
500.00
400.00
300.00
200.00
100.00
0.00
Concentration (µg/L)
2
52
102
152
202
252
302
Time (Days)
DI
LW
Influent Phenanthrene Conc. Vs. Time

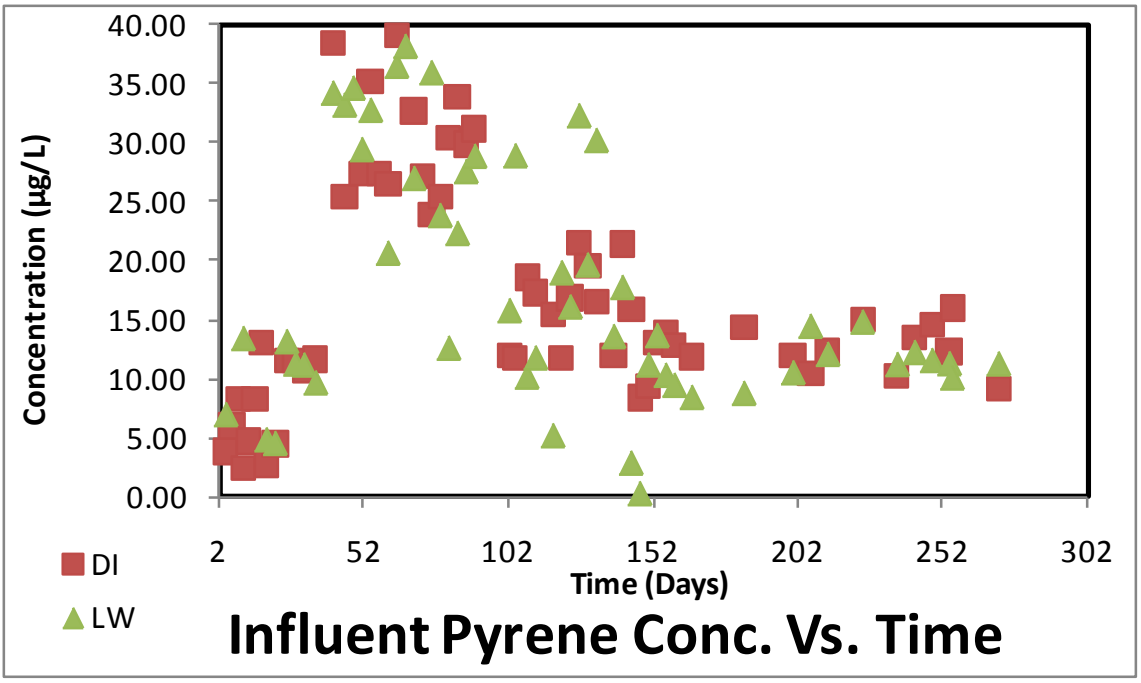
40.00
35.00
30.00
25.00
20.00
15.00
10.00
5.00
0.00
Concentration (µg/L)
2
52
102
152
202
252
302
Time (Days)
DI
LW
Influent Pyrene Conc. Vs. Time

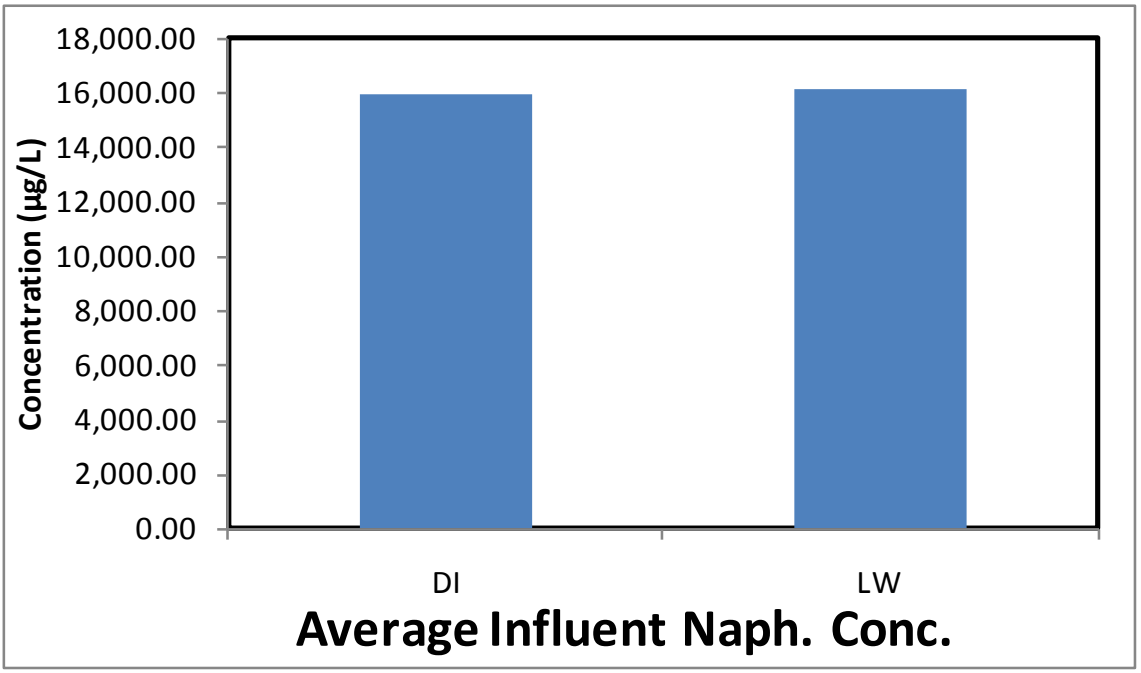
18,000.00
16,000.00
14,000.00
12,000.00
10,000.00
8,000.00
6,000.00
4,000.00
2,000.00
0.00
Concentration (µg/L)
DI
LW
Average Influent Naph. Conc.

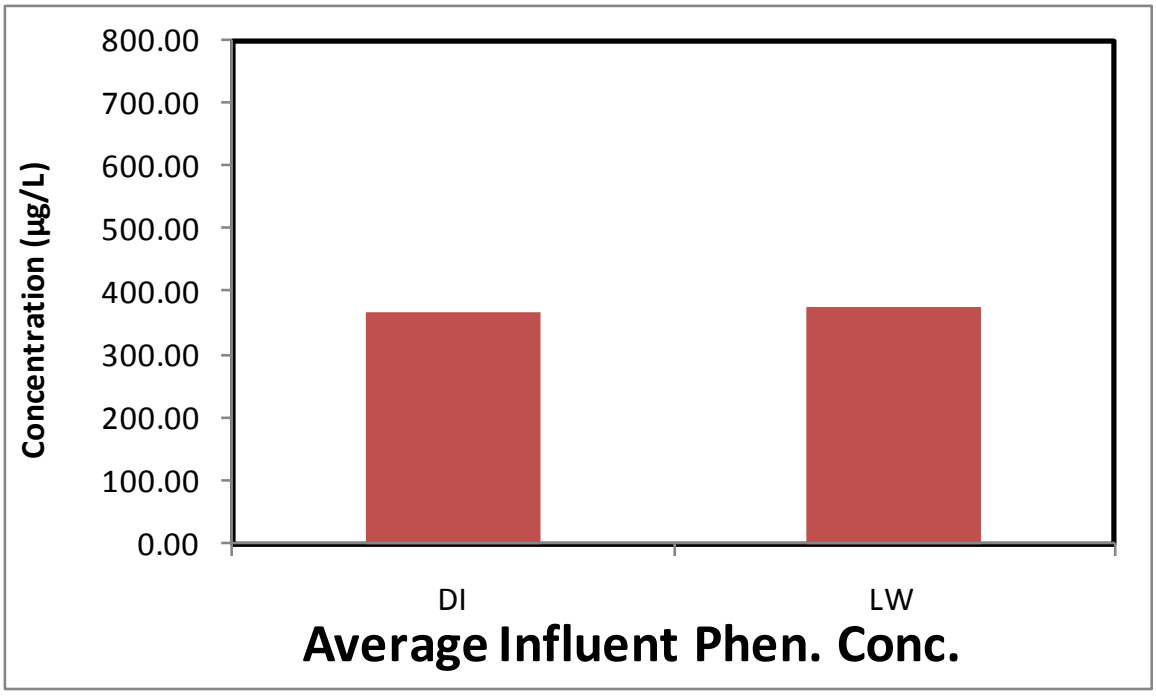
800.00
700.00
600.00
500.00
400.00
300.00
200.00
100.00
0.00
Concentration (µg/L)
DI
LW
Average Influent Phen. Conc.

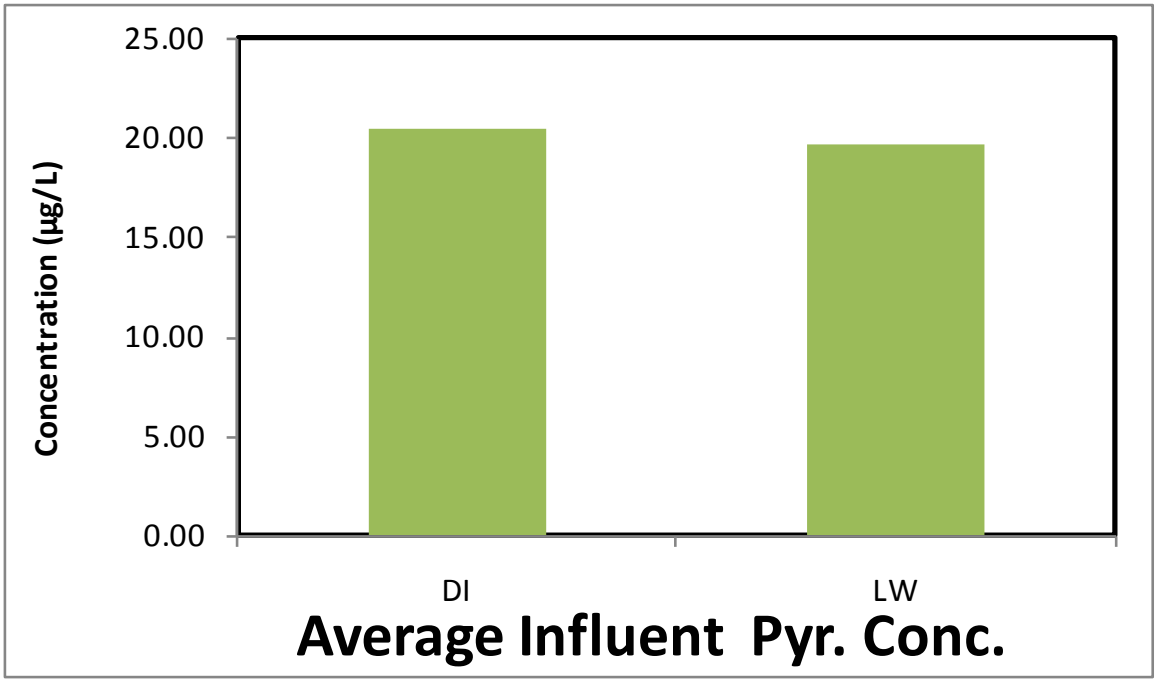
25.00
20.00
15.00
10.00
5.00
0.00
Concentration (µg/L)
DI
LW
Average Influent Pyr. Conc.

APPENDIX J:

Column Studies Standards

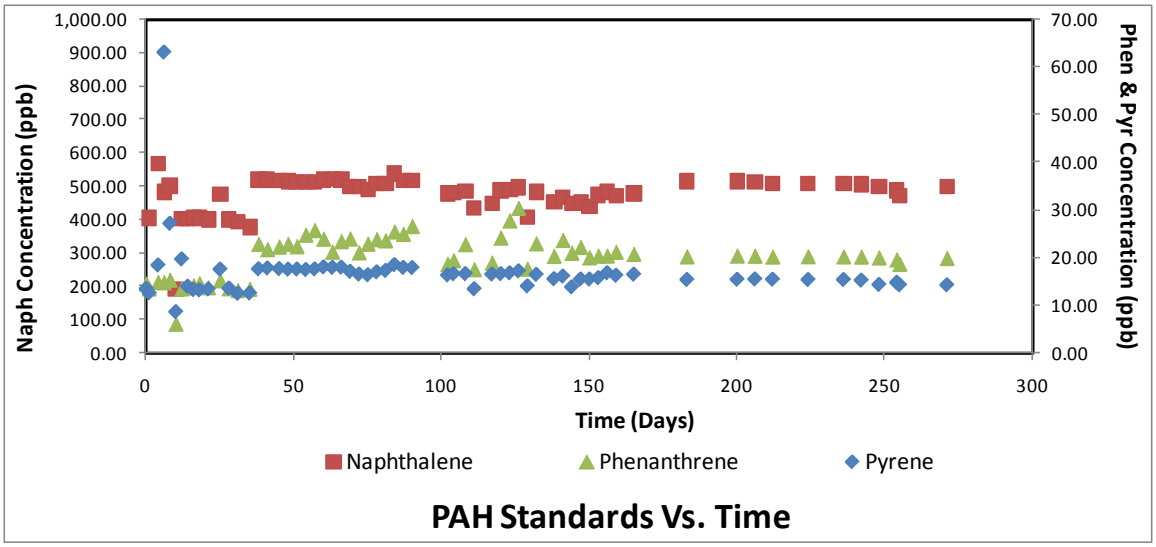
1,000.00
900.00
800.00
700.00
600.00
500.00
400.00
300.00
200.00
100.00
0.00
Naph Concentration (ppb)
70.00
60.00
50.00
40.00
30.00
20.00
10.00
0.00
Phen & Pyr Concentration (ppb)
0
50
100
150
200
250
300
Time (Days)
Naphthalene
Phenanthrene
Pyrene
PAH Standards Vs. Time

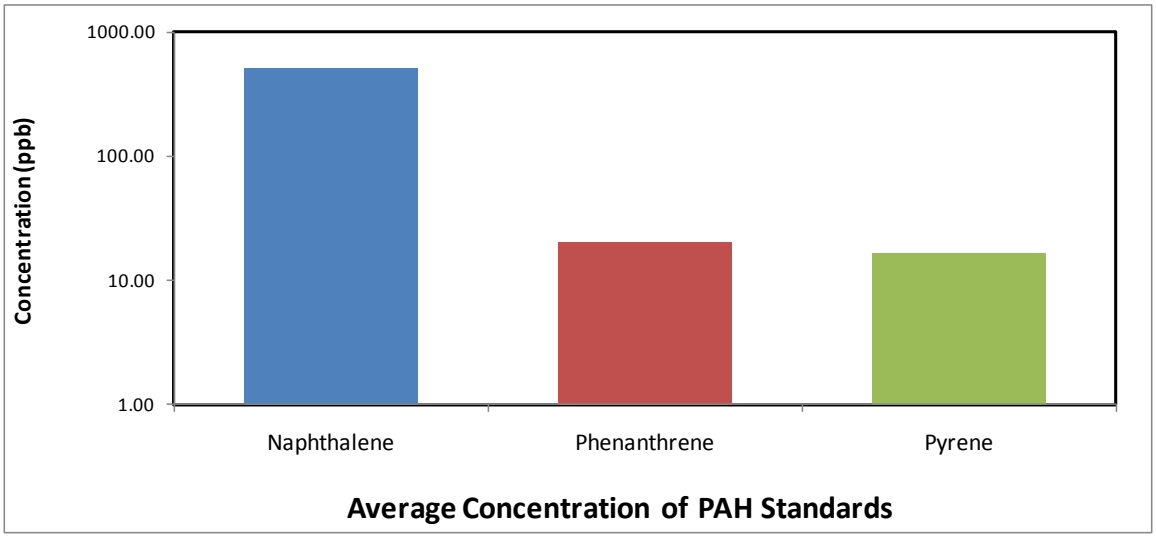
1000.00
100.00
10.00
1.00
Concentration (ppb)
Naphthalene
Phenanthrene
Pyrene
Average Concentration of PAH Standards

APPENDIX K:

Filter Losses

FILTERED SAMPLES

Sample	Naph	Phen	Pyr
1	284.93	17.05	13.95
2	315.59	31.83	14.96
3	297.05	21.49	13.50
4	321.84	29.02	15.90
5	313.16	14.71	14.71
Avg. Conc.	299.19	23.46	14.14
St. Dev.	15.44	7.58	0.75
Coef. Var.	0.05	0.32	0.05

UNFILTERED SAMPLES

Sample	Naph	Phen	Pyr
1	371.80	45.31	26.32
2	395.08	46.25	32.68
3	390.27	38.78	30.84
4	383.62	42.96	29.72
5	379.00	35.10	2.86
Avg. Conc.	385.19	43.33	29.89
St. Dev.	10.09	3.33	2.68
Coef. Var.	0.03	0.08	0.09
Avg. Loss	**86.00**	**19.87**	**15.75**
Avg. Loss (%)	**22.33**	**45.86**	**52.70**

Bibliography

Ahn, Sungwoo, David Werner, and Richard G. Luthy. "Modeling PAH mass transfer in a slurry of comtaminated soil or sediment amended with organic sorbents." *Water Research*, 2008: 2931-2942.

Ake, C.L., et al. "Porous organoclay composite for the sorption of polycyclic aromatic hydrocarbons and pentachlorophenol from groundwater." *Chemosphere*, 2003: 835-844.

Allen-King, Richelle M., Peter Grathwohl, and Billiam P. Ball. "New modeling paradigms for the sprotion of hydrophobic organic chemicals to heterogeneous carbonaceous matter in soils, sediments, and rocks." *Advances in Water Resources*, 2002: 985-1016.

Aqua Technologies of Wyoming Inc. *Organoclay and Organophilic Clay Infromation.* http://www.aquatechnologies.com/info_organoclay.htm (accessed February 26, 2009).

Bandosz, Teresa J. *Activated Carbon Surfaces in Environmental Remediation.* Oxford: Elsevier, 2006.

Bridges, Todd S., et al. *THe Four Rs of Environmental Dredging: Resuspention, Release, Residual, and Risk.* Governmental Research Report, Washington, D.C.: US Army Corps of Engineers, 2008.

Burns, S.E., S.L Bartelt-Hunt, J.A. Smith, and A.Z. Redding. "Coupled MEchanical and Chemical Behavior of Bentonite Engineered with a Controlled Organic Phase." *Journal of Geotechnical and Geoenvironmental Engineering*, 2006: 1404-1412.

Chao, Wen-Lu, J.-Yves Parlange, and Tammos S. Steenhuis. "An Analysis of the Movement of Wetting and Nonwetting Fluids in Homogereous Porous Media." *Transport in Media*, 2000: 121-135.

Conder, J., et al. "Review of Monitored Natural Recovery at Contaminated Sediment Sites." *Fifth International Conference on Remediation of Contaminated Sediments.* Jacksonville: Battelle, 2009.

Conduto, Donald P. *Geotechnical Engineering Principles and Practices.* Upper Saddle River, New Jersey: Prentice Hall, 1999.

Costello, Michael, and Danial Talsma. "Remedial Design Modeling at a Superfund Site." *Proceedings of the Second International Conference on Remediation of Contaminated Sediments.* Venice, Italy, 2003.

Futona, David J., [et al]. *Polycyclic Aromatic Hydrocarbons in Water Systems.* Boca Raton: CRC Press, 1981.

Galjour Dufreche, Jasmine. *Evaluation of Organoclay as an Active Capping Amendment for the Control of Dissolved PAH Contamination.* M.S. Thesis in Civil Engineering, The Univerisity of Texas at Austin, 2008.

Groisman, Ludmila, Chaim Rav-Acha, Zev Gerstl, and Uri Mingelgrin. "Sorption of organic compounds of varying hydrophobicities from water and industrial wastewater by long- and short chain organoclays." *Applied Clay Science*, 2004: 159-166.

GSI. "Remediation Action Conceptual Site Model, McCormick & Baxter Creosoting Company Superfund Site, Portland, Oregon." Portland, 2005.

GSI/Hart Crowser. "Ebullition and Sheen Invenstigation Work Plan, McCormick & Baxter Creosoting Company Superfund Site, Portland, Oregon." Portland, 2008.

Hinkle, S.R., et al. "Linking hyporheic flow and nitrogen cycling near the Willamette River - a large river in Oregon, USA." *Journal of Hydrology*, 2001: 157-180.

Honeywell, Tecsult. *Multi-layer Capping of Contaminated Sediments at Clark Island.* Salaberry-de-Valleyfield, Quebec, Canada, 2006.

Huesker. *FilterMatSeris: Technical Road Show.*

Jankowska, Helena, Andrzej Swiatkowski, and Jerzy Choma. *Active Carbon.* London: Ellis Horwood, 1991.

Jones, Kim D., and Christine L. Tiller. "Effect of Solution Chemestry on the Extent of Binding of Phenanthrene by a Soil Humic Acid: A Comparison of Dissoloved and Clay Bound Humic." *Environmental Science and Technology*, 1999: 580-587.

Khanam, Aiahsa. *Assess Feasibility of Organoclay to retain NAPL (Non Aqueous Phase Liquid) in sediment beneath a cap.* M.S. Thesis in Civil Engineering, The Univerisity of Texas at Austin, 2006.

Kilduff, James E., and Andrew Wigton. "Sorption of TCE by Humic-Preloaded Activated Carbon: Incorporation Size-Exclusion and Pore Blockage Phenomena in a Competitive Adsorption Model." *Environmental Science and Technology*, 1999: 250-256.

Kocan, Anton and et.al. *Persistant Organic Pollutants.* http://www.hearnas.sk/pops/wp2_pops_persistent_organic.htm (accessed March 24, 2009).

Lee, S.Y, S.J. Kim, S.Y. Chung, and C.H. Jeong. "Soprtion of hydrophobic compounds onto organoclays." *Chemosphere*, 2004: 781-785.

Lo, Irene C., and Xiaoyun Yang. "Use of Organoclay as Secondary Containment for Gasoline Storeage Tanks." *Journal of Environmental Engineering*, 2001: 154-161.

Luthy, Richard G., et al. "Sequestration of hydrophobic Organic Contaminants by Geosorbants." *Environmental Science and Technology*, 1997: 3341-3347.

Madalinski, Kelly. *In Situ Technologies for the Remediation of Contaiminated Sediements.* PPT, Washington, D.C.: Office of Superfund Remediation and Technology Innovation, 2008.

Mattson, James S., and Harry B. Mark. *Activated Carbon Surface Chemistry and Adsorption from Solution.* New York: Marcel Dekker, INC., 1971.

McDonough, Kathleen M., Paul Murphy, Jim Olsta, Yuewei Zhu, Danny Reible, and Gregory V. Lowry. "Development and Placement of a Sorband-Amended Thin Lauer Sediment Cap in the Anaostia River." *Soil & Sediment*, 2007: 313-322.

"Sediment Dredging at Superfund Megasites: Assessing the Effectiveness." In *Sediment Dredging at Superfund Megasites: Assessing the Effectiveness*, by Committee on Sediment Dredging at Superfund Megasites, 1-15. Washington, D.C.: The National Academies Press, 2007.

Moretti, Lisa Karen. *Evaluation of Capping NAPL-contaminated Sediment.* M.S. Thesis in Civil Engineering, The Univerisity of Texas at Austin, 2008.

Mulligan, C. N., R. N. Yong, and B. F. Gibbs. "Surfactant-enhanced remediation of contaminated soil: a review." *Engineering Geology*, 2001: 371-380.

Pennell, Kurt D., Minquan Jin, Linda M. Abriola, and Gary A. Pope. "Surfactant enhanced remediation of soil columns contaiminated by residual tetrachloroethylene." *Journal of Contaminated Hydrology*, 1994: 35-53.

Pernyeszi, Timea, Roy Kasteel, Barbara Witthuhn, Peter Klahre, Harry Vereecken, and Erwin Klumpp. "Organoclays for soil remediation: Adsorption of 2,4-dichlorophenol on organoclay/aquiofer material mixtures studies under static and flow condidtions." *Applied Clay Science*, 2006: 179-189.

Pignatello, Joseph J., and Baoshan Xing. "Mechanisms of Slow Sorption Chemicals to Natural Particles." *Environmentla Science and Technology*, 1996: 1-11.

Redding, A.Z., S.E. Burns, R.T. Upson, and E.F. Anderson. "Organoclay Sorption of Benzene as a Fucntion of Total Organic Carbon Content." *Journal of Colloid and Interface Science*, 2002: 261-264.

Reible, Danny, David Lampert, David Constant, Robert D. Jr. Mutch, and Yuewei Zhu. "Active Capping Demonstration in the Anacostia River, Washington, D.C." *Remediation*, 2006: 39-53.

Reucroft, P. J., W. H. Simpson, and L. A. Jonas. "Sorption Properties of Activated Carbon." *The Journal of Physical Chemisty*, 1971: 3526-3531.

Rong, Yue. "Laboratory Detection Limits." *Contaminated Soil, Sediment, and Water*, 2002: 24-26.

Rytwo, Giora, Ynon Kohavi, Ilan Botnick, and Yotam Goenen. "Use of CV- and TTP-montmorillonite for the removal of priority pollutants from water." *Applied Clay Science*, 2007: 182-190.

Sediment Dredging at Superfund Megasites: Assessing the Effectiveness. Washington, D.C.: The National Academies Press, 2007.

Smisek, Milan, and Slavoj Cerny. *Active Carbon Manufacture, Properties and Applications.* Amsterdam-London-New York: Elsevier Publishing Conpany, 1970.

Steward, Kimberly K. *Development of Apparatus and Method for Consolidating Very Soft, Contaminated Sediments.* Austin, 2007.

U.S. EPA. *2005/2006 National Listing of Fish Advisories Fact Sheet.* Fact Sheet, Washington, D.C.: Office of Water, 2007.

U.S. EPA. *Contaminated Sediment Remediation Guidance for Hazardous Waste Sites.* Governmental Report, Washington, D.C.: United States Environmental Protection Agency, 2005.

Van Genuchten, M.T. "Analytical solutions for chemical transport with simultaneous adsorption, zero order production, and first order decay." *Journal of Hydrology*, 1981: 213-233.

Walser, Gabriele S., Tissa H. Illangasekare, and Arthur T. Corey. "Retention of liquid contaminants in layered soils." *Journal of Contaminant Hydrology*, 1999: 91-108.

Walters, Richard W., and Richard G. Luthy. "Equilibrium Adsorption of Polycyclic Aromatic Hydrocarbons from Water onto Activated Carbon." *Environmental Science and Technology*, 1984: 395-403.

Weissenfels, Walter D., Hans-Jurgen Klewer, and Joseph Langhoff. "Adsorption of polycyclic aromatic hydrocarbons (PAHs) by soil particles: influence on biodegradability and biotoxicity." *Applied Microbiology and Biotechnology*, 1992: 869-696.

Wikipedia The Free Encyclopedia. *Activated Carbon.* March 12, 2009. http://en.wikipedia.org/wiki/Activated_carbon (accessed March 23, 2009).

Wiles, Melina C., Hernry J. Huebner, Thomas J. McDonald, Kirby C. Donnelly, and Timothy D. Phillips. "Matrix-immolbilized organoclay for the sorption of polycyclic aromatic hydrocarbons and pentachlorophenol from groundwater." *Chemosphere*, 2005: 1455-1464.

Zeman, Alex J. "Subaqueous capping of very soft contaminated sediments." *Canadian Geotechnical Journal*, 1994: 570-577.

Zimmerman, John R., Upal Ghosh, Rod N. Millward, Todd S. Bridges, and Richard G. Luthy. "Addition of Carbon Sorbants to Reduce PCB and PAH Bioavailability in Marine Sediments: Physicochemical Tests." *Environmental Science and Technology*, 2004: 5458-5464.

Vita

Gabriel Trejo was born, raised, and schooled in El Paso, Texas a stone's throw from the U.S.–Mexico border. He obtained his bachelor's degree in Civil Engineering from the University of Texas at El Paso; affectionally know by many as UTEP. At UTEP, Gabriel worked on a variety of research projects; that ranged from modeling the Hueco Bolson for deep well injection of concentrate from a desalination plant; to comparing the water quality of primary effluent from wastewater treatment plants in El Paso and neighboring Ciudad Juarez. Upon graduation, in 2007 he decided to continue his education at the University of Texas at Austin, and pursue a master's degree in Environmental and Water Resources Engineering. Once in Austin, Gabriel participated extensively in intramural sports, followed the happenings of Texas Longhorn Football, dabbled in cycling and rock climbing, and began his journey on becoming an outdoorsman.

Permanent Address: 9304 Ramirez Ct.; El Paso, TX 79907

This thesis was typed by Gabriel Trejo.